USGS
science for a changing world

Three Approaches for Estimating Recovery Factors in Carbon Dioxide Enhanced Oil Recovery

Scientific Investigations Report 2017–5062

U.S. Department of the Interior
U.S. Geological Survey

Three Approaches for Estimating Recovery Factors in Carbon Dioxide Enhanced Oil Recovery

Mahendra K. Verma, Editor

Scientific Investigations Report 2017–5062

U.S. Department of the Interior
U.S. Geological Survey

U.S. Department of the Interior
RYAN K. ZINKE, Secretary

U.S. Geological Survey
William H. Werkheiser, Acting Director

U.S. Geological Survey, Reston, Virginia: 2017

Suggested citation:
Verma, M.K., ed., 2017, Three approaches for estimating recovery factors in carbon dioxide enhanced oil recovery: U.S. Geological Survey Scientific Investigations Report 2017–5062–A–E, variously paged, https://doi.org/10.3133/sir20175062.

ISSN 2328-0328 (online)

Preface

The Energy Independence and Security Act of 2007 authorized the U.S. Geological Survey (USGS) to conduct a national assessment of geologic storage resources for carbon dioxide (CO_2) and requested the USGS to estimate the "potential volumes of oil and gas recoverable by injection and sequestration of industrial carbon dioxide in potential sequestration formations" (42 U.S.C. 17271(b)(4)). Geologic CO_2 sequestration associated with enhanced oil recovery (EOR) using CO_2 in existing hydrocarbon reservoirs has the potential to increase the U.S. hydrocarbon recoverable resource. The objective of this report is to provide detailed information on three approaches that can be used to calculate the incremental recovery factors for CO_2-EOR. Therefore, the contents of this report could form an integral part of an assessment methodology that can be used to assess the sedimentary basins of the United States for the hydrocarbon recovery potential using CO_2-EOR methods in conventional oil reservoirs.

Acknowledgments

The authors would like to express their gratitude to Reid B. Grigg (Petroleum Recovery Research Center, New Mexico Tech, Socorro) and Donald J. Remson (National Energy Technology Laboratory, Pittsburgh, Pa.), who kindly agreed to review this manuscript and made constructive comments. The authors would also like to thank Jacqueline N. Roueche (Petroleum Engineer, Lynxnet LLC, contracted to the U.S. Geological Survey in Reston, Va.) for her review and valuable comments. Thanks are also due to James L. Coleman (U.S. Geological Survey), whose critique resulted in significant improvements to the report. Finally, the authors would like to thank members of the U.S. Geological Survey, especially Peter D. Warwick and Philip A. Freeman, for their continuous support and help in making improvements to this report and Elizabeth Good and Jeannette Foltz for assistance in preparing the report for release.

Contents

[Letters designate the chapters]

Conversion Factors

Multiply	By	To obtain
	Length	
foot (ft)	0.3048	meter (m)
	Area	
acre	4,047	square meter (m^2)
acre	0.4047	hectare (ha)
	Volume	
acre-foot (acre-ft)	1,233	cubic meter (m^3)
acre-foot (acre-ft)	7,758.4	barrel (bbl)
cubic foot (cf, ft^3)	0.02832	cubic meter (m^3)
standard cubic foot (SCF)	0.02832	standard cubic meter
thousands of cubic feet (mcf) of CO_2 per barrel of produced oil at the surface at standard conditions of 14.7 psi and 60 °F	0.3328	metric ton of CO_2 per cubic meter of produced oil at the surface at standard conditions of 14.7 psi (101.4 kilopascals) and 60 °F (15.6 °C)
barrel (bbl; petroleum, 1 barrel=42 gallons)	0.1590	cubic meter (m^3)
stock tank barrel (STB)	0.1590	cubic meter (m^3)
million barrels (MMbbl)	0.1590	million cubic meters (m^3)
cubic meter (m^3)	35.315	cubic foot (cf, ft^3)
cubic meter (m^3)	6.29	barrel (bbl; petroleum, 1 barrel=42 gallons)
	Density	
pound per cubic foot (lb/cf, lb/ft^3)	0.01602	gram per cubic centimeter (g/cm^3)
gram per cubic centimeter (g/cc, g/cm^3)	62.428	pound per cubic foot (lb/cf, lb/ft^3)
	Permeability	
millidarcy	9.869×10^{-16}	square meter (m^2)
	Pressure	
pound-force per square inch (psi, lbf/in^2)	6.895	kilopascal (kPa)
	Viscosity	
centipoise (cP)	1	millipascal second (mP·s)

Temperature in degrees Celsius (°C) may be converted to degrees Fahrenheit (°F) as follows:

$$°F = (1.8 \times °C) + 32.$$

Temperature in degrees Fahrenheit (°F) may be converted to degrees Celsius (°C) as follows:

$$°C = (°F - 32) / 1.8.$$

General Introduction and Recovery Factors

By Mahendra K. Verma

Chapter A of
Three Approaches for Estimating Recovery Factors in Carbon Dioxide Enhanced Oil Recovery
Mahendra K. Verma, Editor

Scientific Investigations Report 2017–5062–A

U.S. Department of the Interior
U.S. Geological Survey

U.S. Department of the Interior
RYAN K. ZINKE, Secretary

U.S. Geological Survey
William H. Werkheiser, Acting Director

U.S. Geological Survey, Reston, Virginia: 2017

Suggested citation:
Verma, M.K., 2017, General introduction and recovery factors, chap. A *of* Verma, M.K., ed., Three approaches for estimating recovery factors in carbon dioxide enhanced oil recovery: U.S. Geological Survey Scientific Investigations Report 2017–5062, p. A1–A3, https://doi.org/10.3133/sir20175062A.

ISSN 2328-0328 (online)

Contents

Chapter A. General Introduction and Recovery Factors

By Mahendra K. Verma[1]

Introduction

The U.S. Geological Survey (USGS) compared methods for estimating an incremental recovery factor for the carbon dioxide enhanced oil recovery (CO_2-EOR) process involving the injection of CO_2 into oil reservoirs. In order to show the significance of the recovery factor (*RF*), equation A1 relating the recoverable hydrocarbon volume with the *RF* and various reservoir parameters is given below. Although the reservoir parameters used in equation A1 are generally known, the *RF* for CO_2-EOR is unknown for individual oil reservoirs and needs to be established for estimating the recoverable hydrocarbon volume. This chapter first provides some basic information on the *RF,* including its dependence on various reservoir and operational parameters, and then discusses the three development phases of oil recovery—primary, secondary, and tertiary (EOR). It ends with a brief discussion of the three approaches for estimating recovery factors, which are detailed in subsequent chapters.

For calculating technically recoverable hydrocarbon volumes from a volumetric approach, it is necessary to have the values of all the reservoir parameters that make up the volumetric equation, as given below:

$$\text{recoverable } HC = RF\left[7758.4 \cdot \frac{A \times h \times \phi \times (1 - S_{wi})}{FVF_{oil}}\right] \qquad \text{(A1)}$$

where

HC	is the hydrocarbon volume, in stock tank barrels (STB);
RF	is the recovery factor;
7758.4	is the conversion factor from acre-foot (acre-ft) to barrel (bbl);
A	is the area, in acres;
h	is the formation average net thickness, in feet;
ϕ	is the porosity, expressed as a fraction;
S_{wi}	is the initial or connate water saturation, expressed as a fraction; and
FVF_{oil}	is the formation volume factor for oil, in reservoir barrel per stock tank barrel of oil (bbl/STB).

The values of all the parameters except for the *RF* are available from the comprehensive resource database (CRD) developed by INTEK Inc., a petroleum engineering consulting company under contract to the USGS (Carolus and others, in press). The data within the CRD are proprietary because they include field and reservoir properties from the "Significant Oil and Gas Fields of the United States Database" (NRG) from Nehring Associates Inc. (2012) and proprietary production and drilling data from IHS Inc. (2012). These proprietary data cannot be released directly to the public in this or other related reports.

The recovery factor for a reservoir is a function of lithology; porosity; rock permeability (including relative permeability of the fluids present in the reservoir); capillary size; rock wettability; oil properties such as oil gravity, viscosity, and percentage of medium to higher molecular weight components; and the reservoir driving mechanism in two types of oil reservoirs that are potentially suitable for CO_2-EOR: (1) undersaturated oil reservoirs with or without aquifer support and (2) saturated oil reservoirs with a gas cap with or without aquifer support. The recovery factor may also be affected to some extent by other factors, such as using advanced technologies for drilling horizontal wells and multilateral wells and using more effectively the interpretation of production logs as well as seismic surveys. Of course, good reservoir management plays an important role in improving the recovery factor as managers continuously monitor the reservoir performance and proactively take measures to remedy various adverse operational situations.

Of the three approaches that are included in this report, the decline curve analysis and review of papers and reports on reservoirs with CO_2-EOR do provide the *RF* information for a certain number of reservoirs but do not help establish a technically sound basis for estimating recoverable hydrocarbon volumes for a large number of reservoirs. The third approach, reservoir simulation, is a proven and reliable procedure to estimate the *RF* and hence help assess the technically recoverable hydrocarbon potential of all oil reservoirs that meet the screening criteria.

[1]U.S. Geological Survey.

Three Phases of Oil Recovery in Oil Fields

The history of an oil field may have three main developmental phases—primary, secondary, and tertiary recovery, also known as enhanced oil recovery (EOR)—all of which are intended to progressively improve the total recovery. Wells are drilled during the reservoir development phase, which is generally associated with the **primary production phase** when the reservoir is produced under its own energy that is manifested through the expansion of oil and rock with the decline in reservoir pressure. In **conventional reservoirs** (where oil is trapped due to the low permeability of an overlying formation), continued development calls for drilling more wells either as step-out wells or as in-fill wells to reduce the spacing among the existing wells. All these development wells accelerate the reservoir depletion rate, but the increase in the overall recovery factor depends on the permeability distribution and fluid properties of the individual reservoir. In **unconventional reservoirs** (where oil is trapped due to the ultralow permeability of the reservoir rock), additional wells are continually drilled to maximize the recoverable hydrocarbon volumes and thereby directly affect the recovery factor.

During the primary phase, oil production eventually declines to such a low level that the project becomes only marginally profitable, at which point, a **secondary recovery phase** is introduced. During this phase, either water is injected at the bottom of the reservoir structure or gas is injected at the top of the reservoir structure to raise the reservoir pressure, augmenting the reservoir energy for improved recovery. However, such injections are effective only if the reservoir has good horizontal and vertical permeability allowing gravity to keep the fluid segregated and resulting in higher displacement efficiency. In other places, where the geology is complex, the reservoir is produced with a waterflood on a line-drive or a normal or inverted five-spot, seven-spot, or nine-spot well pattern for better sweep efficiency and hence an improved recovery. During this phase, additional producers and injectors are drilled, and old wells are recompleted, worked over, or converted to either production or injection wells across the entire reservoir. In large reservoirs, the development is often carried out in phases.

At the end of the secondary phase, as the production begins to decline because of increasing water-cut or producing gas:oil ratio (GOR), the profitability once again becomes marginal. The decline in profitability may prompt the initiation of a **tertiary phase**, also called **enhanced oil recovery** (EOR). There are several EOR methods (chemical, thermal, and CO_2 injection) for improving the oil recovery, but for the purpose of this study, the focus is on the CO_2-EOR process. During the CO_2-EOR phase, more wells may be drilled and existing wells recompleted or worked over depending on the well pattern for optimum recovery. Under CO_2-EOR miscible conditions, theoretically oil recoveries could be as high as 90 percent of the oil in place in the CO_2-swept region (Taber and others, 1997), but they are generally lower because of reservoir complexity in terms of lithology, structure, fractures, capillary pressure, rock wettability, oil viscosity and gravity, and permeability contrast between various zones in the reservoir. Application of economic filters to the CO_2-EOR project further lowers the recovery factors.

Three Approaches for Determining the Recovery Factor

Due to the reliability and the ease of its use, reservoir simulation by CO_2 Prophet was considered the preferred approach by the USGS for determining recovery factors for the CO_2-EOR application in oil reservoirs within the United States. Two additional methods were considered valuable and were used to verify *RF* values obtained from the simulation—the widely used empirical decline curve analysis (DCA) for estimating recoverable hydrocarbon volumes, and a review of published papers and reports on the performance of active or previously active CO_2-EOR fields and reservoirs.

CO_2 Prophet.—The CO_2 Prophet model was developed for the U.S. Department of Energy by Texaco Inc. under contract DE–FC22–93BC14960 and was described by Dobitz and Prieditis (1994). Its application for reservoir simulation in this study is discussed in chapter B of this report.

Decline curve analysis.—Decline curve analysis is an empirical method and is used to estimate recoverable hydrocarbon volumes by analyzing the plots of the historical production rate against time or cumulative production from a reservoir. The *RF* is determined by dividing the recoverable hydrocarbon volume with CO_2-EOR method by the original-oil-in-place (OOIP) volume. This simple method for estimating the *RF* is discussed in chapter C of this report.

Literature review.—A review of the publicly available literature has identified 53 CO_2-EOR projects in the United States and 17 abroad. The available information on *RF* values from these 70 projects has been analyzed and is discussed in chapter D of this report.

Because the production data for the DCA are from either EOR pilot projects or portions of reservoirs, they pose a challenge for the estimation of oil-in-place values due to uncertainty in defining the area and (or) the layers within a reservoir affected by the EOR. Therefore, even with good values of ultimate production from DCA, there is a certain amount of uncertainty in the *RF*, which is a function of both the ultimate production and the oil-in-place values. The *RF* values from a review of published papers and reports come from reservoirs with profitable CO_2-EOR projects. Because of economic factors, they may be lower than *RF* values obtained by CO_2 Prophet for technically recoverable oil resources that are calculated as being producible by using current technology and industry practices without any economic constraint.

However, the *RF* values from DCA and from the review of published papers and reports will still help provide values of the *RF* range, which will be useful in preparing a probabilistic estimate of technically recoverable oil volumes.

With the advancement of computer technology in terms of its affordability and the versatility of available models, reservoir simulation has become an invaluable tool to evaluate reservoir performance and recovery factors. Because CO_2 Prophet models a simplified physical process occurring in the reservoir and does not capture the chemical processes that would be described by a sophisticated compositional model, it should not be expected to reflect all the subtleties of real-world petroleum operations. All three approaches will help to establish the range of recovery factors for various reservoir types and therefore are discussed in chapters B, C, and D.

References Cited

Carolus, Marshall, Biglarbigi, Khosrow, Warwick, P.D., Attanasi, E.D., Freeman, P.A., and Lohr, C.D., in press, Overview of a comprehensive resource database for the assessment of recoverable hydrocarbons produced by carbon dioxide enhanced oil recovery: U.S. Geological Survey Techniques and Methods, book 7, chap. C16.

Dobitz, J.K., and Prieditis, John, 1994, A steam tube model for the PC: SPE/DOE Ninth Symposium on Improved Oil Recovery, Tulsa, Oklahoma, 17–20 April 1994, paper SPE–27750–MS, 8 p.

IHS Inc., 2012, PIDM [Petroleum Information Data Model] relational U.S. well data [data current as of December 23, 2011]: Englewood, Colo., IHS Inc.

Nehring Associates Inc., 2012, Significant oil and gas fields of the United States database [data current as of December 2012]: Colorado Springs, Colo., Nehring Associates Inc.

Taber, J.J., Martin, F.D., and Seright, R.S., 1997, EOR screening criteria revisited—Part 1: Introduction to screening criteria and enhanced recovery field projects: SPE (Society of Petroleum Engineers) Reservoir Engineering, v. 12, no. 3 (August 1997), p. 189–198, paper SPE–35385–PA.

Using CO_2 Prophet to Estimate Recovery Factors for Carbon Dioxide Enhanced Oil Recovery

By Emil D. Attanasi

Chapter B of
Three Approaches for Estimating Recovery Factors in Carbon Dioxide Enhanced Oil Recovery
Mahendra K. Verma, Editor

Scientific Investigations Report 2017–5062–B

U.S. Department of the Interior
U.S. Geological Survey

U.S. Department of the Interior
RYAN K. ZINKE, Secretary

U.S. Geological Survey
William H. Werkheiser, Acting Director

U.S. Geological Survey, Reston, Virginia: 2017

Suggested citation:
Attanasi, E.D., 2017, Using CO_2 Prophet to estimate recovery factors for carbon dioxide enhanced oil recovery, chap. B *of* Verma, M.K., ed., Three approaches for estimating recovery factors in carbon dioxide enhanced oil recovery: U.S. Geological Survey Scientific Investigations Report 2017–5062, p. B1–B10, https://doi.org/10.3133/sir20175062B.

ISSN 2328-0328 (online)

Contents

Figures

Table

Chapter B. Using CO_2 Prophet to Estimate Recovery Factors for Carbon Dioxide Enhanced Oil Recovery

By Emil D. Attanasi[1]

Introduction

The Oil and Gas Journal's enhanced oil recovery (EOR) survey for 2014 (Koottungal, 2014) showed that gas injection is the most frequently applied method of EOR in the United States and that carbon dioxide (CO_2) is the most commonly used injection fluid for miscible operations. The CO_2-EOR process typically follows primary and secondary (waterflood) phases of oil reservoir development. The common objective of implementing a CO_2-EOR program is to produce oil that remains after the economic limit of waterflood recovery is reached. Under conditions of miscibility or multicontact miscibility, the injected CO_2 partitions between the gas and liquid CO_2 phases, swells the oil, and reduces the viscosity of the residual oil so that the lighter fractions of the oil vaporize and mix with the CO_2 gas phase (Teletzke and others, 2005). Miscibility occurs when the reservoir pressure is at least at the minimum miscibility pressure (MMP). The MMP depends, in turn, on oil composition, impurities of the CO_2 injection stream, and reservoir temperature. At pressures below the MMP, component partitioning, oil swelling, and viscosity reduction occur, but the efficiency is increasingly reduced as the pressure falls farther below the MMP.

CO_2-EOR processes are applied at the reservoir level, where a reservoir is defined as an underground formation containing an individual and separate pool of producible hydrocarbons that is confined by impermeable rock or water barriers and is characterized by a single natural pressure system. A field may consist of a single reservoir or multiple reservoirs that are not in communication but which may be associated with or related to a single structural or stratigraphic feature (U.S. Energy Information Administration [EIA], 2000).

The purpose of modeling the CO_2-EOR process is discussed along with the potential CO_2-EOR predictive models. The data demands of models and the scope of the assessments require tradeoffs between reservoir-specific data that can be assembled and simplifying assumptions that allow assignment of default values for some reservoir parameters. These issues are discussed in the context of the CO_2 Prophet EOR model, and their resolution is demonstrated with the computation of recovery-factor estimates for CO_2-EOR of 143 reservoirs in the Powder River Basin Province in southeastern Montana and northeastern Wyoming.

Modeling CO_2-EOR Production and Assessment of Recovery Potential

The technical performance of an EOR project is measured by the volume of incremental oil that can be produced beyond the oil that would have been produced through the waterflood stage of reservoir development. If the CO_2-EOR recovery factors are sufficiently high, producers will have an incentive to profitably recover the remaining oil after waterflood. From a national or regional prospective, the aggregate volume of oil that remains after waterflood is large,[2] and the percentage that can be commercially recovered is of interest to industry and government decisionmakers. Unlike undiscovered oil accumulations, the candidate reservoirs are already identified, and most have a documented production history. For assessments of potential EOR recovery at the national or regional levels, analysts might have to screen and evaluate thousands of reservoirs. Each reservoir, however, has some production history and possibly other data that may allow the analyst to estimate values of reservoir temperature, pressure, porosity, permeability, net pay, and oil in place. The parameter values assigned to each reservoir are assumed to represent average values for the reservoir. Ideally, the data available for each potential candidate reservoir are sufficient to determine, at the reconnaissance level, amenability to miscible CO_2-EOR (Taber and others, 1997) and to predict reservoir performance.

A numerical reservoir model is a tool to predict reservoir response, in terms of produced oil, natural gas, and CO_2, to the injection of CO_2 and water. In actual EOR project developments, the operator commonly has a sophisticated simulation model prepared that characterizes reservoir and fluid

[1]U.S. Geological Survey.

[2]If 600 billion barrels of original oil in place has been discovered in the United States and primary and waterflood phases of development have recovered only one-third of that, then about 400 billion barrels remain in discovered reservoirs as a target for enhanced oil recovery (Kuuskraa and others, 2013).

composition spatially at individual grid points. The model is used in the design of the EOR project and later for the daily operations and management of reservoir production. Such models are three-dimensional and provide an array of reservoir attributes at each grid point, which is identified with a physical location in the reservoir. Compositional reservoir models also show the changes in the chemical composition of reservoir fluids as injection and production progress. Data required to populate such models include a site-specific geochemical characterization of the crude oil, reservoir rocks, and reservoir parameters that is well beyond what is available from public and commercial data sources. During the last two decades of the 20th century, the Federal Government sponsored development of at least two public domain CO_2-EOR scoping models: CO_2 PM and CO_2 Prophet.

CO_2 PM is a pattern-level[3] analytical model developed by Paul and others (1984) for the National Petroleum Council's (NPC's) 1984 study to model miscible CO_2-EOR project recoveries for a set of candidate oil reservoirs. It was described by Ray and Munoz (1986), and its application to the NPC study was described by Robl and others (1986). CO_2 PM applies sweep efficiency correlations as a means of relating injected fluids to produced oil, natural gas, water, and CO_2.

CO_2 Prophet is another pattern-level reservoir model. It uses computational algorithms that represent later advances in modeling fluid recovery (Willhite, 1986). CO_2 Prophet predicts the reservoir responses by generating fluid flow streamlines between injection and production wells and models the physical displacement and recovery of oil along stream tubes formed when the streamlines are used as boundaries (Green and Willhite, 1998). This model was developed for the U.S. Department of Energy by Texaco Inc. under contract DE–FC22–93BC14960 and was described by Dobitz and Prieditis (1994). When this model is used for national or regional assessments, the predicted oil recovery factor for a pattern is applied to the entire reservoir. In the past, CO_2 Prophet has been applied to regional and national assessments for the U.S. Department of Energy by Advanced Resources International (ARI, 2006a, b, c, d) and by ARI and the U.S. Department of Energy, National Energy Technology Laboratory (Wallace and others, 2013). Industry applications of CO_2 Prophet include its use as a scoping tool to evaluate potential candidate reservoirs (Hsu and others, 1995).

Estimation of Recovery Factors for Miscible CO_2-EOR

CO_2-EOR process modeling provides predictions of the reservoir's production response to a pre-specified regime of CO_2 and water injection. For this analysis, the forecasts are computed on the basis of a single pattern of injector and producer wells that is assumed to be representative of the reservoir.[4] The CO_2-EOR recovery factor as defined here represents the fraction of the pattern's original oil in place (OOIP) that is recovered over the duration of the EOR project and is interpreted to represent technically recoverable[5] oil because no economic screen or cutoff is applied.

A CO_2-EOR process will be miscible if the reservoir pressure is maintained at least as high as the MMP of the oil. The MMP depends on the composition of the oil and reservoir temperature (Mungan, 1981). The formation fracture pressure, which is calculated by using an appropriate pressure gradient and depth, must also be greater than the MMP to assure that miscibility can actually be attained. In the implementation of an actual CO_2-EOR program, the reservoir pressure is commonly increased to the MMP by shutting in producing wells and continuing to inject water after the waterflood program has been discontinued.

Initial Reservoir Conditions and Injection Regime

The application of CO_2 Prophet to the suite of carbonate and clastic reservoirs that are suitable candidates for miscible CO_2-EOR requires a number of simplifying assumptions. The computational program requires the entry of data that represent the nature of the reservoir and associated fluids at the start of the CO_2-EOR process. The simplifying assumptions are the major determinants for the values of these data. An assumed parameter used as the initial oil saturation at the start of the CO_2-EOR evaluation is the residual oil saturation to water (oil saturation after the waterflood). For the clastic reservoirs, this value is assumed to be 0.25, and for carbonate reservoirs, the value is assumed to be 0.305. These values are based on past high-level reconnaissance-type CO_2-EOR oil recovery assessments such as the 1984 NPC study (Robl and others, 1986) and subsequent industry and government adjustments (Donald J. Remson, National Energy Technology Laboratory, written commun., 2015).

The water and CO_2 injection rates and the injection regime also reflect initial conditions. These rates were set so that the reservoir pressure remains at or above the MMP but below fracture pressure less a safety margin of 400 pounds-force per square inch (psi),[6] and the analyst assumed a five-spot injector/producer pattern and pattern area (Lyons, 1996). Holtz (2014) reported that after initial CO_2 injection, water and CO_2 injectivity may increase, decline, or remain the same. However, changes in injectivity are specific to individual reservoirs and even individual patterns and cannot

[3]A pattern is a configuration of injector and production wells.

[4]In commercial applications of CO_2 Prophet where pattern-specific data are available, individual patterns across a reservoir can be modeled and then pattern results can be aggregated to arrive at an average recovery factor.

[5]Technically recoverable resources are the resources in accumulations producible by using current recovery technology and industry practices but without reference to economic profitability.

[6]This safety margin of 400 psi is somewhat arbitrary, and there are reservoirs where it may be desirable to have a greater margin.

be accurately predicted. Holtz (2014) and Wallace and others (2013) discussed a number of treatments that are commercially available to remediate the injectivity losses. Consequently, for the calculation of the technically recoverable oil from miscible CO_2-EOR, it is assumed that any decline in injectivity is remediated.

The total volume of CO_2 injected during the EOR project model runs amounts to 100 percent of the hydrocarbon pore volume (HCPV). The assumed injection regime is accomplished in three phases. In phase 1, the volume of injected CO_2 is equivalent to 25 percent of the current HCPV; in phase 2, the volume of injected CO_2 is equivalent to 35 percent of the HCPV; and in phase 3, the volume of injected CO_2 is equivalent to 40 percent of the HCPV. To achieve a tapered water-alternating-with-gas (WAG) injection, for each phase, a different water:gas ratio is specified. Phase 1 has a 1:3 WAG ratio, phase 2 has a 1:2 WAG ratio, and phase 3 has a 1:1.5 WAG ratio. As the WAG is tapered, water is injected in greater cumulative amounts in each phase relative to the injected CO_2 over time.

Reservoir Heterogeneity and Other Default Reservoir Conditions

The model's calculations also require a value for the Dykstra-Parsons coefficient of permeability variation to characterize reservoir heterogeneity. Producers use measured permeability values from well logs or core samples to calculate the Dykstra-Parsons coefficient. Homogeneous reservoirs have permeability variations near 0, and at the extreme, heterogeneous reservoirs have permeability variations near 1. When permeability variation measurements are available for individual patterns, the Dykstra-Parsons coefficient value may be assigned to individual patterns across the reservoir. However, for reconnaissance-type regional or national studies that must evaluate thousands of reservoirs, reservoir-specific values of the Dykstra-Parsons coefficients based on the actual permeability measures are simply not publicly available.

An alternative approach is to use a constructed coefficient, correlated with actual reservoir heterogeneity, to represent the average value of the Dykstra-Parsons coefficient for the reservoir. Hirasaki and others (1984) developed an algorithm for application in the 1984 NPC EOR study to calculate a pseudo-Dykstra-Parsons coefficient derived from the calculated waterflood sweep efficiency and mobility ratio (between water and oil) for each candidate reservoir. The relations among pseudo-Dykstra-Parsons values, sweep efficiency, and mobility ratios were presented in graphical form by Willhite (1986) and Hirasaki and others (1984). The graphs were digitized so that for any given mobility ratio and sweep efficiency, the pseudo-Dykstra-Parsons coefficient could be numerically computed.

Hirasaki and others (1984, 1989) suggested some adjustments in the values of the pseudo-Dykstra-Parsons coefficient calculated from their sweep efficiency formula to more closely align values with the Dykstra-Parsons coefficient based on measurements of permeability variability. If the calculated coefficient value was positive but less than 0.5, it was set to 0.5. When the coefficient value exceeded 0.98, it was set to a default value of 0.72, and calculated coefficient values that were between 0.72 and 0.98 were left unchanged (Hirasaki and others, 1989). According to J.K. Dobitz (Windy Cove Energy, written commun., 2015), an author of CO_2 Prophet, the program uses a maximum of 10 layers to describe variations in permeability, and that maximum limits the maximum distinguishable value of the pseudo-Dykstra-Parsons coefficient to 0.86. So if the pseudo-Dykstra-Parsons coefficient given by the method of Hirasaki and others (1984) is greater than 0.86, then it is reset to 0.86.

Other assumptions about the initial conditions follow. The connate water or irreducible water saturation values were assumed to be 0.2 for all reservoirs. On the basis of data presented by Lange (1998), a value of 0.08 was selected in this study for all reservoirs suitable for miscible CO_2-EOR to represent the residual oil saturation following multiple passes (contacts) of the CO_2 solvent. The specific gravity for casing-head gas, with respect to air (where the specific gravity of air equals 1.0), was assumed to be 0.7. The values of the endpoints of the relative permeability functions were based on default values for mildly water-wet reservoirs suggested by Michael Stein (BP, retired, written commun., 2014).[7]

Recovery-Factor Determinants

CO_2 Prophet models the physical process occurring in the reservoir when water and CO_2 are injected. It is a simplification of the actual physical processes and does not capture the chemical processes that would be described by a sophisticated compositional model. Nor does the modeling capture the unanticipated operational factors such as fractures or thief zones that affect the actual recovery factors. A number of numerical experiments were carried out with the same reservoir model in order to understand the primary determinants of the EOR recovery factor as computed by the CO_2 Prophet model. The experiments showed that the principal determinants of the recovery factors were the residual oil saturation at the start of the CO_2-EOR program and the measure of reservoir heterogeneity; to a much smaller extent, the injected volume of CO_2 beyond 100 percent of the HCPV, the water:CO_2 gas ratio, and the oil viscosity[8] affect the recovery factors.

[7]In particular, the following parameters are specified: the endpoint relative permeability of oil at connate water saturation is 1, the endpoint relative permeability of water at residual oil saturation is 0.3, the endpoint relative permeability of CO_2 at connate water saturation is 0.4, the endpoint relative permeability of gas-to-connate-water saturation is 0.4, and the exponents on the relative permeability equations are 2.0.

[8]The maximum viscosity allowed for miscible CO_2-EOR is 10 centipoises. Measuring the effect of the oil viscosity is somewhat more complicated. A change in oil viscosity that changes the API gravity of the oil will change the MMP, which will also affect the required reservoir operating pressure and injection rates.

The reservoir heterogeneity, represented by the Dykstra-Parsons coefficient, is used directly by the model to create permeability layers that exhibit the inferred permeability variability and resistance to fluid flow. Figure B1 shows the recovery factor as a surface function of the residual oil saturation, which ranges from 0.13 to 0.33, and the Dykstra-Parsons coefficient, which ranges from 0.50 to 0.85. For figure B1, the volume of injected CO_2 is 100 percent of the HCPV.

Figure B2 shows the effects of increasing the injected volume of CO_2 to 150 percent of the HCPV. The curve labeled 100 percent of HCPV can be visualized as a slice of the recovery-factor model in figure B1 for a reservoir where the assumed residual oil saturation to water is 0.305, which is characteristic of carbonate reservoirs that are candidates for miscible CO_2-EOR. The absolute value of the improvement in the recovery factor ranges from 2.5 to 3.5 percent, and the incremental increases in the recovery factor decline as the residual oil saturation declines.

Along with the recovery-factor estimates, the reservoir simulation provides the volumes of injected CO_2 and produced CO_2 and oil. The net utilization of CO_2 over the life of the EOR program is the arithmetic difference between the volume of injected and produced CO_2 divided by the volume of oil produced. The injected minus the recovered CO_2 is the amount of CO_2 lost during the recovery process. The net utilization of CO_2 over the life of the project can be used to estimate the amount of CO_2 that will naturally be retained in the reservoir when the CO_2-EOR program is completed. Figure B3 shows how the net utilization varies with the residual oil saturation and the Dykstra-Parsons coefficient. For the set of data points generated to the recovery-factor surface shown in figure B1, the correlation coefficient between recovery factor and net utilization was calculated to capture the strength and direction of the relationship. The calculated correlation coefficient is –0.86. This correlation coefficient suggests for an individual reservoir that the greater the recovery factor, the lower the net utilization will be. The estimate of the retained CO_2 is obtained by taking the product of the oil produced and the net utilization factor; the estimate is based on the assumption that the operator will not try to capture and re-sell CO_2 remaining in the reservoir.

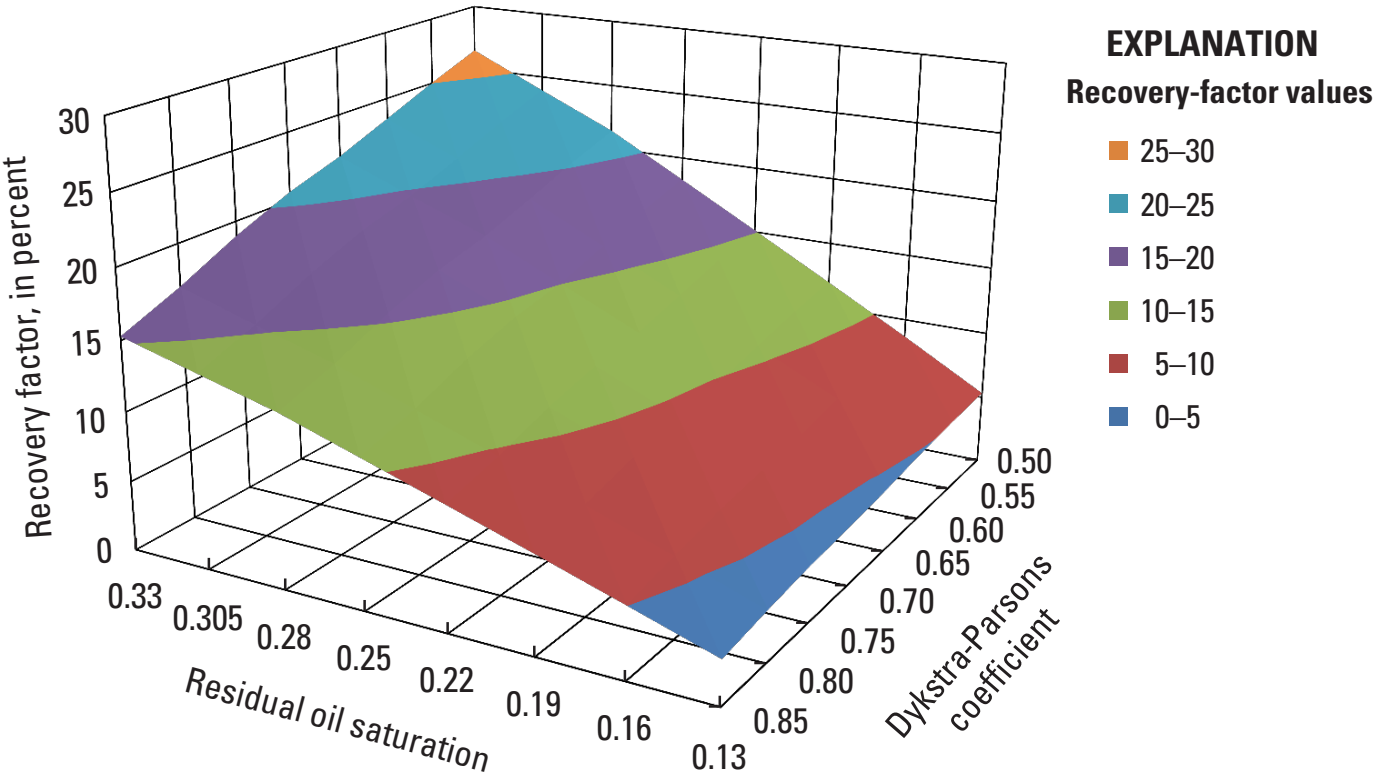

Figure B1. Three-dimensional graph showing estimated recovery factors during miscible carbon dioxide (CO_2) enhanced oil recovery (EOR), in percentage of the original oil in place, shown as a function of reservoir heterogeneity as represented by the Dykstra-Parsons coefficient and the residual oil saturation to water at the start of the EOR program. The residual oil saturation of 0.305 is assumed to be characteristic of carbonate reservoirs that are candidates for miscible CO_2-EOR. The CO_2 Prophet model was used to compute recovery factors for a representative reservoir.

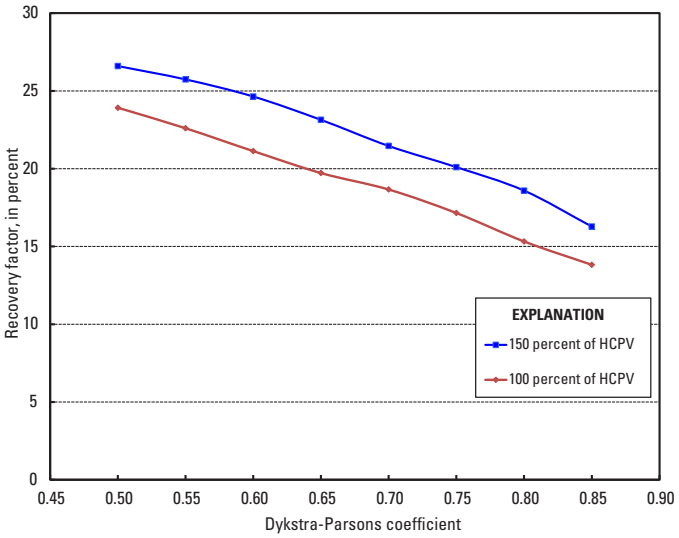

Figure B2. Two-dimensional graph showing estimated recovery factors during miscible carbon dioxide (CO_2) enhanced oil recovery (EOR), in percentage of the original oil in place, shown as a function of reservoir heterogeneity when the residual oil saturation at the start of the EOR program is 0.305. The red line represents a slice of figure B1, at 0.305 residual oil saturation. Figure B1 is based on a volume of CO_2 equivalent to 100 percent of the hydrocarbon pore volume (HCPV). The CO_2 Prophet model was used to compute recovery factors for a representative reservoir.

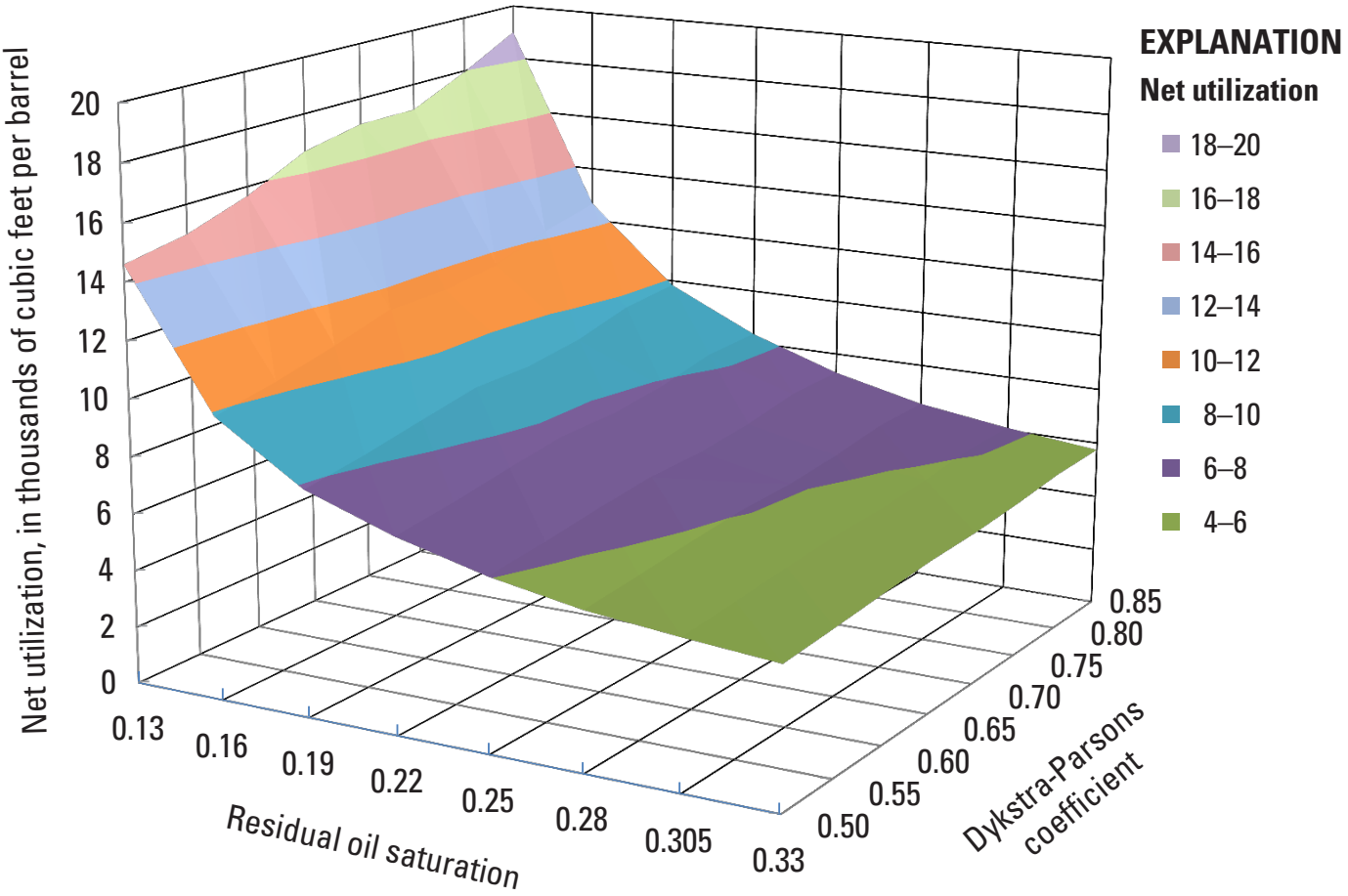

Figure B3. Three-dimensional graph showing estimated net carbon dioxide (CO_2) utilization factors during miscible CO_2 enhanced oil recovery (EOR), in thousands of cubic feet per barrel (both measured at standard surface conditions), shown as a function of reservoir heterogeneity as represented by the Dykstra-Parsons coefficient and the residual oil saturation at the start of the EOR program. The CO_2 Prophet model was used to compute net CO_2 utilization factors for a representative reservoir.

Recovery-Factor Estimates for Reservoirs in the Powder River Basin Province

Selection of Reservoirs for Recovery-Factor Calculations

Several criteria were imposed on the reservoirs selected from the candidates that were considered for miscible CO_2-EOR and that conformed to the requirements set out by Taber and others (1997). Reservoirs that had recovery factors evaluated by using the CO_2 Prophet model had an average permeability of at least 2 millidarcies, a net pay thickness of at least 5 feet, and an estimate of OOIP of at least 5 million barrels. Recovery factors for selected reservoirs in the conterminous United States were presented by Attanasi and Freeman (2016). As a related report from the same study, this chapter uses the Powder River Basin Province, which includes reservoirs in Wyoming and Montana, as an example and provides additional data; recovery factors were estimated for 143 clastic reservoirs in this province.

Distributions of Recovery Factors and Net Utilization Factors

The play and province classification scheme followed here corresponds to the definitions used in the 1995 USGS National Oil and Gas Assessment (NOGA; Gautier and others, 1996). The play names and codes are identified in table B1. There were no miscible carbonate reservoirs identified in the Powder River Basin Province, so the recovery factors are representative of clastic reservoirs. Distributions of the recovery factors and net utilization factors for 143 reservoirs in the 7 conventional plays evaluated for the Powder River Basin are shown in figures B4 and B5, respectively. Boxplots display the distribution of values where the interquartile range is shown between the 25th percentile (bottom of box) and the 75th percentile (top of box). The median value is the thick line, and the minimum and maximum values are shown by the vertical lines outside the box. Table B1 provides characteristics of each play distribution.

For each of the reservoirs evaluated, the residual oil saturation at the initiation of CO_2-EOR recovery was assigned a value of 0.25 because the candidates were classified as clastic reservoirs. Each reservoir was assumed to have 100 percent of the HCPV injected with CO_2 over the duration of the EOR recovery program. The range of calculated recovery factors therefore reflects variations in reservoir heterogeneity as measured by the pseudo-Dykstra-Parsons coefficient, oil viscosity, and other variables that may affect recovery. The play-level recovery-factor distributions, as shown by each boxplot in figure B4, are generally right skewed. A right-skewed distribution is not symmetric and is indicated by the boxplots when the vertical distances between the minimum and first quartile to the median value are much shorter than the vertical distances from the median to the third quartile and maximum value. Across plays, median recovery factors (represented by the heavy line inside the box) range from 9.50 to 13.43 percent of the OOIP (table B1). These values are well within the published records (Christensen and others, 2001) when adjustments are made to the data to account for the percentage of the HCPV injected with CO_2.

Figure B5 shows the play distributions of the net CO_2 utilization factors, represented as boxplots. The net utilization factor indicates the rate at which CO_2 is retained per barrel of oil produced over the entire CO_2-EOR program. On an annual basis, the modeling results show that the net utilization is generally highest during the initial years of EOR production. Higher utilization is consistent with a greater percentage of the injected CO_2 being retained in the reservoir. The retention factor is simply the percentage of injected CO_2 that is retained in the reservoir. Table B1 shows the relevant retention statistics for each evaluated play of the Power River Basin Province. These median play values are consistent with the empirical findings of Olea (2015).

Table B1. Estimated recovery factors, net carbon dioxide utilization factors, and carbon dioxide retention factors during miscible carbon dioxide enhanced oil recovery (CO_2-EOR) for 143 clastic reservoirs in 7 plays in the Powder River Basin Province.

[Play codes and names are from 1995 U.S. Geological Survey National Oil and Gas Assessment (NOGA; Gautier and others, 1996). The recovery factors and median net CO_2 utilization factors from this study were also published in Attanasi and Freeman (2016, table 7). Estimates of recovery factors, net CO_2 utilization factors, and CO_2 retention factors were calculated by the CO_2 Prophet model. Net CO_2 utilization factors are in thousands of cubic feet of CO_2 per barrel of produced oil at standard surface conditions]

Play code	Play name	Number of oil reservoirs eligible for CO_2-EOR	Distribution of data					
			Minimum	Maximum	1st quartile	Median	Mean	3d quartile
			Recovery factor, in percent					
3302	Basin Margin Anticline	21	8.43	17.33	9.25	9.50	9.99	9.83
3304	Upper Minnelusa Sandstone	45	8.90	18.44	9.23	9.65	11.10	11.86
3306	Fall River Sandstone	14	9.16	18.42	9.64	9.79	11.61	12.74
3307	Muddy Sandstone	27	8.37	17.83	9.54	9.91	10.59	10.24
3309	Deep Frontier Sandstone	11	9.74	14.15	10.02	13.43	12.07	13.92
3312	Sussex-Shannon Sandstone	9	9.61	14.29	9.96	10.05	10.63	10.11
3313	Mesaverde-Lewis	16	9.45	13.75	9.61	9.85	10.79	11.46
			Net CO_2 utilization factor, in thousands of cubic feet per barrel of oil produced					
3302	Basin Margin Anticline	21	4.79	6.96	5.09	5.31	5.50	5.89
3304	Upper Minnelusa Sandstone	45	4.29	6.85	5.39	5.73	5.78	6.32
3306	Fall River Sandstone	14	4.98	7.47	5.96	6.44	6.27	6.58
3307	Muddy Sandstone	27	5.13	7.89	6.01	6.48	6.52	7.20
3309	Deep Frontier Sandstone	11	5.13	6.99	5.98	6.27	6.31	6.80
3312	Sussex-Shannon Sandstone	9	6.33	8.34	6.83	7.13	7.13	7.33
3313	Mesaverde-Lewis	16	5.63	6.77	5.89	6.34	6.26	6.53
			CO_2 retention factor, in percent					
3302	Basin Margin Anticline	21	21.42	33.85	22.25	22.63	23.53	23.03
3304	Upper Minnelusa Sandstone	45	21.93	36.55	22.97	24.40	26.24	28.17
3306	Fall River Sandstone	14	21.81	35.03	22.14	22.86	25.38	27.43
3307	Muddy Sandstone	27	21.60	36.59	22.42	23.06	24.32	23.92
3309	Deep Frontier Sandstone	11	24.47	31.99	24.83	30.44	28.22	31.06
3312	Sussex-Shannon Sandstone	9	22.91	30.61	23.66	23.80	24.71	23.90
3313	Mesaverde-Lewis	16	22.62	30.60	23.36	23.41	25.07	25.85

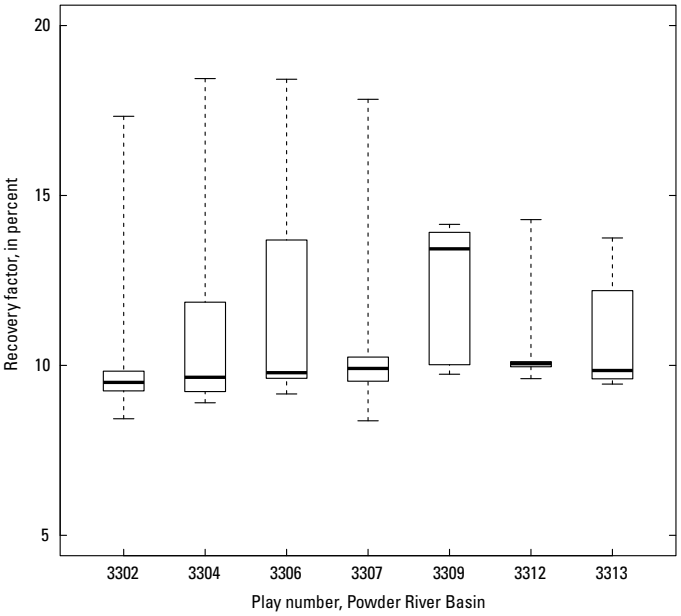

Figure B4. Boxplots showing distributions of the estimated recovery factors for clastic reservoirs by play in the Powder River Basin Province during miscible carbon dioxide enhanced oil recovery. The CO_2 Prophet model was used to compute recovery factors. Play codes and names are provided in table B1. Box extremities represent the first and third quartiles, and extreme values of the linear members are the minimum and maximum values. The darkened horizontal line inside each box is the median value.

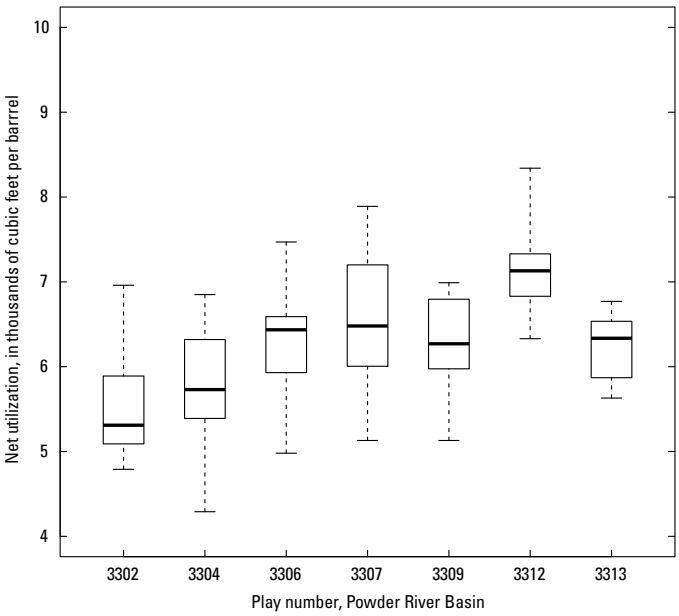

Figure B5. Boxplots showing distributions of the estimated net carbon dioxide (CO_2) utilization factors for clastic reservoirs by play in the Powder River Basin Province during miscible CO_2 enhanced oil recovery. The CO_2 Prophet model was used to compute the net CO_2 utilization factors, which are in thousands of cubic feet of CO_2 per barrel of produced oil (both measured at standard surface conditions). Play codes and names are provided in table B1. Box extremities represent the first and third quartiles, and extreme values of the linear members are the minimum and maximum values. The darkened horizontal line inside each box is the median value.

Summary and Conclusions

This chapter has demonstrated a scheme for calculating reservoir-level estimates of miscible CO_2-EOR recovery factors for application to assessments of potentially recoverable oil from EOR for entire petroleum provinces and regions. The scheme uses the CO_2 Prophet model. The scope of the regional or national assessments may require the evaluation of thousands of candidate reservoirs. Although numerical reservoir modeling requires specific data for individual reservoirs, the modeler will need to formulate a set of reasonable assumptions to provide default parameter values. This modeling approach allows one to clearly identify the oil production attributable to CO_2-EOR. For the modeling presented here, the residual oil saturation to water (that is, the oil that remains at the completion of a waterflood program), was the starting point for evaluation of potential CO_2-EOR production. All models are simplifications of the actual processes and should therefore not be expected to reflect all the subtleties of real-world petroleum operations.

CO_2 Prophet (Dobitz and Prieditis, 1994) was applied to calculate the technically recoverable oil to provide an estimate of the miscible CO_2-EOR recovery factor. The estimated recovery factors were highly sensitive to the reservoir heterogeneity and the assumed values for residual oil saturation to water. Other variables that affect recovery factors to varying degrees are the percentage of HCPV injected with CO_2 and the viscosity of the oil.

An advantage of applying rudimentary reservoir models, such as CO_2 Prophet, for calculating miscible CO_2-EOR recovery factors is that the oil attributed to the EOR program can be clearly delineated from oil produced under secondary recovery. Furthermore, the model provides a production profile for the oil as a function of the injected fluids. This profile allows the analyst to quantify the effects of alternative injection regimes on recovery factors. CO_2 Prophet, by predicting production, also allows the analyst to estimate the commercially recoverable oil from EOR. Estimates of net utilization and CO_2 retention are byproducts of the model's results. A significant challenge to using reservoir models in high-level assessments is the requirement for reservoir-level data.

References Cited

Advanced Resources International (ARI), 2006a, Basin oriented strategies for CO_2 enhanced oil recovery; Illinois and Michigan Basins [of Illinois, Indiana, Kentucky, and Michigan]: Prepared for U.S. Department of Energy, Office of Fossil Energy–Office of Oil and Natural Gas, variously paged [104 p.], accessed July 15, 2015, at http://www.adv-res.com/pdf/Basin%20Oriented%20Strategies%20-%20Illinois_Michigan_Basin.pdf.

Advanced Resources International (ARI), 2006b, Basin oriented strategies for CO_2 enhanced oil recovery; Permian Basin: Prepared for U.S. Department of Energy, Office of Fossil Energy–Office of Oil and Natural Gas, variously paged [117 p.], accessed September 17, 2014, at http://www.adv-res.com/pdf/Basin%20Oriented%20Strategies%20-%20Permian_Basin.pdf.

Advanced Resources International (ARI), 2006c, Basin oriented strategies for CO_2 enhanced oil recovery; Rocky Mountain region [of Colorado, Utah, and Wyoming]: Prepared for U.S. Department of Energy, Office of Fossil Energy–Office of Oil and Natural Gas, variously paged [98 p.], accessed September 17, 2014, at http://www.adv-res.com/pdf/Basin%20Oriented%20Strategies%20-%20Rocky_Mountain_Basin.pdf.

Advanced Resources International (ARI), 2006d, Basin oriented strategies for CO_2 enhanced oil recovery; Williston Basin [of South Dakota, North Dakota, and Montana]: Prepared for U.S. Department of Energy, Office of Fossil Energy–Office of Oil and Natural Gas, variously paged [96 p.], accessed July 13, 2015, at http://www.adv-res.com/pdf/Basin%20Oriented%20Strategies%20-%20Williston_Basin.pdf.

Attanasi, E.D., and Freeman, P.A., 2016, Play-level distributions of estimates of recovery factors for a miscible carbon dioxide enhanced oil recovery method used in oil reservoirs in the conterminous United States: U.S. Geological Survey Open-File Report 2015–1239, 36 p., accessed October 4, 2016, at http://dx.doi.org/10.3133/ofr20151239.

Christensen, J.R., Stenby, E.H., and Skauge, A., 2001, Review of WAG field experience: SPE Reservoir Evaluation and Engineering, v. 4, no. 2, p. 97–106, paper SPE–71203–PA.

Dobitz, J.K., and Prieditis, John, 1994, A steam tube model for the PC: SPE/DOE Ninth Symposium on Improved Oil Recovery, Tulsa, Oklahoma, 17–20 April 1994, paper SPE–27750–MS, 8 p.

Gautier, D.L., Dolton, G.L., Takahashi, K.I., and Varnes, K.L., eds., 1996, 1995 national assessment of United States oil and gas resources; Results, methodology, and supporting data (release 2): U.S. Geological Survey Digital Data Series DDS–30, 1 CD-ROM.

Green, D.W., and Willhite, G.P., 1998, Enhanced oil recovery: Society of Petroleum Engineers Textbook Series, v. 6, 545 p.

Hirasaki, G.J., Morra, Frank, and Willhite, G.P., 1984, Estimation of reservoir heterogeneity from waterflood performance: Society of Petroleum Engineers, SPE–13415–MS, 10 p.

Hirasaki, G., Stewart, W.C., Elkins, L.E., and Willhite, G.P., 1989, Reply to discussion of the 1984 National Petroleum Council studies on EOR: Journal of Petroleum Technology, v. 41, no. 11, p. 1218–1222.

Holtz, M.H., 2014, Insights and managing CO_2 WAG injectivity: 8th Annual CO_2 Conference, University of Wyoming, Casper, Wyoming, July 8–10, 2014, presentation, 42 p., accessed August 17, 2015, at http://www.uwyo.edu/eori/_files/co2conference14/holtz.pdf.

Hsu, C.-F., Koinis, R.L., and Fox, C.E., 1995, Technology, experience speed CO_2 flood design: Oil and Gas Journal, v. 93, no. 43, p. 51–59.

Koottungal, Leena, ed., 2014, 2014 worldwide EOR survey: Oil and Gas Journal, v. 112, no. 4 (April 7, 2014), p. 78–97. [Also available at http://www.ogj.com/articles/print/volume-112/issue-4/special-report-eor-heavy-oil-survey/2014-worldwide-eor-survey.html].

Kuuskraa, V.A., Godec, M.L., and Dipietro, Phil, 2013, CO_2 utilization from "next generation" CO_2 enhanced oil recovery technology: Energy Procedia, v. 37, p. 6854–6866.

Lange, E.A., 1998, Correlation and prediction of residual oil saturation for gas-injection EOR processes: SPE Reservoir Evaluation and Engineering, v. 1, no. 2, p. 127–133, paper SPE–35425–PA.

Lyons, W.C., ed., 1996, Standard handbook of petroleum and natural gas engineering, volume 2: Houston, Texas, Gulf Publishing Company, 1,090 p.

Mungan, Necmettin, 1981, Carbon dioxide flooding; Fundamentals: Journal of Canadian Petroleum Technology, v. 20, no. 1 (January–March), p. 87–92.

National Petroleum Council (NPC), 1984, Enhanced oil recovery: Washington, D.C., National Petroleum Council, variously paged [285 p.]. [Also available at http://www.npc.org/reports/rby.html.]

Olea, R.A., 2015, CO_2 retention values in enhanced oil recovery: Journal of Petroleum Science and Engineering, v. 129 (May 2015), p. 23–28. [Also available at http://dx.doi.org/10.1016/j.petrol.2015.03.012.]

Paul, G.W., Lake, L.W., and Gould, T.L., 1984, A simplified predictive model for CO_2 miscible flooding: SPE (Society of Petroleum Engineers), Annual Technical Conference and Exhibition, 59th, Houston, Texas, September 16–19, 1984, paper SPE–13238–MS, 12 p.

Ray, R.M., and Munoz, J.D., 1986, Supporting technology for enhanced oil recovery—CO_2 miscible flood predictive model: U.S. Department of Energy [technical report] DOE/BC–86/12/SP, variously paged.

Robl, F.W., Emanuel, A.S., and Van Meter, O.E., Jr., 1986, The 1984 National Petroleum Council estimate of potential EOR for miscible processes: Journal of Petroleum Technology, v. 38, no. 8 (August), p. 875–882.

Taber, J.J., Martin, F.D., and Seright, R.S., 1997, EOR screening criteria revisited—Part 1, Introduction to screening criteria and enhanced recovery field projects: SPE Reservoir Engineering, v. 12, no. 3, p. 189–198, paper SPE–35385–PA.

Teletzke, G.F., Patel, P.D., and Chen, Amy, 2005, Methodology for miscible gas injection for EOR screening: SPE International Improved Oil Recovery Conference in Asia Pacific, Kuala Lumpur, Malaysia, 5–6 December 2005, paper SPE–97650–MS, 11 p.

U.S. Energy Information Administration (EIA), 2000, U.S. crude oil, natural gas, and natural gas liquids reserves; 1999 annual report: U.S. Energy Information Administration [Report] DOE/EIA–0216(99), 156 p. [Also available at http://www.eia.gov/pub/oil_gas/natural_gas/data_publications/crude_oil_natural_gas_reserves/historical/1999/pdf/arr.pdf.]

Wallace, Matthew, Kuuskraa, V.A., and Dipietro, Phil, 2013, An in-depth look at "next generation" CO_2-EOR technology: U.S. Department of Energy, National Energy Technology Laboratory (NETL) presentation, 207 p., accessed February 2, 2015, at http://www.netl.doe.gov/File%20Library/Research/Energy%20Analysis/Publications/Disag-Next-Gen-CO2-EOR_full_v6.pdf. [Prepared collaboratively by staff from Advanced Resources International and NETL under contract DE–FE0004001.]

Willhite, G.P., 1986, Waterflooding: Society of Petroleum Engineers Textbook Series, v. 3, 326 p.

Application of Decline Curve Analysis To Estimate Recovery Factors for Carbon Dioxide Enhanced Oil Recovery

By Hossein Jahediesfanjani

Chapter C of
Three Approaches for Estimating Recovery Factors in Carbon Dioxide Enhanced Oil Recovery
Mahendra K. Verma, Editor

Scientific Investigations Report 2017–5062–C

U.S. Department of the Interior
U.S. Geological Survey

U.S. Department of the Interior
RYAN K. ZINKE, Secretary

U.S. Geological Survey
William H. Werkheiser, Acting Director

U.S. Geological Survey, Reston, Virginia: 2017

Suggested citation:
Jahediesfanjani, Hossein, 2017, Application of decline curve analysis to estimate recovery factors for carbon dioxide enhanced oil recovery, chap. C *of* Verma, M.K., ed., Three approaches for estimating recovery factors in carbon dioxide enhanced oil recovery: U.S. Geological Survey Scientific Investigations Report 2017–5062, p. C1–C20, https://doi.org/10.3133/sir20175062C.

ISSN 2328-0328 (online)

Contents

Figures

Tables

Chapter C. Application of Decline Curve Analysis To Estimate Recovery Factors for Carbon Dioxide Enhanced Oil Recovery

By Hossein Jahediesfanjani[1]

Background

In the decline curve analysis (DCA) method of estimating recoverable hydrocarbon volumes, the analyst uses historical production data from a well, lease, group of wells (or pattern), or reservoir and plots production rates against time or cumulative production for the analysis. The DCA of an individual well is founded on the same basis as the fluid-flow principles that are used for pressure-transient analysis of a single well in a reservoir domain (Fetkovich, 1987; Fetkovich and others, 1987) and therefore can provide scientifically reasonable and accurate results. However, when used for a group of wells, a lease, or a reservoir, the DCA becomes more of an empirical method. Plots from the DCA reflect the reservoir response to the oil withdrawal (or production) under the prevailing operating and reservoir conditions, and they continue to be good tools for estimating recoverable hydrocarbon volumes and future production rates. For predicting the total recoverable hydrocarbon volume, the DCA results can help the analyst to evaluate the reservoir performance under any of the three phases of reservoir productive life—primary, secondary (waterflood), or tertiary (enhanced oil recovery) phases—so long as the historical production data are sufficient to establish decline trends at the end of the three phases.

Basis for Decline Curve Analysis

The DCA method is used to predict the future oil production rate of an oil-producing well or reservoir. Theoretically, according to this method, the oil production rate for a given entity will first reach its maximum output and then decline according to the following generalized relationship (Fetkovich, 1987):

$$\frac{q}{q_i} = (1 + bD_i t)^{-\frac{1}{b}} \tag{C1}$$

where

q is the time-dependent oil production rate, in barrels per day (bbl/day);

q_i is the initial oil production rate, in barrels per day;

D_i is the initial decline rate per year;

b represents the degree of curvature of the shape of the decline trend, which is dimensionless; and

t is the oil production time, in years.

Theoretically, the parameters, such as q_i, D_i, and b, have defined meanings only if equation C1 is applied for a single well that produces from a single reservoir under appropriate fluid-flow conditions. However, if equation C1 is applied to larger entities such as a number of wells, a reservoir, or a field, these parameters are only empirical and are obtained by a curve-fitting process. Practically, this equation represents three different types of declines depending on the value of b; namely, an exponential decline for $b = 0$, a hyperbolic decline for $b > 0$ and $b < 1$, and a harmonic decline for $b = 1$. On the basis of the explanations above and for the sake of simplicity, in many of the industrial applications of evaluating reservoir oil production decline, the value of b is often assumed to be zero, and, hence, equation C1 takes the form:

$$q = q_i \exp(-D_i t) \tag{C2}$$

[1]Lynxnet LLC, under contract to the U.S. Geological Survey.

Equation C2 is rewritten in terms of cumulative oil production in the following form:

$$Q = \frac{(q_i - q)}{D_i} \tag{C3}$$

where

Q is the cumulative oil production, in barrels.

These two equations, C2 and C3, were used for the analysis of oil production decline in this current study to determine the values of constants "D_i" and "q_i" in the above equations. For this purpose, these equations can be written as:

$$\ln(q) = \ln(q_i) - D_i t \tag{C4}$$

$$q = q_i - D_i Q \tag{C5}$$

On the basis of equation C4, plotting the oil production rate (q) versus production time (t) on a semi-log graph will result in a straight line having an intercept equal to $\ln(q_i)$ and a slope equal to D_i. Alternatively, on the basis of equation C5, plotting the oil production rate (q) versus cumulative oil production (Q) will result in a straight line having an intercept and slope equal to q_i and D_i, respectively. After values are determined for D_i and q_i, equations C4 and C5 are used to predict the future oil production rate and the cumulative amount of recoverable oil, respectively. The current assessment methodology is designed to assess only the technically recoverable hydrocarbon for the carbon dioxide enhanced oil recovery (CO_2-EOR) application, implying no economic limit. If an economic evaluation is required in the future, first an appropriate economic hydrocarbon production rate (q_{ec}) in reservoir barrels per day (bbl/day) needs to be defined below which hydrocarbon production from a given reservoir is considered to be uneconomic. The magnitude of the introduced value of q_{ec} depends on each project configuration and specifications and external factors such as hydrocarbon prices that vary from one project to another. After the value of q_{ec} is chosen, the field's productive life (t_{ec}) and total economically recoverable hydrocarbon volume (Q_{ec}) can be calculated by applying the following equations:

$$t_{ec} = -\frac{1}{D_i}\ln\left(\frac{q_{ec}}{q_i}\right) \tag{C6}$$

$$Q_{ec} = -\frac{1}{D_i}(q_i - q_{ec}) \tag{C7}$$

For a technically recoverable hydrocarbon volume, designated as Q_{max}, the recovery factor (RF) under current production conditions is estimated from the following:

$$RF = \frac{Q_{max}}{OOIP} \times 100 \tag{C8}$$

where

Q_{max} is the maximum cumulative oil production, in barrels (bbl);

$OOIP$ is the original oil in place, in stock tank barrels (STB); and

RF is the recovery factor, expressed as a percentage.

If an incremental recovery factor is required for any phase (that is, primary, secondary, or tertiary), it is determined as the total calculated RF at phase i minus the total calculated RF at the previous phase ($i - 1$):

$$RF_{Incremental} = RF_i - RF_{i-1} \tag{C9}$$

where

i is 1 for primary, 2 for secondary, and 3 for tertiary production.

For example, if the reservoir is currently under CO_2-EOR, which was initiated after a waterflood, the calculated RF at the current stage represents the total recovery, including all three stages of primary, waterflood, and CO_2-EOR. Therefore, on the basis of equation C9, the additional recovery factor due to CO_2-EOR is obtained by subtracting the calculated RF values of the waterflood from the RF value calculated for the CO_2-EOR.

Case Study

The Oil and Gas Journal's 2012 survey of EOR projects (Koottungal, 2012; Kuuskraa, 2012) indicated that about 123 CO_2-EOR projects were active within the United States in 2012. Twenty-four fields (28 reservoirs) of these projects were initially selected for DCA. However, after the initial investigation, almost half of these projects were excluded from the DCA because they either did not develop long enough CO_2-EOR decline periods appropriate for the DCA or were not in their decline phases yet. Data for the DCA were obtained from the comprehensive resource database (CRD), which was described by Carolus and others (in press); the CRD was developed from two proprietary databases by Nehring Associates Inc. (2012) and IHS Inc. (2012) and provided adequate injection and production data for only 12 fields containing 15 reservoirs. Therefore, the DCA was successfully applied

only on these fields that have established a good CO_2-EOR decline trend. The results of DCA on 15 reservoirs from these 12 fields are summarized in table C1 (tables follow the "References Cited"). The DCA for the Sable oil field in the west Texas section of the Permian Basin Province is presented here to show the procedure, and the details of the DCA for all the 15 reservoirs are provided in appendix C1. It is important to note that the Sable oil field was under a CO_2-EOR operation from 1984 to 2001 and hence was not an active CO_2-EOR project in 2012. However, because it makes a great example of the application of DCA, this field is being analyzed and presented herein.

In order to present the DCA procedure and demonstrate its applicability in modeling both waterflood and CO_2-EOR decline periods for the Sable oil field, two figures were generated and are discussed. Figure C1 shows the semi-log plot of oil production rate versus production time for the Sable oil field. This graph shows that the oil production decline during waterflood that began in 1976 continued until 1984, when the CO_2-EOR project was initiated. Because of CO_2-EOR, the field production remained stable until 1993, when the production decline started again.

Figure C2 shows the oil production rate versus the cumulative oil production for the Sable oil field. As shown in the figure, the technically recoverable oil volume has increased from 9.85 million barrels (MMbbl) for the waterflood phase to 13.1 MMbbl for the CO_2-EOR phase.

The oil production data for DCA are from IHS Inc. (2012), and the calculated *OOIP* values are from the CRD (Carolus and others, in press), which is based on data from the Nehring Associates Inc. database (2012) and IHS Inc. (2012). Because the *OOIP* values from the CRD are proprietary, the *OOIP* values of reservoirs are reported qualitatively in table C2 and appendix C1 as small, medium, and large: a small *OOIP* is less than or equal to 100 MMbbl, a medium *OOIP* is between 100 and 1,000 MMbbl, and a large *OOIP* is larger than or equal to 1,000 MMbbl. The *OOIP* of the San Andres Limestone of the Sable oil field was estimated volumetrically to be less than 100 MMbbl, thus classifying the reservoir in the Sable field as a small reservoir. By applying equation C8, the calculated recovery factors are 27.2 and 36.2 percent for waterflood and CO_2-EOR, respectively (table C2). On the basis of equation C9, the additional recovery-factor value due to CO_2-EOR is 9.0 percent. A similar process has been repeated for the selected 14 reservoirs located in Colorado, Wyoming, and the Permian Basin of Texas and New Mexico that were under CO_2-EOR in 2012.

The additional recoverable oil volumes for CO_2-EOR in 15 selected reservoirs were estimated by using DCA. Recovery factors were calculated by dividing the recoverable oil volumes at the end of the waterflood and at the end of CO_2-EOR by the *OOIP* of the individual reservoirs.

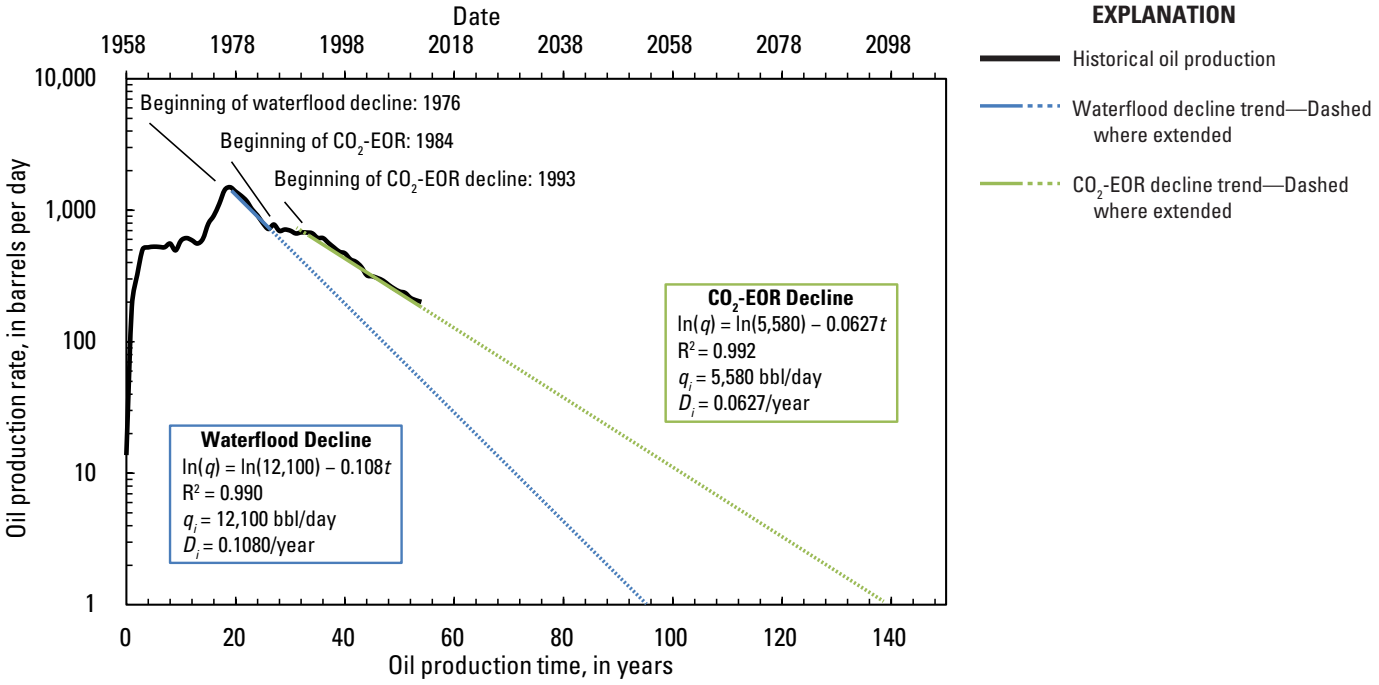

Figure C1. Semi-log plot of the oil production rate versus the oil production time for the San Andres Limestone in the Sable oil field in the west Texas section of the Permian Basin Province, showing the decline trends for both the waterflood and the carbon dioxide enhanced oil recovery (CO_2-EOR) phases. Data are from IHS Inc. (2012). Terms used in the decline equations on the graph: D_i = initial decline rate per year; q = oil production rate, in barrels per day (bbl/day); q_i = initial oil production rate, in barrels per day (bbl/day); R^2 = coefficient of determination; t = oil production time, in years.

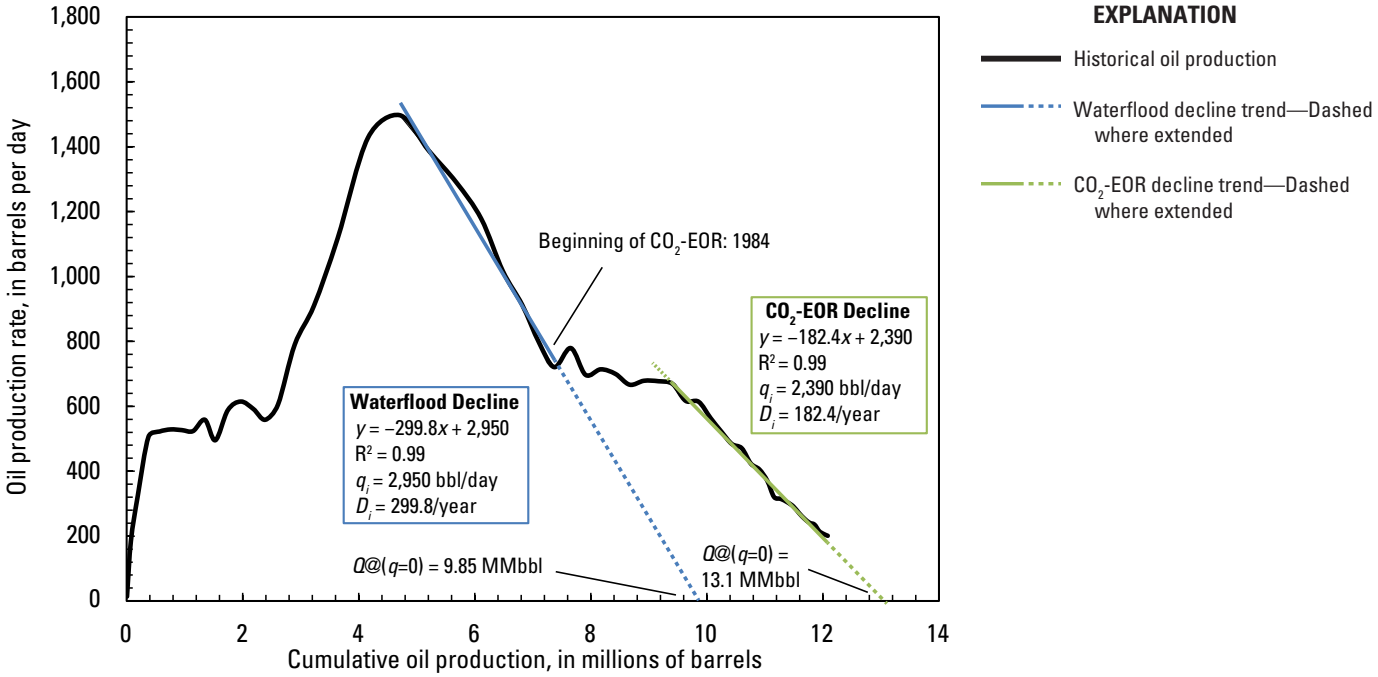

Figure C2. Graph of the oil production rate versus the cumulative oil production for the San Andres Limestone in the Sable oil field, Texas, showing the decline trends for both the waterflood and the carbon dioxide enhanced oil recovery (CO_2-EOR) phases. Data are from IHS Inc. (2012). Terms used in the decline equations on the graph: D_i = initial decline rate per year; q = oil production rate, in barrels per day (bbl/day); q_i = initial oil production rate, in barrels per day (bbl/day); Q = cumulative oil production, in millions of barrels (MMbbl); R^2 = coefficient of determination; x = cumulative oil production in the trendline equation, in millions of barrels; y = oil production rate in the trendline equation, in barrels per day.

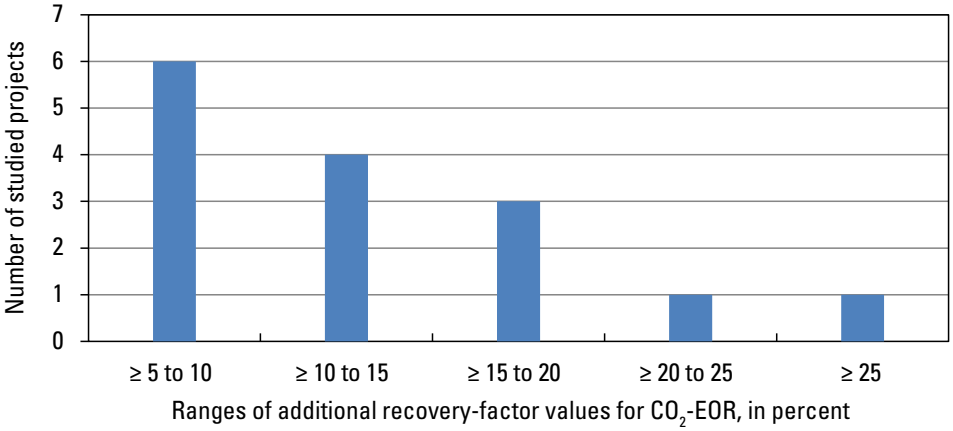

Figure C3. Bar graph showing the number of studied reservoirs having values of additional oil recovery factors due to carbon dioxide enhanced oil recovery (CO_2-EOR) in five different ranges. Recovery-factor values estimated by decline curve analysis are from table C2.

Discussion

Generally speaking, the DCA is utilized in this study as a method that enables calculating both current and projected values of reservoir oil recovery-factor values at the end of a waterflood period and a subsequent CO_2-EOR period. Table C1 summarizes the best match values of the initial oil production rate (q_i) and the initial decline rate for oil production (D_i) and the corresponding values of the coefficient of determination (R^2) values in the DCA equation for both waterflood and CO_2-EOR decline periods of the studied reservoirs. As explained above, the q_i and D_i values are empirical matching parameters and do not carry any physical meanings. For comparison purposes, it can be observed from this table that the overall average values of q_i and D_i are 72,500 bbl/day and 360.7/year for the waterflood period and 125,400 bbls/day and 190.5/year for the CO_2-EOR period, respectively. It is important to note that the overall average values of R^2 are 0.951 and 0.952 for the waterflood and CO_2-EOR periods, respectively, indicating a good to excellent match for the waterflood and CO_2-EOR periods. This observation highlights an important point that the basic DCA method as it has been routinely applied to model waterflood decline in performance analysis can also be utilized to model the CO_2-EOR decline period with similar accuracy.

The calculated recovery factors for the technically recoverable oil volumes for the waterflood and CO_2-EOR phases and the additional oil recovery for the CO_2-EOR phase for all 15 studied reservoirs are reported in table C2. The results of this table indicate that the incremental oil recovery factor by CO_2-EOR ranges from 6.6 percent for the Weber Sandstone in the Rangely field to 25.7 percent for the San Andres Limestone (dolomite) in the Wasson field, whereas the average overall calculated recovery factor for the studied reservoirs is 13.2 percent. The ranges of the additional recovery factor due to CO_2-EOR from DCA along with the values from the review of literature on CO_2-EOR in chapter D are utilized to substantiate the estimated values from the reservoir modeling as described in chapter B.

Data from table C2 reveal that the average additional recovery factor with CO_2-EOR from the seven dolomite reservoirs producing from the San Andres Limestone is around 13.5 percent, whereas the other five carbonate reservoirs have an average additional recovery of 14.3 percent. The average additional recovery factor for the 3 clastic (sandstone) reservoirs is 10.9 percent, which is lower than the 13.8 percent for the 12 carbonate reservoirs. However, the data are limited in terms of samples and, therefore, it is hard to make any conclusive observations. In figure C3, the reservoirs that were evaluated for DCA are grouped according to their *RF* values for CO_2-EOR, and the graph shows that most of them are in the lower range (13 out of 15 are less than 20 percent)—6 are in the range of ≥5 to 10 percent, 4 are in the range of ≥10 to 15 percent, and 3 are in the range of ≥15 to 20 percent.

From the lithology point of view, the majority of the studied reservoirs (12 out of 15) are carbonates and only 3 are sandstone reservoirs. This small sample size of sandstone reservoirs makes the comparison of the CO_2-EOR performance in these two lithological classes practically impossible.

References Cited

Carolus, Marshall, Biglarbigi, Khosrow, Warwick, P.D., Attanasi, E.D., Freeman, P.A., and Lohr, C.D., in press, Overview of a comprehensive resource database for the assessment of recoverable hydrocarbons produced by carbon dioxide enhanced oil recovery: U.S. Geological Survey Techniques and Methods, book 7, chap. C16.

Fetkovich, M.J., 1980, Decline curve analysis using type curves: Journal of Petroleum Technology, v. 32, no. 6 (June 1980), p. 1065–1077, paper SPE–4629–PA.

Fetkovich, M.J., Vienot, M.E., Bradley, M.D., and Kiesow, U.G., 1987, Decline curve analysis using type curves—Case histories: SPE (Society of Petroleum Engineers) Formation Evaluation, v. 2, no. 4 (December 1987), p. 637–656, paper SPE–13169–PA.

Holm, L.W., and Josendal, V.A., 1974, Mechanisms of oil displacement by carbon dioxide: Journal of Petroleum Technology, v. 26, no. 12 (December 1974), p. 1427–1438, paper SPE–4736–PA.

IHS Inc., 2012, PIDM [Petroleum Information Data Model] relational U.S. well data [data current as of December 23, 2011]: Englewood, Colo., IHS Inc.

Koottungal, Leena, ed., 2012, 2012 worldwide EOR survey: Oil and Gas Journal, v. 110, no. 4 (April 2, 2012), p. 1–4, accessed in 2014 at http://www.ogj.com/articles/print/vol-110/issue-4/general-interest/special-report-eor-heavy-oil-survey/2012-worldwide-eor-survey.html.

Kuuskraa, Vello, 2012, QC updates carbon dioxide projects in OGJ's enhanced oil recovery survey: Oil and Gas Journal, v. 110, no. 7 (July 2, 2012), p. 1–4, accessed [in 2014] at http://www.ogj.com/articles/print/vol-110/issue-07/drilling-production/qc-updates-carbon-dioxide-projects.html.

Nehring Associates Inc., 2012, Significant oil and gas fields of the United States database [data current as of December 2012]: Colorado Springs, Colo., Nehring Associates Inc.

Table C1. Best match values of the initial oil production rate, the initial decline rate for oil production, and the corresponding coefficient of determination (R^2) values for both waterflood and carbon dioxide enhanced oil recovery (CO_2-EOR) decline periods of the studied reservoirs.

[The selection of the 15 studied reservoirs and the sources of data are described in chapter C of this report. Fourteen of the reservoirs had active CO_2-EOR projects in 2012. The reservoir in the Sable oil field did not have an active CO_2-EOR project in 2012, but it is included because it is a good example. The values in this table were determined by decline curve analysis. Each reservoir is described as a case study in appendix C1. State abbreviations: CO, Colorado; NM, New Mexico; TX, Texas; WY, Wyoming. Variables: D_i, initial decline rate per year in oil production; q_i, initial oil production rate, in barrels per day (bbl/day)]

Case study number in appendix C1	Oil field	State	Stratigraphic unit containing the reservoir	Waterflood			CO_2-EOR		
				q_i (bbl/day)	D_i (/year)	R^2	q_i (bbl/day)	D_i (/year)	R^2
1	Sable*	TX	San Andres Limestone	2,950	299.8	0.99	2,390	182.4	0.99
2	Rangely	CO	Weber Sandstone	89,500	215.9	0.98	88,000	169.9	0.92
3	Lost Soldier	WY	Tensleep Formation	18,000	427.8	0.95	23,000	314.3	0.96
4	Lost Soldier	WY	Madison Formation	6,900	497.9	0.98	8,500	329.9	0.96
5	Wasson	TX	San Andres Limestone	421,000	300.9	0.98	120,000	43.1	0.95
6	Wasson	TX	Clear Fork Group	26,000	279.3	0.99	20,000	65.0	0.93
7	Dollarhide	TX	Thirtyone Formation	23,000	405.9	0.89	11,000	87.6	0.85
8	Dollarhide	TX	Clear Fork Group	7,500	426.8	0.95	9,000	213.3	0.97
9	Salt Creek	TX	“Canyon-age reservoir”	49,000	154.3	0.94	116,000	295.1	0.96
10	Seminole	TX	San Andres Limestone	106,000	232.3	0.87	97,000	129.4	0.96
11	Twofreds	TX	Ramsey Member	6,000	1,042.5	0.91	2,400	176.1	0.96
12	Vacuum	NM	San Andres Limestone	61,000	271.6	0.96	44,000	132.7	0.97
13	Cedar Lake	TX	San Andres Limestone	14,000	217.6	0.99	14,500	94.8	0.96
14	North Hobbs	NM	San Andres Limestone	1,200	387.3	0.97	1,900	402.6	0.96
15	Yates	TX	San Andres Limestone	256,000	250.2	0.91	244,000	221.7	0.98
Average				**72,500**	**360.7**	**0.951**	**125,400**	**190.5**	**0.952**

*The Sable oil field was under a CO_2-EOR operation from 1984 to 2001 and hence is not included in the list of CO_2-EOR projects that were active in 2012. Because it makes a great example of the application of decline curve analysis, this field is being analyzed and presented in chapter C and appendix C1 of this report.

Table C2. Additional oil recovery factors estimated by using decline curve analysis for carbon dioxide enhanced oil recovery (CO_2-EOR) projects in 15 selected reservoirs.

[The selection of the 15 studied reservoirs and the sources of data are described in chapter C of this report. Each reservoir is described as a case study in appendix C1. Reservoirs are classified on the basis of the estimated original oil in place (*OOIP*) as small, medium, or large; a small reservoir has less than or equal to100 million barrels (MMbbl) of *OOIP*, a medium reservoir has between 100 and 1,000 MMbbl of *OOIP*, and a large reservoir has more than or equal to 1,000 MMbbl of *OOIP*. State abbreviations: CO, Colorado; NM, New Mexico; TX, Texas; WY, Wyoming. Terms: *RF*, recovery factor; WF, waterflood; %, percent]

Case study number in appendix C1	Oil field	State	Stratigraphic unit containing the reservoir	Lithology	Reservoir size classification	*RF* after WF (%)*	*RF* after CO_2-EOR (%)*	Additional *RF* due to CO_2-EOR (%)
1	Sable**	TX	San Andres Limestone	Dolomite	Small	27.2	36.2	9.0
2	Rangely	CO	Weber Sandstone	Sandstone	Large	26.2	32.8	6.6
3	Lost Soldier	WY	Tensleep Formation	Sandstone	Medium	17.7	30.0	12.3
4	Lost Soldier	WY	Madison Formation	Limestone-dolomite	Medium	8.6	16.2	7.6
5	Wasson	TX	San Andres Limestone	Dolomite	Large	26.2	51.9	25.7
6	Wasson	TX	Clear Fork Group	Dolomite	Large	9.3	30.0	20.7
7	Dollarhide	TX	Thirtyone Formation	Dolomite	Medium	14.8	31.9	17.1
8	Dollarhide	TX	Clear Fork Group	Dolomite	Medium	11.4	27.7	16.3
9	Salt Creek	TX	“Canyon-age reservoir”	Limestone	Large	21.4	31.2	9.8
10	Seminole	TX	San Andres Limestone	Dolomite	Large	18.9	31.0	12.1
11	Twofreds	TX	Ramsey Member	Sandstone	Small	12.4	26.2	13.8
12	Vacuum	NM	San Andres Limestone	Dolomite	Large	19.5	28.9	9.4
13	Cedar Lake	TX	San Andres Limestone	Dolomite	Medium	19.5	27.9	8.4
14	North Hobbs	NM	San Andres Limestone	Dolomite	Small	15.2	33.2	18.0
15	Yates	TX	San Andres Limestone	Dolomite	Large	19.7	31.6	11.9
	Average for clastic (sandstone) reservoirs					**18.8**	**29.7**	**10.9**
	Average for carbonate (mostly dolomite) reservoirs					**17.6**	**31.4**	**13.8**
	Average for all 15 reservoirs					**17.9**	**31.1**	**13.2**

*The obtained recovery factors are based on the projection that both waterflood and CO_2-EOR continue until oil production of zero (q = 0 barrels).

**The Sable oil field was under a CO_2-EOR operation from 1984 to 2001 and hence is not included in the list of CO_2-EOR projects that were active in 2012. Because it makes a great example of the application of decline curve analysis, this field is being analyzed and presented in chapter C and appendix C1 of this report.

Appendix C1. Decline Curve Analysis of Selected Reservoirs

Appendix C1. Decline Curve Analysis of Selected Reservoirs

The 15 reservoirs for case studies of decline curve analysis (DCA) were chosen because adequate geologic, reservoir, and production data were available for them. They all possess specific data on reservoir and fluid properties and vary significantly in terms of (1) size, as is obvious from their reported original oil in place (OOIP), (2) rock types, as they contain both clastic and carbonate reservoirs, (3) geographical locations, being distributed in different basins throughout Texas, New Mexico, Wyoming, and Colorado, and (4) source of carbon dioxide (CO_2), as they use both natural and industrial CO_2. Miscible carbon dioxide enhanced oil recovery (CO_2-EOR) operations were used in 14 reservoirs, and an immiscible operation was used in 1 reservoir (case study 15). Fourteen of the reservoirs had active CO_2-EOR projects in 2012. The reservoir in the Sable oil field (case study 1) did not have an active CO_2-EOR project in 2012, but it is included because it is a good example. The 15 reservoirs all make great examples and case studies in demonstrating the applicability of DCA in predicting the behavior of decline periods for both waterflood and CO_2-EOR phases.

The DCA was applied to the period of declining production of each reservoir separately, and the DCA parameters were obtained by curve fitting. The goodness of the obtained fit is presented by values for the coefficient of determination, R^2, which are reported separately on the graph for each reservoir analyzed (figs. C1–1 to C1–15). The closer the value of R^2 is to 1, the better the quality of the fit. The obtained DCA parameters were utilized to forecast the cumulative oil production when the oil production rates were available over the life of the reservoir for both waterflood and CO_2-EOR phases; for this study, the economic hydrocarbon production rate (q_{ec}) is assumed to be 0 reservoir barrels per day. This process also made it possible to estimate the reservoir's additional oil recovery due to the CO_2-EOR operation that was modeled.

It is important to note that this study does not present the technical and operational details of reservoirs described in the case studies. Nor does it provide a detailed insight into the extent of the CO_2-EOR operation for each investigated project.

Case Study 1. San Andres Limestone, Sable Oil Field

The San Andres Limestone in the Sable oil field in Texas is an oil-bearing dolomite formation that was under CO_2-EOR operation between 1984 and 2001. On the basis of its OOIP, the San Andres Limestone in this field is considered a relatively small oil reservoir. The production decline under waterflood started in 1976 and continued until 1984 when the CO_2-EOR operation was initiated in various sections of the reservoir. As a result of the CO_2-EOR, the field's oil production rate remained stable over the course of 9 years until 1993, when the oil production began to decline again. The details of both waterflood and CO_2-EOR declines and the relevant DCA equations and parameters are presented in figure C1–1.

Case Study 2. Weber Sandstone, Rangely Oil Field

The Weber Sandstone in the Rangely oil field in Colorado is an oil-bearing sandstone formation that was under CO_2-EOR operations in 2012. On the basis of its OOIP, the Weber Sandstone in this field is classified as a large oil reservoir. The waterflood decline of the field started in 1978 and continued until 1986, when the CO_2-EOR operation started in various sections of the reservoir. As a result of the CO_2-EOR, the field's oil production rate increased approximately 10 percent over the course of 5 years until 1991, when the decline in production started again. This reservoir was among the largest clastic reservoirs undergoing CO_2-EOR in 2012. The details of both waterflood and CO_2-EOR declines and the obtained relevant DCA equations and parameters are presented in figure C1–2.

Case Study 3. Tensleep Formation, Lost Soldier Oil Field

The Tensleep Formation in the Lost Soldier oil field in Wyoming is an oil-bearing sandstone formation that was under CO_2-EOR operations in 2012. On the basis of its OOIP, the Tensleep Formation in this field is classified as a medium-sized oil reservoir. The waterflood decline of the field started in 1978 and continued until 1988, when the CO_2-EOR operation started in various sections of the reservoir. As a result of the CO_2-EOR, the field's oil production rate increased approximately 300 percent over the course of 3 years until 1991, when the decline in production started again. The production profile of this reservoir shows two distinct and classical declines for both waterflood and CO_2-EOR periods. The details of both waterflood and CO_2-EOR declines and the obtained relevant DCA equations and parameters are presented in figure C1–3.

Case Study 4. Madison Formation, Lost Soldier Oil Field

The Madison Formation in the Lost Soldier oil field in Wyoming is an oil-bearing carbonate (limestone-dolomite) formation that was under CO_2-EOR operations in 2012. On the basis of its OOIP, the Madison Formation in this field is classified as a medium-sized oil reservoir. The waterflood decline of the field started in 1984 and continued until 1989, when the CO_2-EOR operation started in various sections of the reservoir. As a result of the CO_2-EOR, the field's oil production rate increased approximately 40 percent over the course of 16

years until 2005, when the decline in production started again. The production profile of this reservoir shows two distinct and classical declines for both waterflood and CO_2-EOR periods. The details of both waterflood and CO_2-EOR declines and the obtained relevant DCA equations and parameters are presented in figure C1–4.

Case Study 5. San Andres Limestone, Wasson Oil Field

The San Andres Limestone in the Wasson oil field in the Permian Basin in Texas is an oil-bearing carbonate (dolomite) formation that was under CO_2-EOR operations in 2012. On the basis of its OOIP, the San Andres Limestone in this field is classified as a large oil reservoir. The waterflood decline of the field started in 1975 and continued until 1983, when the CO_2-EOR operation started in various sections of the reservoir. As a result of the CO_2-EOR, the field's oil production decline rate has decreased since. The San Andres Limestone in the Wasson field is one of the largest carbonate reservoirs undergoing CO_2-EOR worldwide. The details of both waterflood and CO_2-EOR declines and the obtained relevant DCA equations and parameters are presented in figure C1–5.

Case Study 6. Clear Fork Group, Wasson Oil Field

The Clear Fork Group in the Wasson oil field in the Permian Basin in Texas is an oil-bearing carbonate (dolomite) formation that was under CO_2-EOR operations in 2012. On the basis of its OOIP, the Clear Fork Group in this field is classified as a large oil reservoir. The waterflood decline of the field started in 1968 and continued until 1984, when the CO_2-EOR operation started in various sections of the reservoir. As a result of the CO_2-EOR, the field's oil production rate increased approximately 93 percent over the course of 13 years until 1997, when it started to decline again. The details of both waterflood and CO_2-EOR declines and the obtained relevant DCA equations and parameters are presented in figure C1–6.

Case Study 7. Thirtyone Formation, Dollarhide Oil Field

The Thirtyone Formation in the Dollarhide oil field in the Permian Basin in Texas is an oil-bearing chert and carbonate (dolomite) formation that was under CO_2-EOR operations in 2012. On the basis of its OOIP, the Thirtyone Formation in this field is classified as a medium-sized oil reservoir. The waterflood decline of the field started in 1965 and continued until 1985, when the CO_2-EOR operation started in various sections of the reservoir. As a result of the CO_2-EOR, the field's oil production rate increased approximately 118 percent over the course of 13 years until 1998, when it started to decline again. This reservoir is one of the best examples to demonstrate clearly the effect of CO_2-EOR on a reservoir's oil production rate and cumulative production. The details of both waterflood and CO_2-EOR declines and the obtained relevant DCA equations and parameters are presented in figure C1–7.

Case Study 8. Clear Fork Group, Dollarhide Oil Field

The Clear Fork Group in the Dollarhide oil field in the Permian Basin in Texas is an oil-bearing carbonate (dolomite) formation that was under CO_2-EOR operations in 2012. On the basis of its OOIP, the Clear Fork Group in this field is classified as a medium-sized oil reservoir. The waterflood decline of the field started in 1970 and continued until 1977. On the basis of the available production data, it is not possible to investigate what happened between 1977 and 1995, during which time the reservoir oil production rate stopped declining and increased slightly. This change in the oil production decline could be due to infill drilling and (or) changes in the waterflood scheme in different sections of the reservoir. In November 1995, the CO_2-EOR operation started in this reservoir. As a result of the CO_2-EOR, the field's oil production rate increased approximately 139 percent over the course of 4 years until 1999, when it started to decline again. The details of both waterflood and CO_2-EOR declines and the obtained relevant DCA equations and parameters are presented in figure C1–8.

Case Study 9. "Canyon-age reservoir," Salt Creek Oil Field

The "Canyon-age reservoir" in the Salt Creek oil field in the Permian Basin in Texas is an oil-bearing carbonate (limestone) formation that was under CO_2-EOR operations in 2012. On the basis of its OOIP, the "Canyon-age reservoir" in this field is classified as a large oil reservoir. The waterflood decline of the field started in 1972 and continued until 1993, when the CO_2-EOR operation started in various sections of the reservoir. As a result of the CO_2-EOR, the field's oil production rate increased approximately 38 percent over the course of 4 years until 1997, when it started to decline again. The details of both waterflood and CO_2-EOR declines and the obtained relevant DCA equations and parameters are presented in figure C1–9.

Case Study 10. San Andres Limestone, Seminole Oil Field

The San Andres Limestone in the Seminole oil field in the Permian Basin in Texas is an oil-bearing carbonate (dolomite) formation that was under CO_2-EOR operations in 2012. On the basis of its OOIP, the San Andres Limestone in this field is classified as a large oil reservoir. The waterflood decline of the field started in 1977 and continued until 1983, when the CO_2-EOR operation started in various sections of the reservoir.

As a result of the CO_2-EOR, the field's oil production rate increased approximately 37 percent over the course of 8 years until 1991, when it started to decline again. The details of both waterflood and CO_2-EOR declines and the obtained relevant DCA equations and parameters are presented in figure C1–10.

Case Study 11. Ramsey Member, Twofreds Oil Field

The Ramsey Member of the Bell Canyon Formation in the Twofreds oil field in the Permian Basin in Texas contains an oil-bearing sandstone that was under CO_2-EOR operations in 2012. On the basis of its OOIP, the sandstone of the Ramsey Member in this field is classified as a small oil reservoir. The waterflood decline of the field started in 1967 and continued until 1974, when the CO_2-EOR operation started in various sections of the reservoir. As a result of the CO_2-EOR, the field's oil production rate increased approximately 323 percent over the course of 11 years until 1985, when it started to decline again. The details of both waterflood and CO_2-EOR declines and the obtained relevant DCA equations and parameters are presented in figure C1–11.

Case Study 12. San Andres Limestone, Vacuum Oil Field

The San Andres Limestone in the Vacuum oil field in the Permian Basin in New Mexico is an oil-bearing carbonate (dolomite) formation that was under CO_2-EOR operations in 2012. On the basis of its OOIP, the San Andres Limestone in this field is classified as a large oil reservoir. The waterflood decline of the field started in 1983 and continued until 1997, when the CO_2-EOR operation started in various sections of the reservoir. As a result of the CO_2-EOR, the field's oil production rate stayed stable until 2001, when it started to decline again. The details of both waterflood and CO_2-EOR declines and the obtained relevant DCA equations and parameters are presented in figure C1–12.

Case Study 13. San Andres Limestone, Cedar Lake Oil Field

The San Andres Limestone in the Cedar Lake oil field in the Permian Basin in Texas is an oil-bearing carbonate (dolomite) formation that was under CO_2-EOR operations in 2012. On the basis of its OOIP, the San Andres Limestone in this field is classified as a medium-sized oil reservoir. The waterflood decline of the field started in 1983 and continued until 1994, when the CO_2-EOR operation started in various sections of the reservoir. As a result of the CO_2-EOR, the field's oil production rate increased approximately 25 percent over the course of 7 years until 2001, when it started to decline again. The details of both waterflood and CO_2-EOR declines and the obtained relevant DCA equations and parameters are presented in figure C1–13.

Case Study 14. San Andres Limestone, North Hobbs Oil Field

The San Andres Limestone in the North Hobbs oil field in the Permian Basin in New Mexico is an oil-bearing carbonate (dolomite) formation that was under CO_2-EOR operations in 2012. On the basis of its OOIP, the San Andres Limestone in this field is classified as a small oil reservoir. The waterflood decline of the field started in 2000 and continued until 2003, when the CO_2-EOR operation started in various sections of the reservoir. As a result of the CO_2-EOR, the field's oil production rate increased approximately 104 percent over the course of 3 years until 2006, when it started to decline again. The details of both waterflood and CO_2-EOR declines and the obtained relevant DCA equations and parameters are presented in figure C1–14.

Case Study 15. San Andres Limestone, Yates Oil Field

The San Andres Limestone in the Yates oil field in the Permian Basin in Texas is an oil-bearing carbonate (dolomite) formation that was under CO_2-EOR operations in 2012. It should be noted that unlike the previous examples, the CO_2-EOR operation in this field is immiscible. On the basis of its OOIP, the San Andres Limestone in this field is classified as a large oil reservoir. The waterflood decline of the field started in 2000 and continued until 2004, when the CO_2-EOR operation started in various sections of the reservoir. As a result of the CO_2-EOR, the field's oil production rate increased approximately 48 percent over the course of 2 years until 2006, when it started to decline again. The details of both waterflood and CO_2-EOR declines and the obtained relevant DCA equations and parameters are presented in figure C1–15.

Reference Cited

IHS Inc., 2012, PIDM [Petroleum Information Data Model] relational U.S. well data [data current as of December 23, 2011]: Englewood, Colo., IHS Inc.

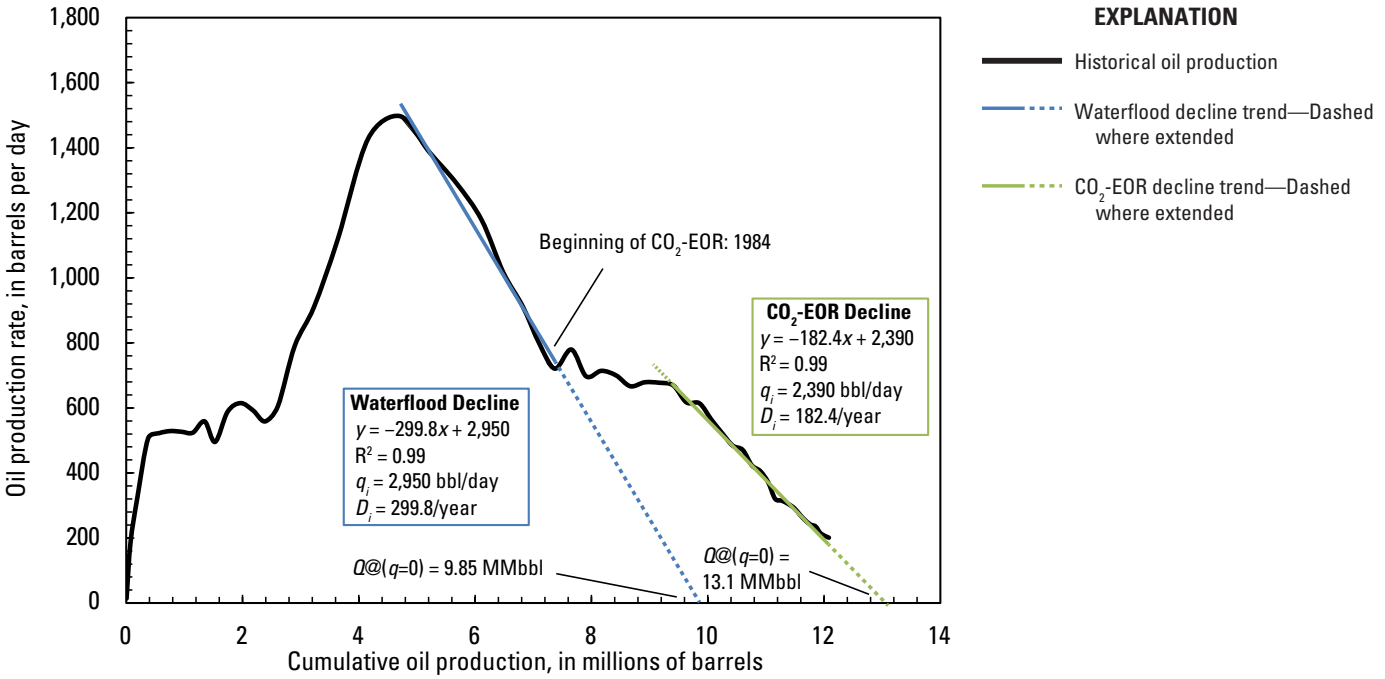

Figure C1–1. Graph of the oil production rate versus the cumulative oil production for the San Andres Limestone in the Sable oil field, Texas, showing the decline trends for both the waterflood and the carbon dioxide enhanced oil recovery (CO_2-EOR) phases. Data are from IHS Inc. (2012). Terms used in the decline equations on the graph: D_i = initial decline rate per year; q = oil production rate, in barrels per day (bbl/day); q_i = initial oil production rate, in barrels per day (bbl/day); Q = cumulative oil production, in millions of barrels (MMbbl); R^2 = coefficient of determination; x = cumulative oil production in the trendline equation, in millions of barrels; y = oil production rate in the trendline equation, in barrels per day.

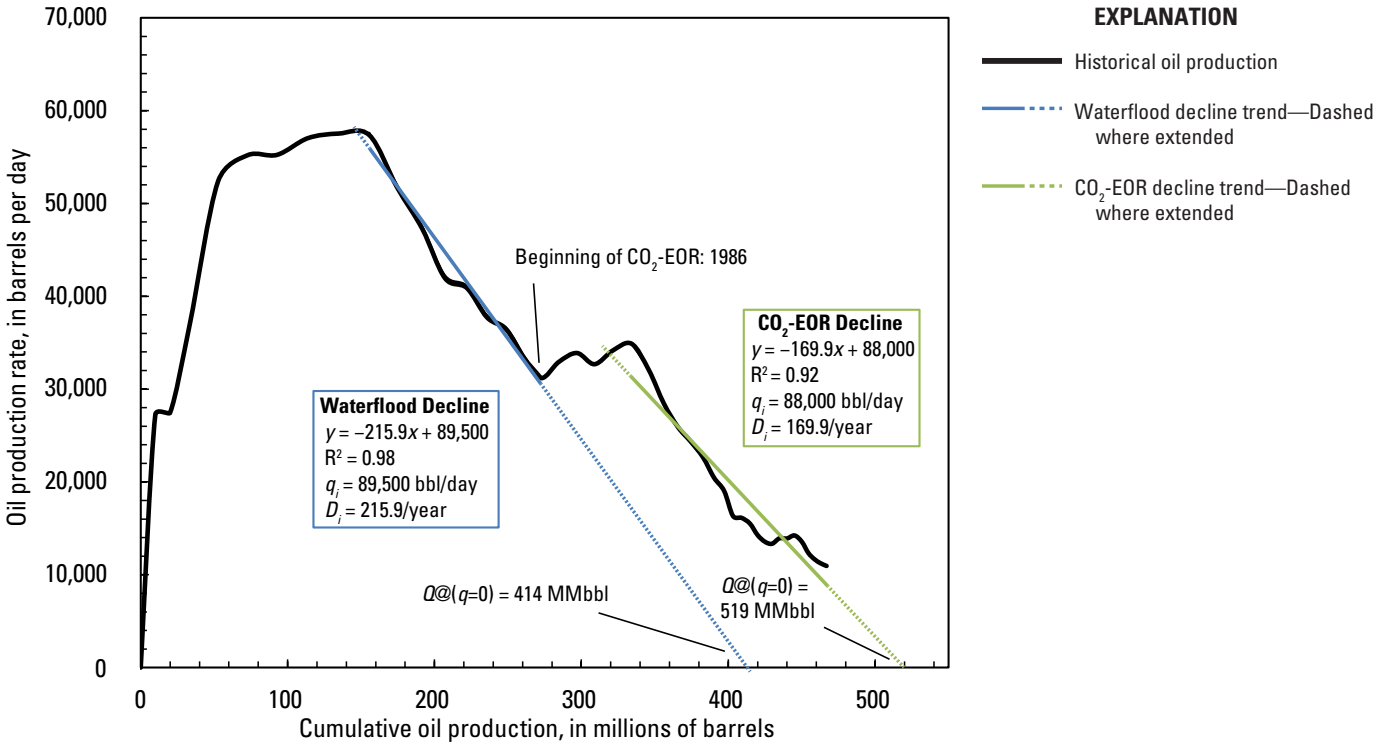

Figure C1–2. Graph of the oil production rate versus the cumulative oil production for the Weber Sandstone in the Rangely oil field, Colorado, showing the decline trends for both the waterflood and the carbon dioxide enhanced oil recovery (CO_2-EOR) phases. Data are from IHS Inc. (2012). Terms are as defined for figure C1–1. For completeness, this figure is included in the appendix even though it is also shown as text-figure C2.

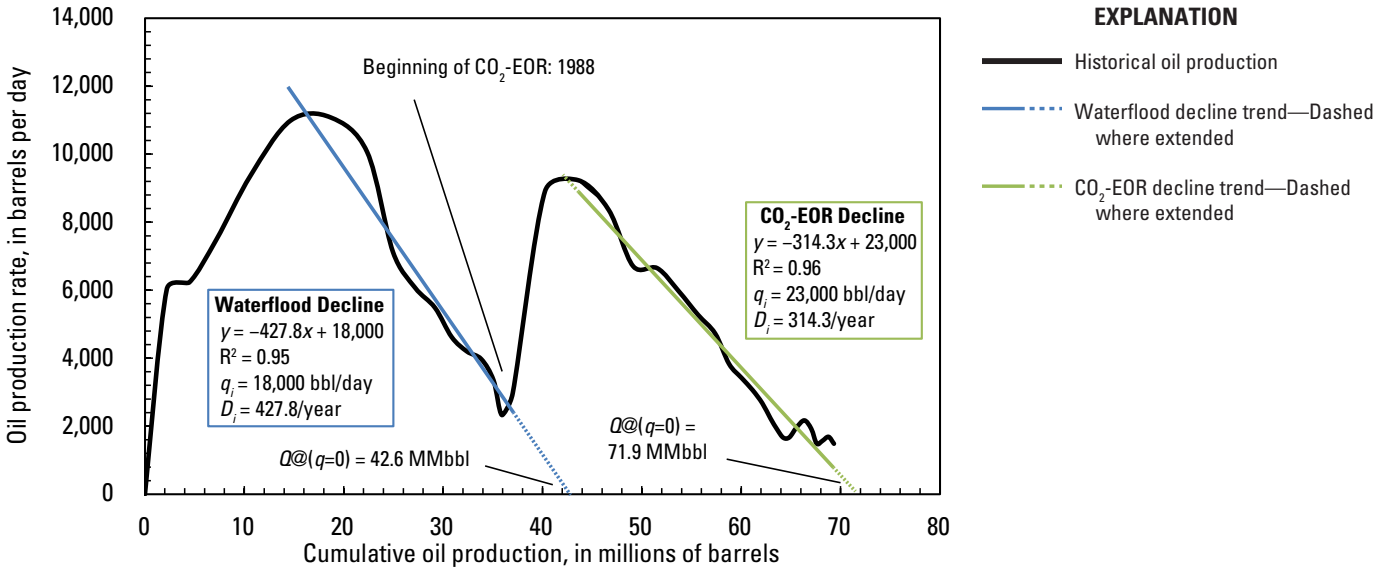

Figure C1–3. Graph of the oil production rate versus the cumulative oil production for the Tensleep Formation in the Lost Soldier oil field, Wyoming, showing the decline trends for both the waterflood and the carbon dioxide enhanced oil recovery (CO_2-EOR) phases. Data are from IHS Inc. (2012). Terms are as defined for figure C1–1.

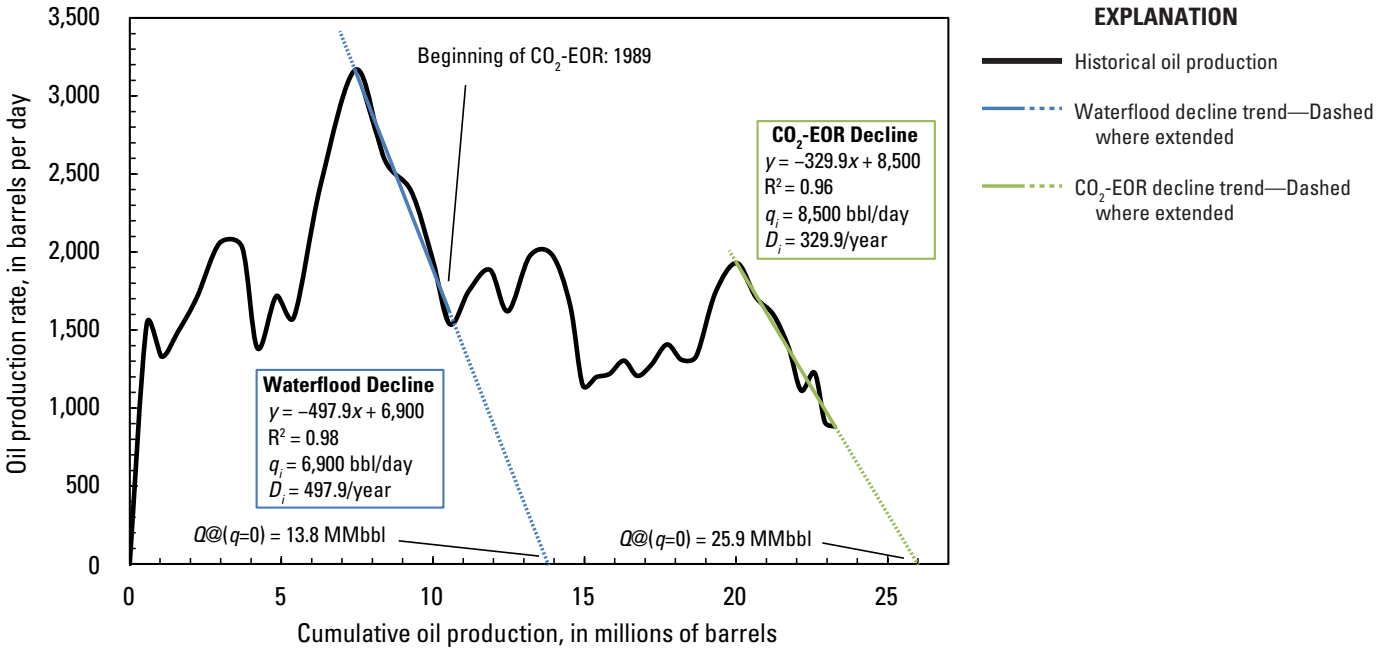

Figure C1–4. Graph of the oil production rate versus the cumulative oil production for the Madison Formation in the Lost Soldier oil field, Wyoming, showing the decline trends for both the waterflood and the carbon dioxide enhanced oil recovery (CO_2-EOR) phases. Data are from IHS Inc. (2012). Terms are as defined for figure C1–1.

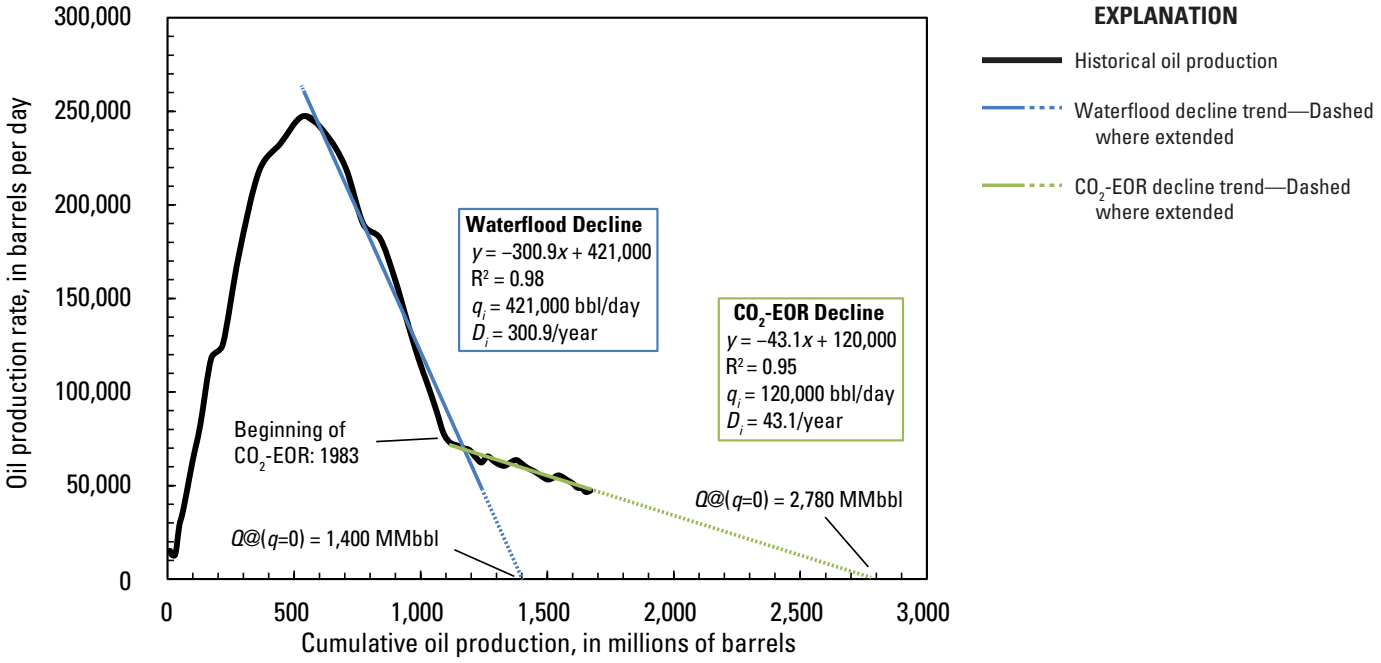

Figure C1–5. Graph of the oil production rate versus the cumulative oil production for the San Andres Limestone in the Wasson oil field, Texas, showing the decline trends for both the waterflood and the carbon dioxide enhanced oil recovery (CO_2-EOR) phases. Data are from IHS Inc. (2012). Terms are as defined for figure C1–1.

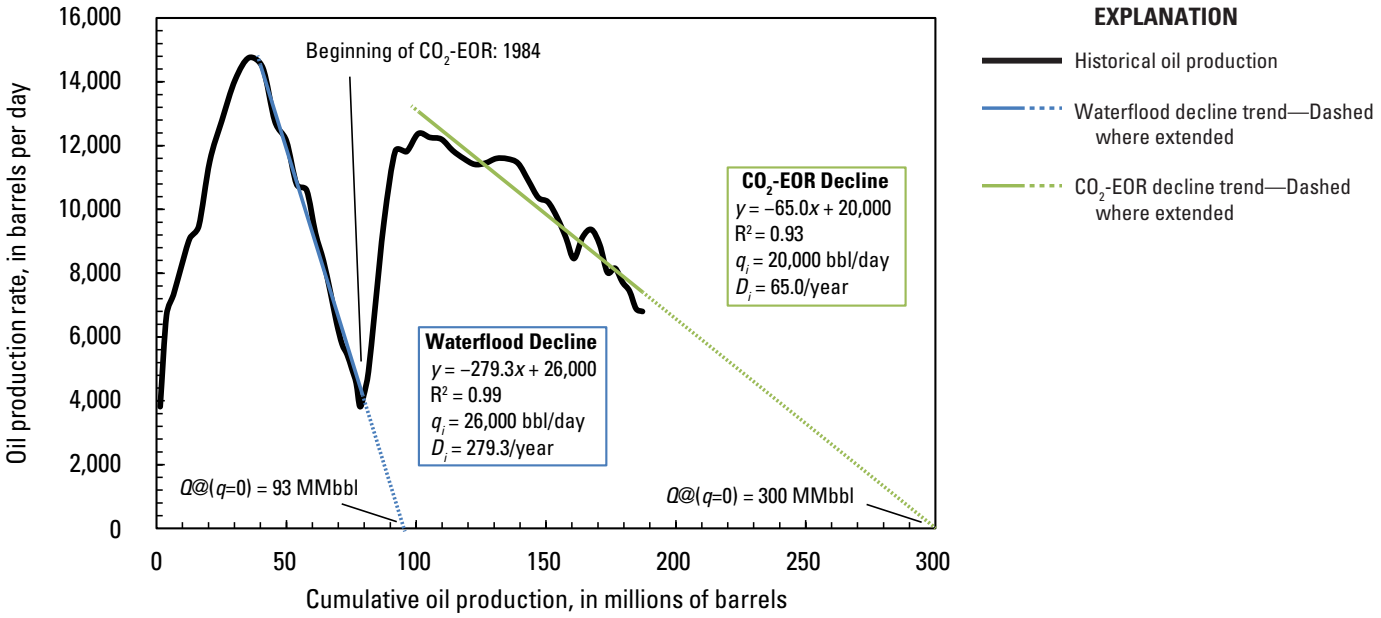

Figure C1–6. Graph of the oil production rate versus the cumulative oil production for the Clear Fork Group in the Wasson oil field, Texas, showing the decline trends for both the waterflood and the carbon dioxide enhanced oil recovery (CO_2-EOR) phases. Data are from IHS Inc. (2012). Terms are as defined for figure C1–1.

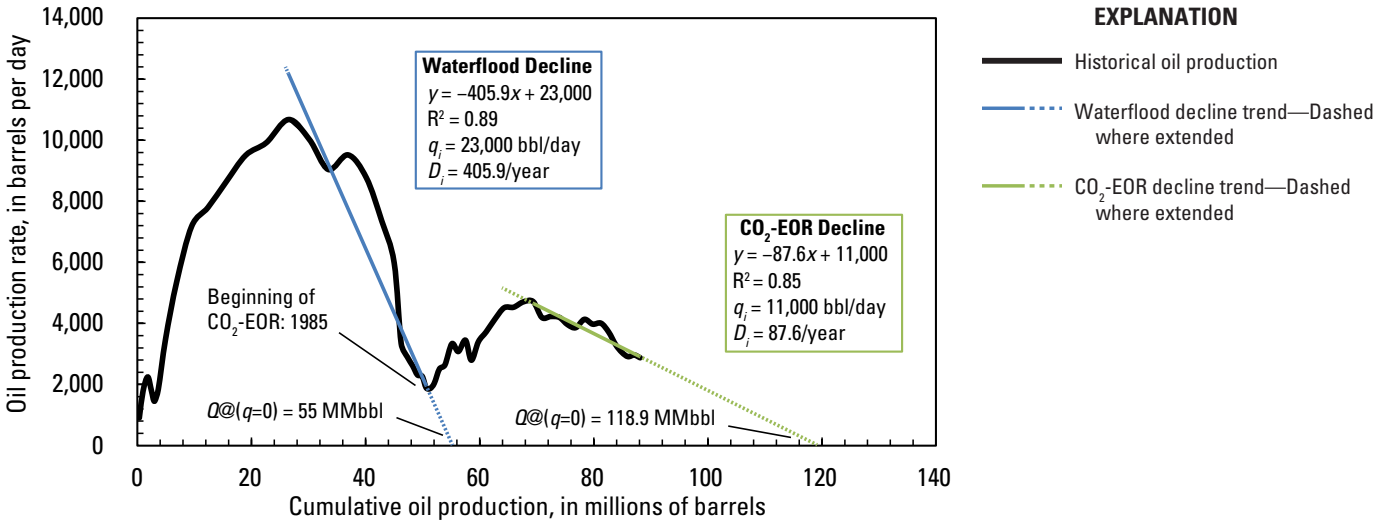

Figure C1–7. Graph of the oil production rate versus the cumulative oil production for the Thirtyone Formation in the Dollarhide oil field, Texas, showing the decline trends for both the waterflood and the carbon dioxide enhanced oil recovery (CO_2-EOR) phases. Data are from IHS Inc. (2012). Terms are as defined for figure C1–1.

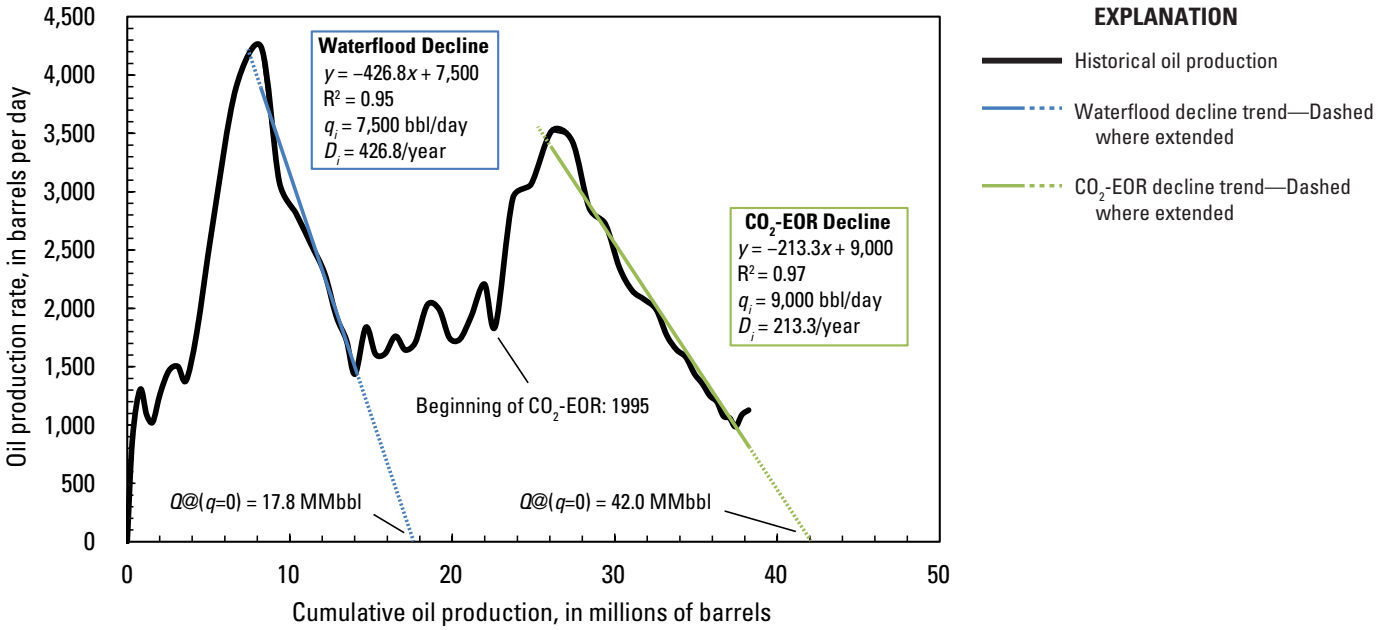

Figure C1–8. Graph of the oil production rate versus the cumulative oil production for the Clear Fork Group in the Dollarhide oil field, Texas, showing the decline trends for both the waterflood and the carbon dioxide enhanced oil recovery (CO_2-EOR) phases. Data are from IHS Inc. (2012). Terms are as defined for figure C1–1.

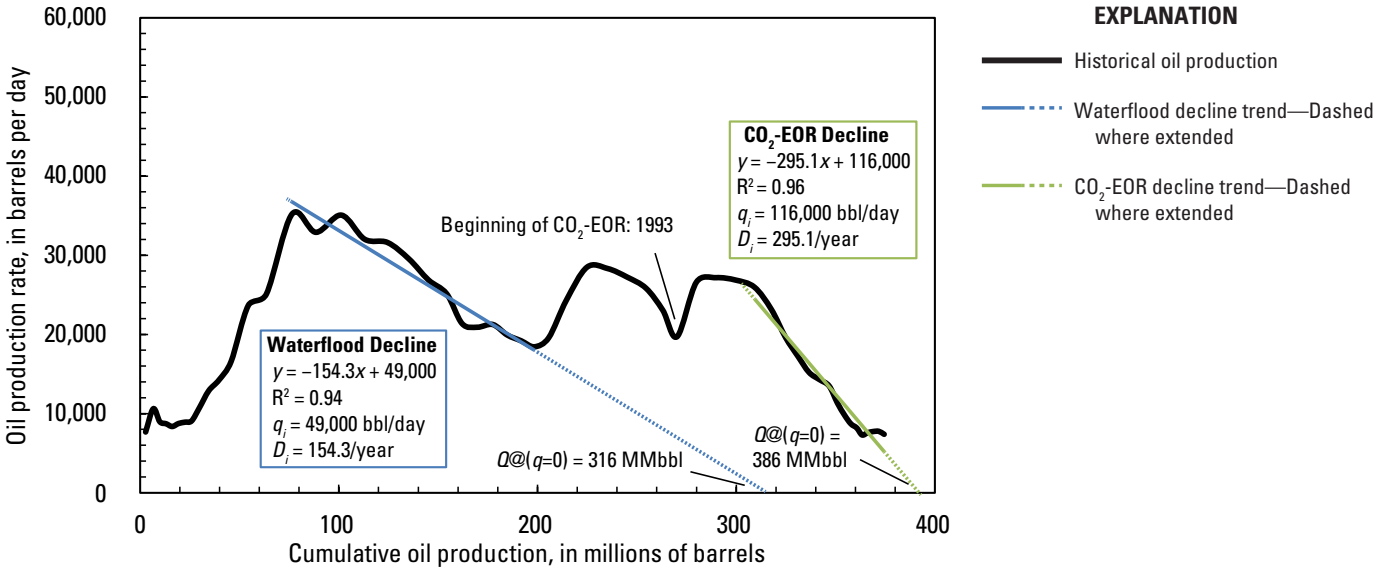

Figure C1–9. Graph of the oil production rate versus the cumulative oil production for the "Canyon-age reservoir" in the Salt Creek oil field, Texas, showing the decline trends for both the waterflood and the carbon dioxide enhanced oil recovery (CO_2-EOR) phases. Data are from IHS Inc. (2012). Terms are as defined for figure C1–1.

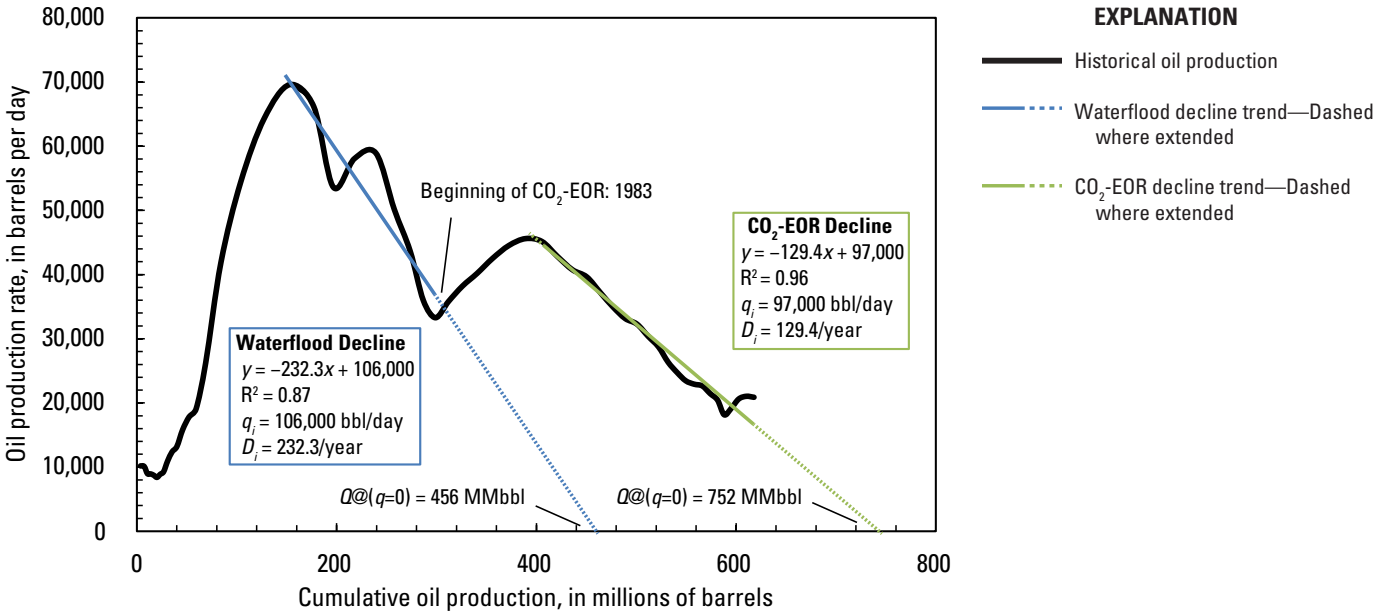

Figure C1–10. Graph of the oil production rate versus the cumulative oil production for the San Andres Limestone in the Seminole oil field, Texas, showing the decline trends for both the waterflood and the carbon dioxide enhanced oil recovery (CO_2-EOR) phases. Data are from IHS Inc. (2012). Terms are as defined for figure C1–1.

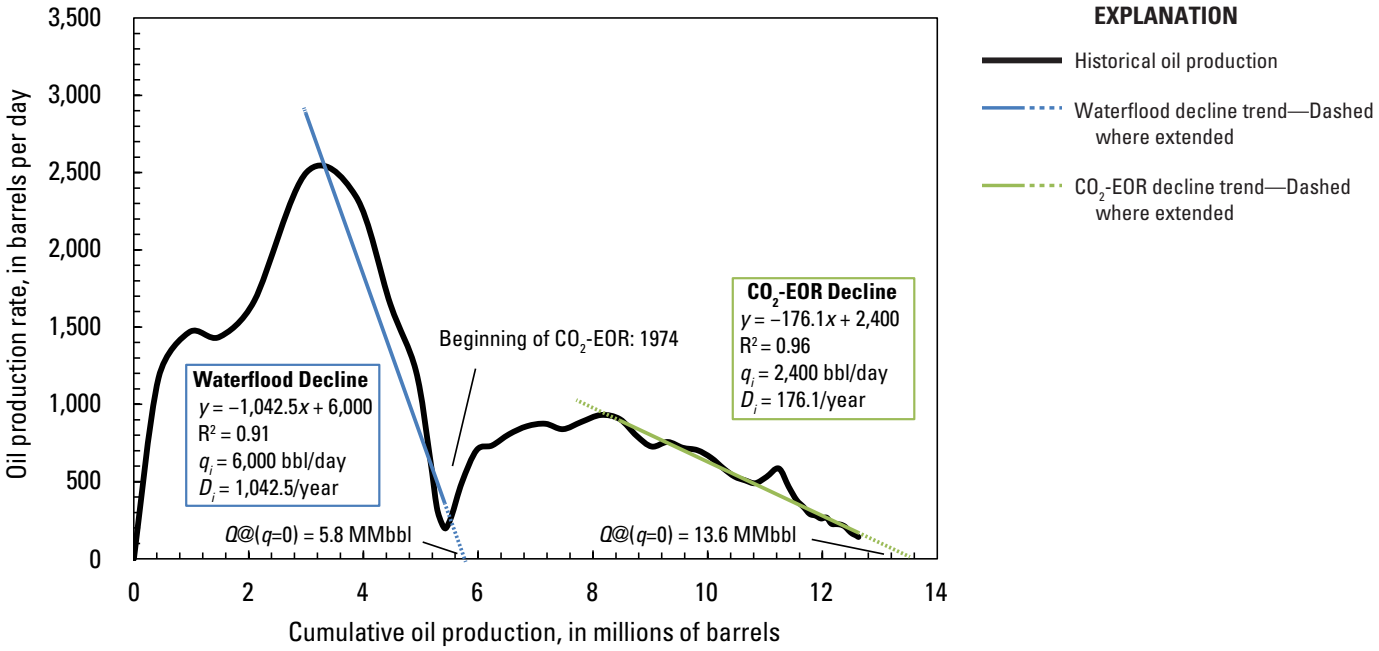

Figure C1–11. Graph of the oil production rate versus the cumulative oil production for the sandstone of the Ramsey Member of the Bell Canyon Formation in the Twofreds oil field, Texas, showing the decline trends for both the waterflood and the carbon dioxide enhanced oil recovery (CO_2-EOR) phases. Data are from IHS Inc. (2012). Terms are as defined for figure C1–1.

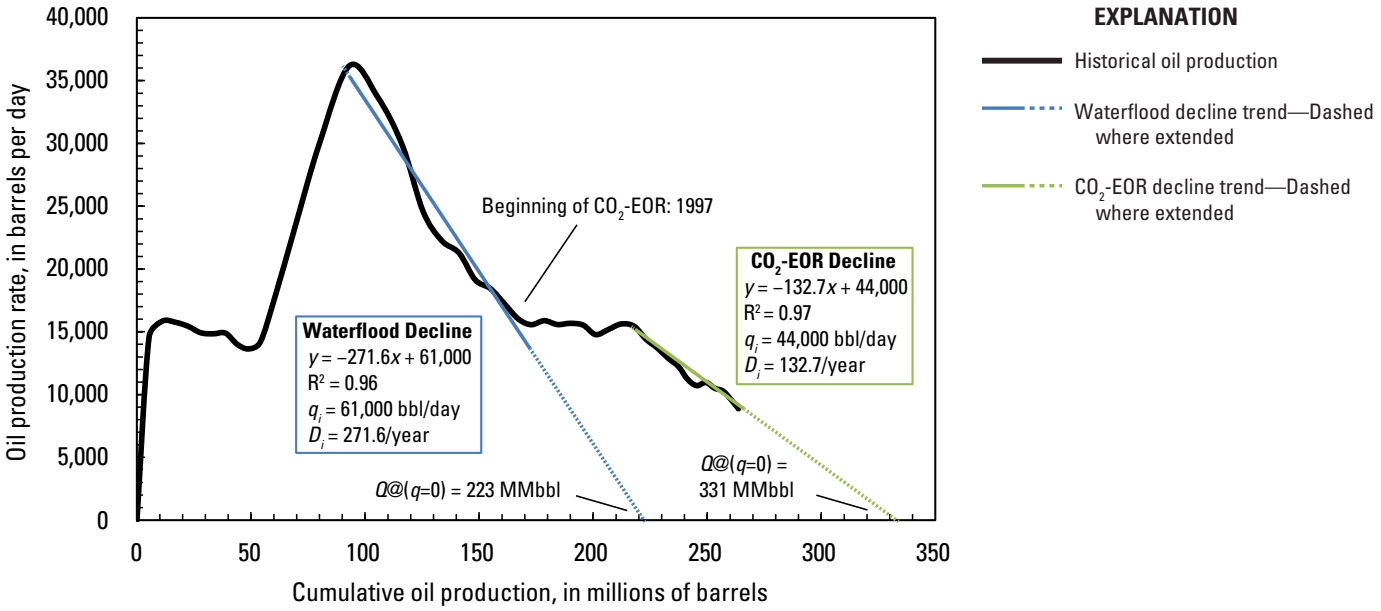

Figure C1–12. Graph of the oil production rate versus the cumulative oil production for the San Andres Limestone in the Vacuum oil field, New Mexico, showing the decline trends for both the waterflood and the carbon dioxide enhanced oil recovery (CO_2-EOR) phases. Data are from IHS Inc. (2012). Terms are as defined for figure C1–1.

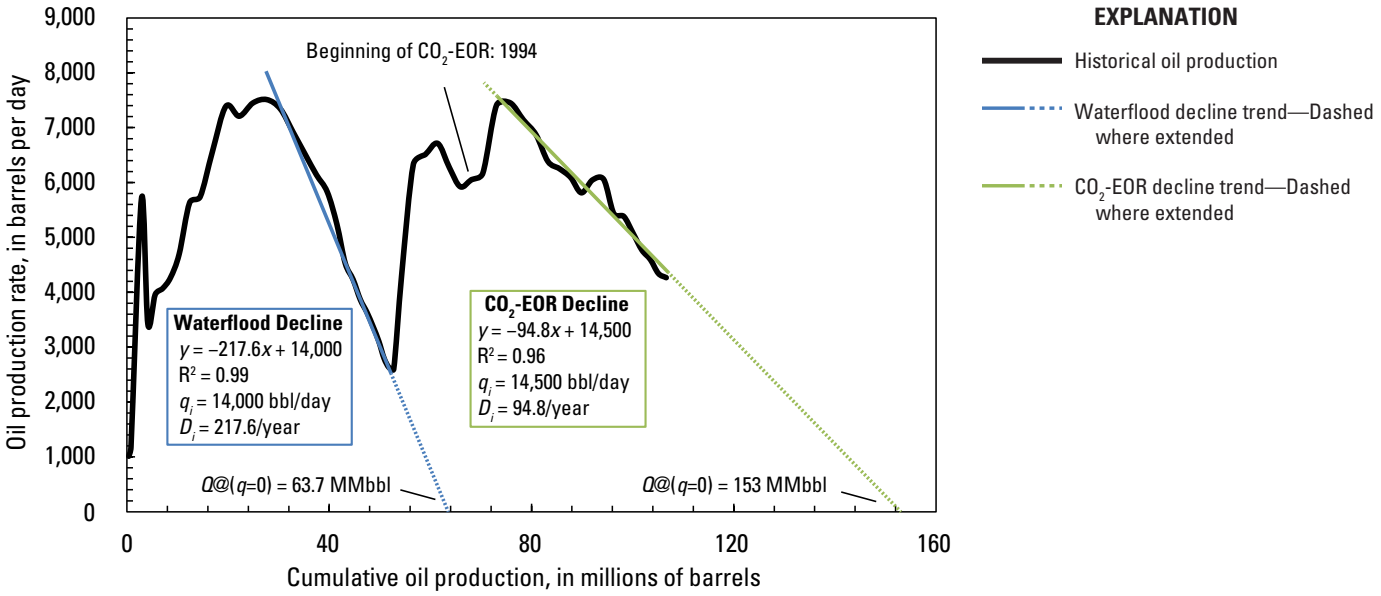

Figure C1–13. Graph of the oil production rate versus the cumulative oil production for the San Andres Limestone in the Cedar Lake oil field, Texas, showing the decline trends for both the waterflood and the carbon dioxide enhanced oil recovery (CO_2-EOR) phases. Data are from IHS Inc. (2012). Terms are as defined for figure C1–1.

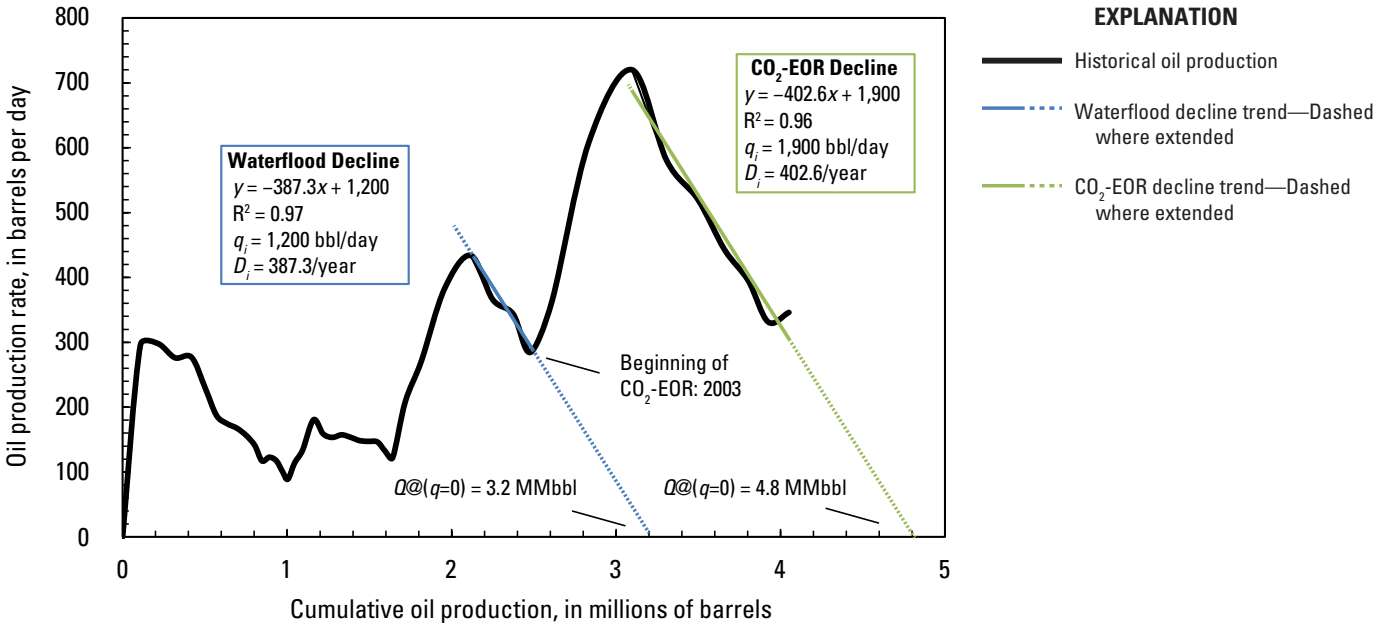

Figure C1–14. Graph of the oil production rate versus the cumulative oil production for the San Andres Limestone in the North Hobbs oil field, New Mexico, showing the decline trends for both the waterflood and the carbon dioxide enhanced oil recovery (CO_2-EOR) phases. Data are from IHS Inc. (2012). Terms are as defined for figure C1–1.

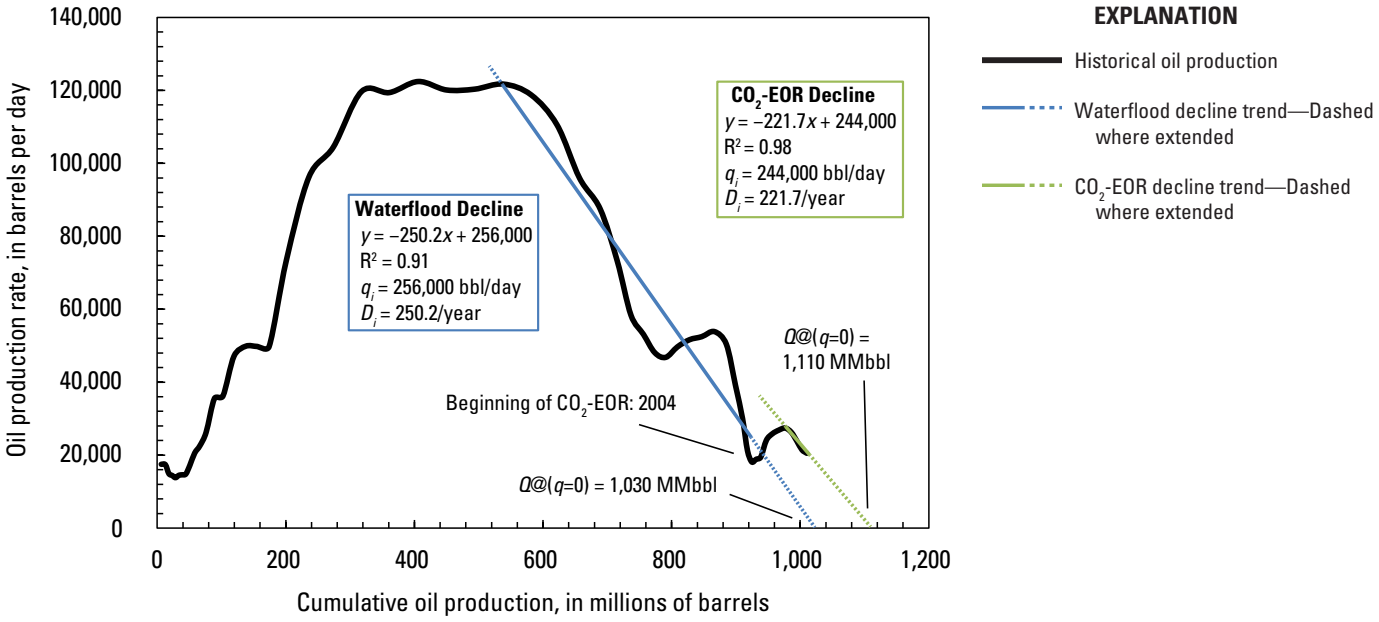

Figure C1–15. Graph of the oil production rate versus the cumulative oil production for the San Andres Limestone in the Yates oil field, Texas, showing the decline trends for both the waterflood and the carbon dioxide enhanced oil recovery (CO_2-EOR) phases. Data are from IHS Inc. (2012). Terms are as defined for figure C1–1.

Carbon Dioxide Enhanced Oil Recovery Performance According to the Literature

By Ricardo A. Olea

Chapter D of
Three Approaches for Estimating Recovery Factors in Carbon Dioxide Enhanced Oil Recovery
Mahendra K. Verma, Editor

Scientific Investigations Report 2017–5062–D

U.S. Department of the Interior
U.S. Geological Survey

U.S. Department of the Interior
RYAN K. ZINKE, Secretary

U.S. Geological Survey
William H. Werkheiser, Acting Director

U.S. Geological Survey, Reston, Virginia: 2017

Suggested citation:
Olea, R.A., 2017, Carbon dioxide enhanced oil recovery performance according to the literature, chap. D *of* Verma, M.K., ed., Three approaches for estimating recovery factors in carbon dioxide enhanced oil recovery: U.S. Geological Survey Scientific Investigations Report 2017–5062, p. D1–D21, https://doi.org/10.3133/sir20175062D.

ISSN 2328-0328 (online)

Contents

Figures

Tables

[Table D1 follows the “References Cited”]

Chapter D. Carbon Dioxide Enhanced Oil Recovery Performance According to the Literature

By Ricardo A. Olea[1]

Introduction

The need to increase the efficiency of oil recovery and environmental concerns are bringing to prominence the use of carbon dioxide (CO_2) as a tertiary recovery agent. Assessment of the impact of flooding with CO_2 all eligible reservoirs in the United States not yet undergoing enhanced oil recovery (EOR) requires making the best possible use of the experience gained in 40 years of applications. Review of the publicly available literature has located relevant CO_2-EOR information for 53 units (fields, reservoirs, pilot areas) in the United States and 17 abroad.

As the world simultaneously faces an increasing concentration of CO_2 in the atmosphere and a higher demand for fossil fuels, the CO_2-EOR process continues to gain popularity for its efficiency as a tertiary recovery agent and for the potential for having some CO_2 trapped in the subsurface as an unintended consequence of the enhanced production (Advanced Resources International and Melzer Consulting, 2009). More extensive application of CO_2-EOR worldwide, however, is not making it significantly easier to predict the exact outcome of the CO_2 flooding in new reservoirs. The standard approach to examine and manage risks is to analyze the intended target by conducting laboratory work, running simulation models, and, finally, gaining field experience with a pilot test. This approach, though, is not always possible. For example, assessment of the potential of CO_2-EOR at the national level in a vast country such as the United States requires making forecasts based on information already available.

Although many studies are proprietary, the published literature has provided reviews of CO_2-EOR projects. Yet, there is always interest in updating reports and analyzing the information under new perspectives. Brock and Bryan (1989) described results obtained during the earlier days of CO_2-EOR from 1972 to 1987. Most of the recovery predictions, however, were based on intended injections of 30 percent the size of the reservoir's hydrocarbon pore volume (HCPV), and the predictions in most cases badly missed the actual recoveries because of the embryonic state of tertiary recovery in general and CO_2 flooding in particular at the time. Brock and Bryan (1989), for example, reported for the Weber Sandstone in the Rangely oil field in Colorado, an expected recovery of 7.5 percent of the original oil in place (OOIP) after injecting a volume of CO_2 equivalent to 30 percent of the HCPV, but Clark (2012) reported that after injecting a volume of CO_2 equivalent to 46 percent of the HCPV, the actual recovery was 4.8 percent of the OOIP. Decades later, the numbers by Brock and Bryan (1989) continue to be cited as part of expanded reviews, such as the one by Kuuskraa and Koperna (2006). Other comprehensive reviews including recovery factors are those of Christensen and others (2001) and Lake and Walsh (2008). The Oil and Gas Journal (O&GJ) periodically reports on active CO_2-EOR operations worldwide, but those releases do not include recovery factors. The monograph by Jarrell and others (2002) remains the most technically comprehensive publication on CO_2 flooding, but it does not cover recovery factors either.

This chapter is a review of the literature found in a search for information about CO_2-EOR. It has been prepared as part of a project by the U.S. Geological Survey (USGS) to assess the incremental oil production that would be technically feasible by CO_2 flooding of all suitable oil reservoirs in the country not yet undergoing tertiary recovery.

Data Acquisition and Normalization

The method of choice for predicting the effectiveness of CO_2-EOR has been to assess the tertiary recovery, *EOR*, as the product of the recovery factor (*RF*) and the original oil in place (*OOIP*) in each reservoir:

$$EOR = RF \cdot OOIP \tag{D1}$$

Although equation D1 is simple in form, the dependence of both variables on several other factors leads to complexity and makes the modeling and displaying of results difficult. In order to obtain more accurate predictions, it is customary to differentiate recovery factors by lithology and prepare two-dimensional graphs as a function of cumulative CO_2 injected.

[1]U.S. Geological Survey.

To express *RF* in percent, convert equation D1 by dividing *EOR* by *OOIP* (that is, normalize *EOR*) and multiply by 100:

$$RF = 100 \cdot \frac{EOR}{OOIP} \tag{D2}$$

The CO_2 injected is also normalized as a fraction of the *OOIP*, except that here the conversion is more elaborate because we are dealing with two different fluids, which in the U.S. system of units are measured in different units (Olea, 2015). The normalized variable is *HCPV,* which is measured as a percentage of the *OOIP*:

$$HCPV = 100 \cdot \frac{inj_{CO2}}{e \cdot OOIP}$$
$$e = 48.156 \cdot B_o \cdot \rho_{CO2res} \tag{D3}$$

where

inj_{CO2} is the cumulative injected CO_2, in standard cubic feet (SCF);

OOIP is the original oil in place, in stock tank barrels (STB);

B_o is the oil formation volume factor, in reservoir barrel per stock tank barrel;

ρ_{CO2res} is the density of CO_2 at reservoir conditions, in pounds per cubic foot (lb/cf); and

e is the conversion factor from *OOIP* to CO_2 volume.

The literature search was done primarily with three engines: OnePetro, Google Search, and Scopus. The results are summarized in table D1 (which follows the "References Cited" for this chapter). The table has 70 entries, of which 76 percent are for operations in the United States. Of the floodings, 73 percent have been clearly identified as operating under miscible conditions, 16 percent operated under immiscible conditions, and the remainder operated in unspecified conditions. Uneven reports of facts were a general problem in the research; it was impossible to collect 100 percent of the information of interest for any of the 70 units.

The minimum requirement for a unit to be included in the table was to have information on recovery after undergoing CO_2 flooding. As much as possible, entries were restricted to actual results from field operations. The table was completed with information about other variables commonly associated with CO_2 flooding recovery.

It was considered convenient to have two entries for recovery: latest reported figure and ultimate recovery. Because most CO_2 floods are still in operation, most of the ultimate recovery values are extrapolated predictions. Field values for ultimate recoveries and associated injection volumes are notoriously scarce. Conversely, most of the other values are actual results. Some of the "last reports" are from several years ago because analysts commonly stop publishing about a reservoir after the initial excitement is over. Numerous fields have never been the subject of a publication, making their inclusion impossible in any review.

The table was completed starting backwards from the most recent reference. When older references did not contribute with information already reported in newer ones, the older references were ignored. For example, eight publications have information on the Lost Soldier Tensleep field in Wyoming, but information relevant to table D1 was covered by only three of the most recent five publications. The Lockhart Crossing field in Louisiana, on the contrary, was only mentioned in the presentation by Wood (2010). As a result, 45 percent of the consulted references are not cited in the table because they have been superseded by more recent data, they are not the original source, or they did not contain information valuable for this compilation.

Analysis of the Information about CO_2-EOR Recovery

An analysis of the values in table D1 allows detecting outliers and providing some perspective. Figures D1 and D2 cover the variations of recovery with HCPV injected for the two main lithologies: clastic and carbonate. For convenience in the display, volumes of CO_2 injections were limited to 150 percent of the HCPV despite availability of three larger values at 320 percent, 242 percent, and 160 percent. The values at 150 percent were interpolated from the original curves. Recoveries for the North Coles Levee field in California were ignored systematically in all figures because they are significantly different from the rest of the reported values.

Instead of mathematically fitting a curve to the cloud of points, actual recovery curves (among the few in the literature) were included to summarize general trends. For the miscible operations in clastic reservoirs (fig. D1), such a curve was a composite of two curves from two fields in Wyoming (Eves and Nevarez, 2009): Wertz Tensleep from 0 to 45 percent of the HCPV and Lost Soldier Tensleep from 50 percent of the HCPV and up. In the immiscible case, the selected curves are from Trinidad and Tobago (Mohammed-Singh and Singhal, 2005): from Forrest Reserve pilot EOR 26 up to 70 percent of the HCPV and from Forrest Reserve pilot EOR 33 above 95 percent of the HCPV. For miscible flooding in carbonate reservoirs (fig. D2), the summary recovery curve is an average between the recoveries for two fields in the Permian Basin of Texas: the Seminole field and the Denver unit of the Wasson field (Stell, 2005). Information was insufficient to investigate a trend in immiscible flooding in carbonate reservoirs.

For clastic reservoirs (fig. D1), except for the abnormal values for the Quarantine Bay pilot in Louisiana and the Oropouche pilot in Trinidad and Tobago (about 14 percent), reported values are roughly within 4 percentage points from the summary recovery curve. Dispersion of data for the carbonate reservoirs follows a different style (fig. D2). Except for four data points with deviations larger than 4 percentage

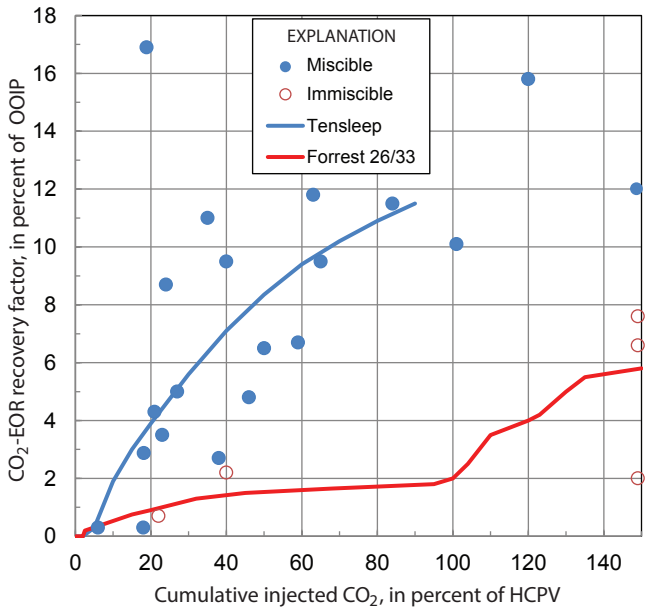

Figure D1. Graph showing recovery factors versus cumulative injected carbon dioxide for clastic reservoirs. Dots denote reported point values summarized in table D1, and the continuous curves are regarded as representative summaries of the general trends. The sources of the composite curves of actual data (Tensleep and Forrest 26/33) are explained in the text. CO_2-EOR, carbon dioxide enhanced oil recovery; HCPV, hydrocarbon pore volume; OOIP, original oil in place.

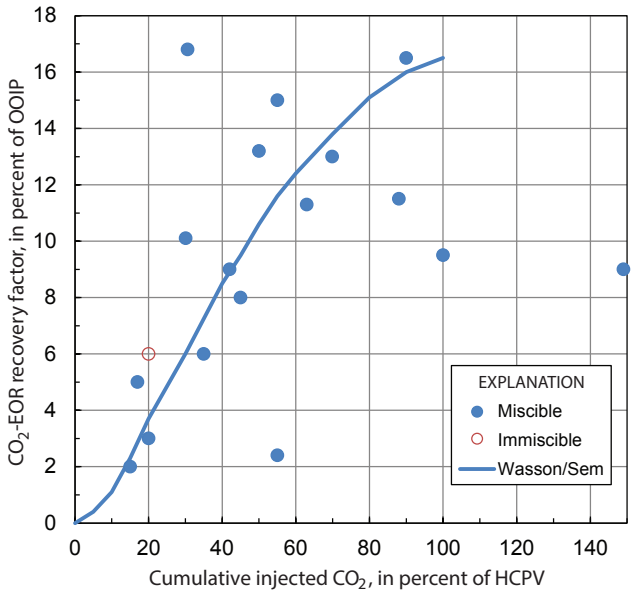

Figure D2. Graph showing recovery factors versus cumulative injected carbon dioxide for carbonate reservoirs. Dots denote reported point values summarized in table D1, and the continuous curve is regarded as a representative summary of the general trend; see details in the text. CO_2-EOR, carbon dioxide enhanced oil recovery; HCPV, hydrocarbon pore volume; OOIP, original oil in place.

points, the remaining points are closer to the type curve. The two most anomalous points, closest to the lower right corner of figure D2, are for the Beaver Creek field in Wyoming. They follow a different trend, which most likely is the result of the highly fractured nature of the reservoir (Peterson and others, 2012).

According to this compilation, there is little difference in recovery below 20 percent of HCPV for CO_2 injection. Above that value, however, the greater the injection, the larger the margin in favor of the carbonate reservoirs. For example, on average, a volume of CO_2 equivalent to 90 percent of the HCPV recovers 16 percent of the original oil in place (OOIP) when injected in a carbonate reservoir, but only 11.5 percent of the OOIP when injected into a clastic reservoir; these results are in close agreement with the 12 percent for clastic reservoirs and 17 percent for carbonate reservoirs reported by van't Veld and Phillips (2010) as ultimate recoveries based on 115 CO_2 floods worldwide.

Analysis of Other Attributes of Interest

Oil density determines to a large extent the feasibility of a reservoir being a candidate for miscible CO_2 flooding. It is often reported in terms of American Petroleum Institute (API) gravity, a dimensionless number comparing the relative density of oil to water, which has a gravity of 10 degrees API (°API). API gravity is loosely and inversely related to viscosity. Unlike geologic characteristics, such as porosity, oil density at standard conditions is a fluid property without significant spatial variation across a reservoir. Consequently, one number is sufficient to characterize exactly a reservoir. In addition, because it is easy to measure, it is one of the variables related to CO_2-EOR most widely reported in the literature, often as degrees of API gravity. The findings are summarized in table D1 and figure D3. There has been a tendency to CO_2-flood reservoirs containing light oils. The average API gravity for clastic and carbonate reservoirs differs by a fraction of one percentage point, not a significant difference. Each histogram in figures D3–D7 includes a list of statistics. For definitions of these terms, see, for example, Olea (2010).

As we have seen, the number of immiscible CO_2 floodings reported in the literature is small. Miscibility is prevented mainly by two factors: (1) oil gravity is too low to have a miscible flood, say, below 25 °API, and (2) gravity is medium to high, but miscibility of CO_2 in oil is not possible because the reservoir is too shallow. The literature reports five reservoirs in the first category, all clastic reservoirs, and three in the second category, with two being carbonate reservoirs.

All other factors being the same, the larger the remaining (or residual) oil saturation of a reservoir, the higher is its CO_2-EOR recovery factor. Oil saturation monotonically declines during production. Thus, the oil saturation at the start of CO_2 flooding will be different depending on the initial conditions and the production history. In the modeling of

CO_2-EOR recovery factors, it is customary to assume that the CO_2 flooding is always preceded by waterflooding. One of the attributes of critical importance in reservoir simulations is the remaining oil saturation in those portions of the reservoir thoroughly flushed by the waterflooding, often denoted as *Sorw* (Verma and others, 1994). In table D1, the similar variable *ResSo* refers to the oil saturation before CO_2 flooding whether or not it was preceded by waterflooding. In other parts of the reservoir, the saturation is higher, closer to the initial oil saturation. Values of *Sorw* imply nothing about the reservoir's volumetric extension. Reported values of *Sorw* are few despite its importance in CO_2-EOR simulation. They are even scarcer when the analysis requires additional evidence that the CO_2 flooding was preceded by waterflooding. The values behind figures D4 and D5 are those listed in table D1. The mean values follow closely the default values of 25 percent for clastic reservoirs and 38 percent for carbonate reservoirs used by the National Petroleum Council (NPC, 1984) and are within the interval of 20 to 35 percent postulated by Tzimas and others (2005). Neither of the numbers published in those two sources, however, is supported with data or references.

Biennially, the Oil and Gas Journal reports results of EOR operations after contacting operators, the latest one being that of Koottungal (2014). The saturation information requested by the journal has been done in terms of "Satur. start" and "Satur. end." Although not reported in the journal version, the saturations are clearly specified as oil saturations in the form distributed by the O&GJ to the operators (Lake and others, 2014). Less clear is the process to which the saturations apply, for which there are discrepancies even among the O&GJ staff (Jacqueline Roueche, Lynxnet LLC, written communications, 2015). Are the data for the start and end of the present recovery process or of the previous one? Even though the most valuable information to have is the starting oil saturation for the current EOR process at those places previously reached by waterflooding (*Sorw*), some of the reported values are so high that they seem to be starting oil saturations before waterflooding. Given this state of confusion, table D1 and the histograms for *Sorw* in figure D4 were prepared by ignoring all the values reported by the O&GJ as well as those from Jarrell and others (2002), who do not disclose sources and also report starting and ending saturations with some quite high values most likely taken from the O&GJ. Nonetheless, it is interesting to note that selected values of "Satur. end" from Koottungal (2014) can produce similar values to those in figure D4, suggesting that some operators interpret "Satur. end" as *Sorw* regardless of the intent of the O&GJ questionnaires. For example, for clastic reservoirs, when four values from Koottungal (2014) are considered in addition to those in figure D4, the mean is 26.8 percent. For carbonate reservoirs, the sample size can significantly increase to 21 by taking 13 of the values from Koottungal (2014) for a mean *Sorw* of 33.5 percent for the sample of size 21.

Bootstrapping is a method to numerically model uncertainty in the calculation of a sample parameter, say, the mean. The method is quite straightforward; it is based on resampling the data, with replacement, multiple times. Given a sample, the bootstrap method allows numerical modeling of any statistics (Efron and Tibshirani, 1993; Pyrcz and Deutsch, 2014), such as the mean. Figure D5 shows the results for the data in figure D4.

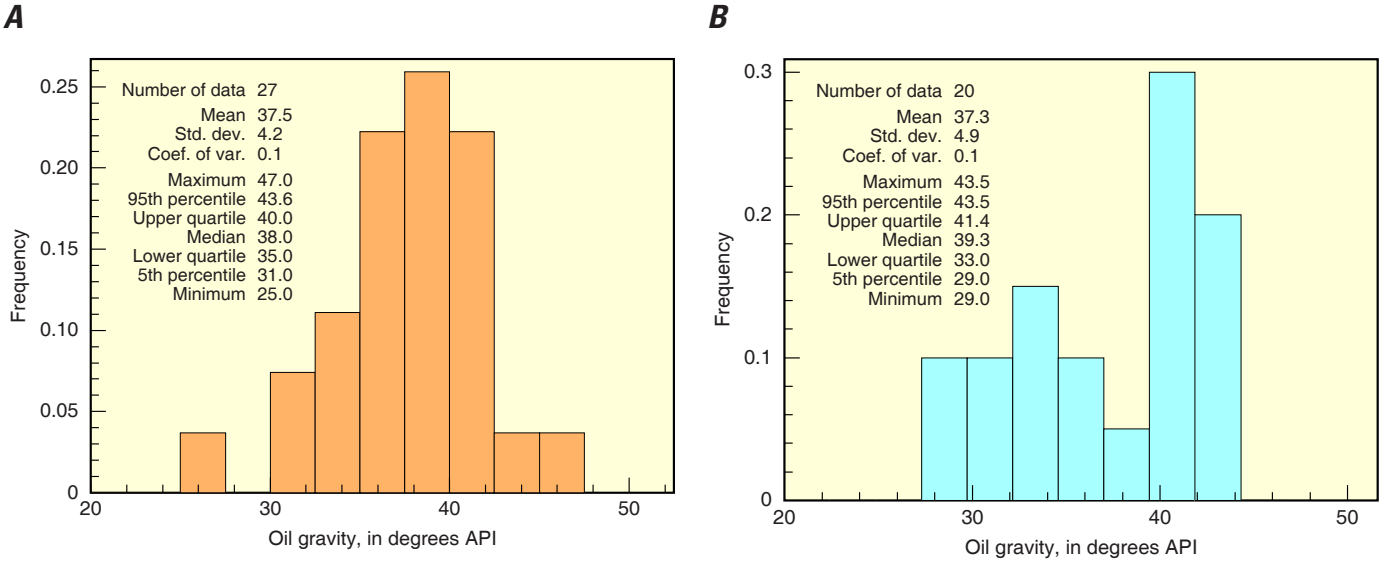

Figure D3. Histograms showing frequency of oil gravity at standard conditions for units under miscible CO_2 flooding for (*A*) clastic reservoirs and (*B*) carbonate reservoirs. Data are from table D1. API, American Petroleum Institute; Coef. of var., coefficient of variation; Std. dev., standard deviation.

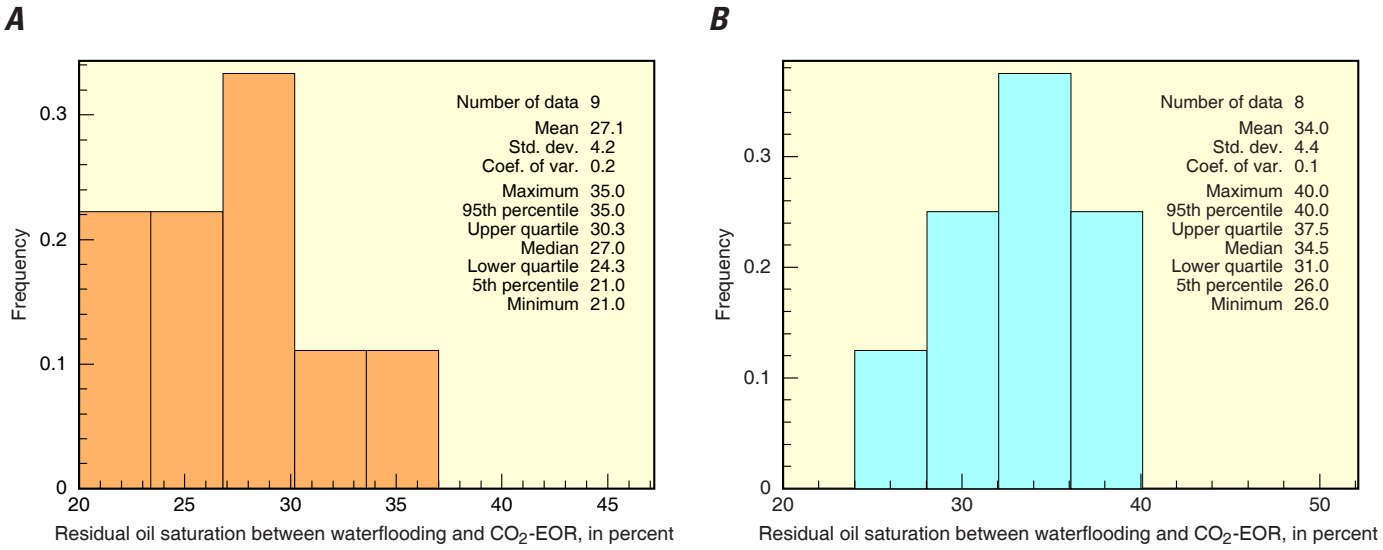

Figure D4. Histograms showng the frequency of residual oil saturation at the beginning of carbon dioxide enhanced oil recovery (CO_2-EOR) when preceded by waterflooding (*Sorw*) for (*A*) clastic reservoirs and (*B*) carbonate reservoirs. Data are from table D1. Coef. of var., coefficient of variation; Std. dev., standard deviation.

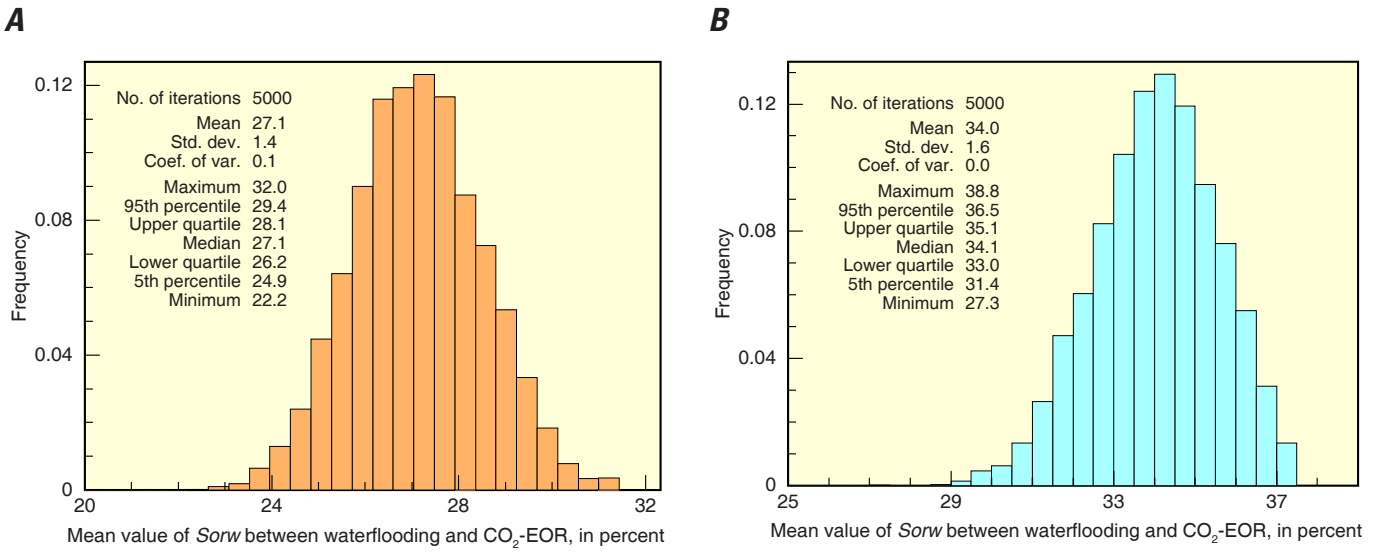

Figure D5. Histograms showing the distribution of the mean value of residual oil saturation (*Sorw*) for the data in figure D4 for (*A*) clastic reservoirs and (*B*) carbonate reservoirs. The distribution shows the proportion of data in each class (frequency). CO_2-EOR, carbon dioxide enhanced oil recovery; Coef. of var., coefficient of variation; No., number; Std. dev., standard deviation.

In reservoir simulation, the value of *Sorw* used ought to be the average value over the field or reservoir. However, the Seminole San Andres unit is the only unit with enough disaggregated information (table D2) to attempt inferring a field average value (fig. D6). It is worth noting that the levels of uncertainty in the national averages and the Seminole average as measured by the interval from the 5th percentile to the 95th percentile are within 1 percentage point (4.5–5.5).

Another variable of the highest importance in CO_2-EOR simulation is the Dykstra-Parsons coefficient (Tiab and Donaldson, 2012). Unfortunately, the information in the literature is minimal and primarily for miscible processes in clastic reservoirs. As reported in table D1, no values were found for the Dykstra-Parsons coefficient of vertical permeability variation (V_{DP}) for any form of CO_2-EOR in carbonates; all the 11 values were for clastic reservoirs, of which 1 was for the immiscible category, and the remaining 10 were for the miscible category. Figure D7 summarizes the findings for clastic reservoirs under miscible CO_2-EOR; the three values for the Katz Strawn unit were averaged so that figure D7 could show one value for each of eight reservoirs. The values closely follow those graphically summarized by Willhite (1986).

Table D2. Residual oil saturation values for flow units within the Seminole San Andres unit, Texas.

[Source: Wang and others (1998). *Sorw*, residual oil saturation after waterflooding; %, percent]

Flow unit	*Sorw* (%)
Wackestone	40
Packstone I	35
Packstone II	35
Packstone III	35
Moldic grainstone I	40
Moldic grainstone II	40
Highly moldic grainstone	40
Grainstone I	35
Grainstone II	25
Grainstone III	25

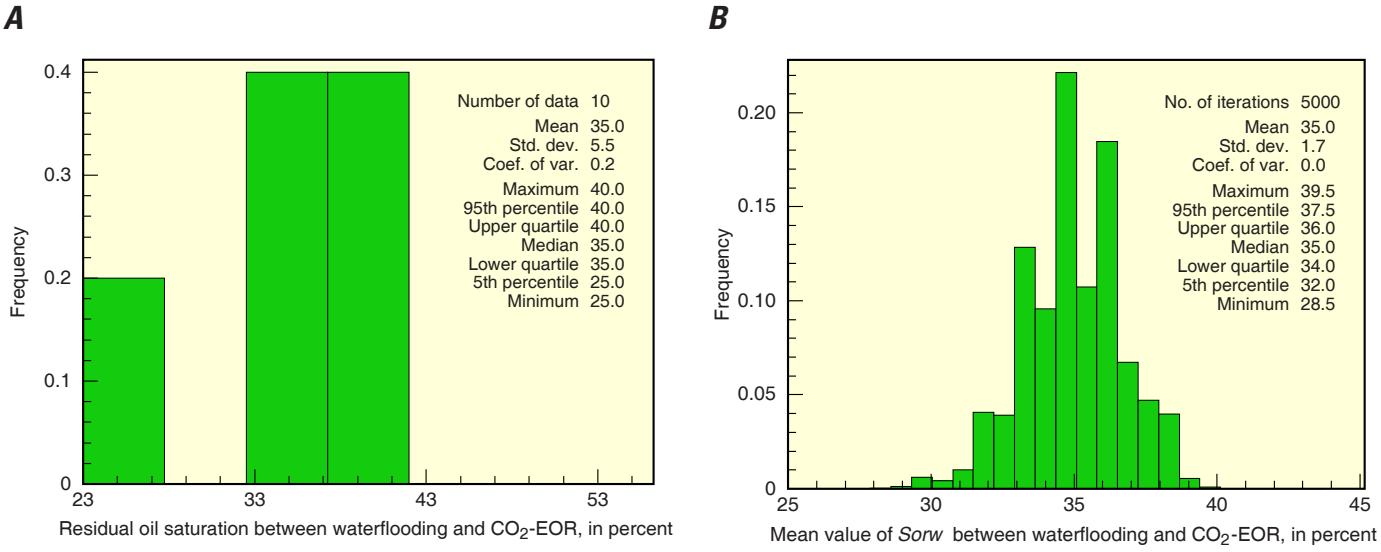

Figure D6. Histograms for residual oil saturation after waterflooding (*Sorw*) for the Seminole San Andres (carbonate) unit showing (*A*) frequency distribution of the data and (*B*) distribution of the mean. CO_2-EOR, carbon dioxide enhanced oil recovery; Coef. of var., coefficient of variation; No., number; Std. dev., standard deviation.

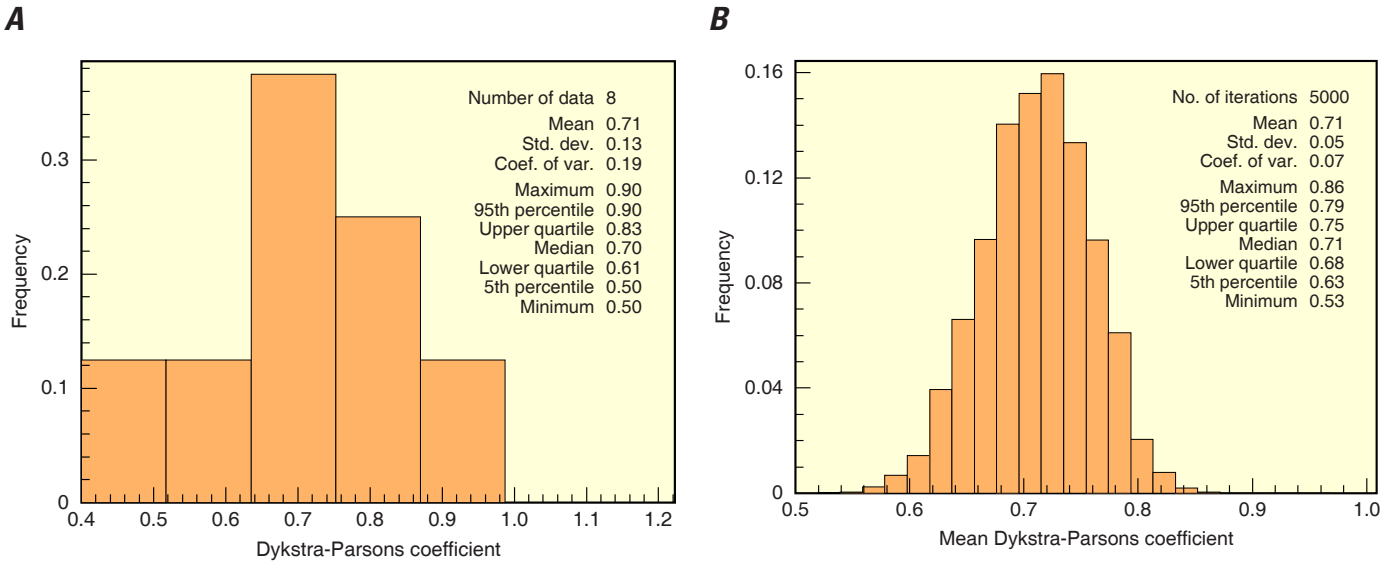

Figure D7. Histograms summarizing reported values for the Dykstra-Parsons coefficient in miscible carbon dioxide (CO_2) flooding of clastic reservoirs and showing (*A*) frequency of 8 values found in the literature (table D1) and (*B*) distribution for the mean obtained by bootstrapping. Coef. of var., coefficient of variation; No., number; Std. dev., standard deviation.

Conclusions

A search of the literature has provided CO_2-EOR data for 70 units (table D1). Recovery-factor values in the dataset and additional values that may be obtained from decline curve analysis should allow calibration against ground truth of hypothetical oil recoveries generated by computer modeling.

Analysis beyond the mere collection of recovery values has provided some results that have been used to formulate generalizations for the national assessment. Lack of complete records reduced the number of units possible to consider in the analyses, compromising the significance of the findings because of the small sample sizes. The main findings are summarized below:

- On average, for large injected CO_2 volumes under miscible conditions, the recovery factors for carbonate reservoirs are larger than those for clastic reservoirs.
- In general, immiscible flooding is significantly less efficient than miscible flooding.
- Despite the dependence of the CO_2-EOR recovery factor on several other attributes than injected volume, there is a general trend in the dependence to injected volume that roughly can be captured by summary recovery curves.
- Of 60 units with both gravity and miscibility information in table D1, 49 are miscible, of which 26 units are clastic reservoirs (ss, sandstone) and 18 are carbonate reservoirs (dl, dolomite; ls, limestone; f.ls, fractured limestone). Independent of the lithology, in the case of miscible flooding, the tendency has been to use CO_2 to flood reservoirs producing light oils that have an average gravity of about 37 °API.
- The mean value of residual oil saturation after waterflooding (*Sorw*) is 27.1 percent for clastic reservoirs and 34.0 percent for carbonate reservoirs. The confidence interval from the 5th to 95th percent for the Seminole San Andres unit in Texas is 5.5 percent, while the same confidence interval from the 5th to 95th percent is remarkably similar for all clastic reservoirs in the literature (4.5 percent) and for all carbonate reservoirs (5.1 percent).
- For the Dykstra-Parsons coefficient of vertical permeability variation, there was enough information to summarize values related to miscible floods in clastic reservoirs. The values are in the range of 0.50–0.90 and have a mean of 0.71.

References Cited

Advanced Resources International (ARI), 2006, Basin oriented strategies for CO_2 enhanced oil recovery; Rocky Mountain region [of Colorado, Utah, and Wyoming]: Prepared for U.S. Department of Energy, Office of Fossil Energy–Office of Oil and Natural Gas, 98 p., accessed October 6, 2016, at http://www.adv-res.com/pdf/Basin%20Oriented%20Strategies%20-%20Rocky_Mountain_Basin.pdf.

Advanced Resources International and Melzer Consulting, 2009, CO_2 storage in depleted oilfields; Global application criteria for carbon dioxide enhanced oil recovery: Report to the International Energy Agency (IAE) Greenhouse Gas R&D Programme, Technical Report 2009–12, 154 p., accessed October 6, 2016, at http://www.ieaghg.org/docs/General_Docs/Reports/2009-12.pdf.

Andrei, Maria, De Simoni, Michela, Delbianco, Alberto, Cazzani, Piero, and Zanibelli, Laura, 2010, Enhanced oil recovery with CO_2 capture and sequestration, *in* World Energy Congress 2010 (WEC Montreal 2010), Montreal, Quebec, Canada, 12–16 September 2010: London, World Energy Council, v. 3, p. 2015–2034. [Also available at http://www.proceedings.com/08705.html.]

Bailey, Alan, 2010, CO_2 triple win at Salt Creek oil field; Injected carbon dioxide acts as a cleaning solvent in wells, forcing out oil: Greening of Oil Web page, accessed May 14, 2015, at http://www.greeningofoil.com/post/CO2-triple-win-at-Salt-Creek-oil-field.aspx.

Beliveau, Dennis, Payne, D.A., and Mundry, Martin, 1993, Waterflood and CO_2 flood of the fractured Midale field: Journal of Petroleum Technology, v. 45, no. 9, p. 881–887, paper SPE–22946–PA.

Bellavance, J.F.R., 1996, Dollarhide Devonian CO_2 flood; Project performance review 10 years later: Paper presented at the SPE Permian Basin Oil & Gas Recovery Conference, Midland, Texas, March 27–29, 1996, p. 395–403, paper SPE–35190–MS.

Birarda, G.S., Dilger, C.W., and McIntosh, Ian, 1990, Re-evaluation of the miscible WAG flood in the Caroline field, Alberta: SPE Reservoir Engineering, v. 5, no. 4, p. 453–458, paper SPE–18066–PA.

Bishop, D.L., Williams, M.E., Gardner, S.E., Smith, D.P., and Cochrane, T.D., 2004, Vertical conformance in a mature carbonate CO_2 flood; Salt Creek field unit, Texas: Paper presented at the Abu Dhabi International Petroleum Exhibition and Conference, paper SPE–88720–MS, 9 p.

Brinkman, F.P., Kane, T.V., McCullough, R.R., and Miertschin, J.W., 1998, Use of full-field simulation to design a miscible CO_2 flood: Paper presented at the 11th SPE/DOE Improved Oil Recovery Symposium, Tulsa, Oklahoma, April 19–22, 1998, p. 265–276, paper SPE–39629–MS.

Brock, W.R., and Bryan, L.A., 1989, Summary results of CO_2 EOR field tests, 1972–1987, *in* Proceedings; SPE Joint Rocky Mountain Regional/Low Permeability Reservoirs Symposium and Exhibition, March 6–8, 1989, Denver, Colorado: [Richardson, Texas,] Society of Petroleum Engineers, p. 499–508, paper SPE–18977–MS.

Brownlee, M.H., and Sugg, L.A., 1987, East Vacuum Grayburg-San Andres unit CO_2 injection project; Development and results to date, *in* Proceedings; 1987 SPE Annual Technical Conference and Exhibition, September 27–30, 1987, Dallas, Texas: [Richardson, Texas,] Society of Petroleum Engineers, p. 241–254, paper SPE–16721–MS.

Chen, T., Kazemi, H., and Davis, T.L., 2014, Integration of reservoir simulation and time-lapse seismic in Delhi field; A continuous CO_2 injection EOR project: Paper presented at the 19th SPE Improved Oil Recovery Symposium, Tulsa, Oklahoma, April 12–16, 2014, paper SPE–169049–MS, 10 p.

Chidsey, T.C., Jr., Allis, R.G., Malkewicz, S.E., Groen, Wilson, McPherson, Brian, and Heath, Jason, 2006, Aneth oil field, southeastern Utah; Demonstration site for geologic sequestration of carbon dioxide: Poster presentation at the 5th Annual Conference on Carbon Capture & Sequestration, Alexandria, Virginia, May 8–11, 2006, 3 panels, accessed October 6, 2016, at http://geology.utah.gov/emp/co2sequest/pdf/poster0506_a.pdf, http://geology.utah.gov/emp/co2sequest/pdf/poster0506_b.pdf, http://geology.utah.gov/emp/co2sequest/pdf/poster0506_c.pdf.

Christensen, J.P., Stenby, E.H., and Skauge, A., 2001, Review of WAG field experience: SPE Reservoir Evaluation and Engineering, v. 4, no. 2, p. 97–106, paper SPE–71203–PA.

Clark, Rory, 2012, Rangely Weber Sand unit case history: Presentation at the 6th Annual Wyoming CO_2 Conference, Casper, Wyoming, July 12, 2012, 31 slides, accessed October 6, 2016, at http://www.uwyo.edu/eori/_files/co2conference12/rory_rangelycasehistory.pdf.

Cook, B.R., 2012, Wyoming's miscible CO_2 enhanced oil recovery potential from main pay zones; An economic scoping study: Laramie, Wyo., University of Wyoming, Department of Economics and Finance, 78 p., accessed October 6, 2016, at http://www.uwyo.edu/eori/_files/docs/wyomings%20miscible%20co2-eor%20potential%20-%20benjamin%20r.%20cook.pdf.

Davis, D.W., 1994, Project design of a CO_2 miscible flood in a waterflooded sandstone reservoir, *in* Proceedings; SPE/DOE Ninth Symposium on Improved Oil Recovery, 17–20 April 1994, Tulsa, Oklahoma: [Richardson, Texas,] Society of Petroleum Engineers, p. 239–252, paper SPE–27758–MS.

Denbury Resources, 2012, All oil companies are not alike: Presentation at the 2012 CO_2 Conference, 31 slides, accessed October 6, 2016, at http://www.co2conference.net/wp-content/uploads/2012/12/1445-Schneider-Denbury-CO2-EOR-Strategies-12-4-12.pdf.

Desch, J.B., Larsen, W.K., Lindsay, R.F., and Nettle, R.L., 1984, Enhanced oil recovery by CO_2 miscible displacement in the Little Knife field, Billings County, North Dakota: Journal of Petroleum Technology, v. 36, no. 9, p. 1592–1602, paper SPE–10696–PA.

Dutton, S.P., Flanders, W.A., and Barton, M.D., 2003, Reservoir characterization of a Permian deep-water sandstone, East Ford field, Delaware basin, Texas: AAPG Bulletin, v. 87, no. 4, p. 609–627.

Efron, Bradley, and Tibshirani, R.J., 1993, An introduction to the bootstrap: Dordrecht, The Netherlands, Springer Science + Business Media, 436 p.

Electric Power Research Institute, 1999, Enhanced oil recovery scoping study: Electric Power Research Institute [report] TR–113836, prepared for EPRI by Advanced Resources International, variously paged [137 p.], accessed October 6, 2016, at http://www.energy.ca.gov/process/pubs/electrotech_opps_tr113836.pdf.

Estublier, Audrey, Dino, Rodolfo, Schinelli, M.C., Barroux, Claire, and Munoz Beltran, Alvaro, 2011, CO_2 injection in Buracica; Long-term performance assessment: Energy Procedia, v. 4, p. 4028–4035, accessed October 6, 2016, at http://www.sciencedirect.com/science/article/pii/S1876610211006230.

Eves, K.E., and Nevarez, J.J., 2009, Update of Lost Soldier/Wertz floods; Living in a constrained CO_2 environment: Presentation at the 15th Annual CO_2 Flooding Conference, Midland, Texas, December 10–11, 2009, 21 slides, accessed October 6, 2016, at http://www.co2conference.net/wp-content/uploads/2012/12/2009CO2FloodingConference_MeritEnergyBaroilPresentation_Nevarez-Eves.pdf.

Evolution Petroleum Corporation, 2013, Delhi field EOR project: Evolution Petroleum Corporation Web site, accessed October 6, 2016, at http://www.evolutionpetroleum.com/delhi.html.

Flanders, W.A., and DePauw, R.M., 1993, Update case history; Performance of the Twofreds tertiary CO_2 project, *in* Proceedings; 68th SPE Annual Technical Conference and Exhibition, Houston, Texas, October 3–6, 1993: [Richardson, Texas,] Society of Petroleum Engineers, p. 41–50, paper SPE–26614–MS.

Flanders, W.A., Stanberry, W.A., and Martínez, Manuel, 1990, CO_2 injection increases Hansford Marmaton production: Journal of Petroleum Technology, v. 42, no. 1, p. 68–73, paper SPE–17327–PA.

Folger, L.K., and Guillot, S.N., 1996, A case study of the development of the Sundown Slaughter unit CO_2 flood, Hockley County, Texas, *in* Proceedings; [SPE] Permian Basin Oil and Gas Recovery Conference, Midland, Texas, March 27–29, 1996: [Richardson, Texas,] Society of Petroleum Engineers, p. 381–393, paper SPE–35189–MS.

Fox, M.J., Simlote, V.N., Stark, K.L., and Brinlee, L.D., 1988, Review of CO_2 flood, Springer "A" sand, Northeast Purdy unit, Garvin County, Oklahoma: SPE Reservoir Engineering, v. 3, no. 4, p. 1161–1167, paper SPE–14938–PA.

Gaines, Jason, 2008, Monell unit CO_2 flood, Patrick Draw field, Sweetwater County, Wyoming: Presentation at the 2d Annual Wyoming CO_2 Conference, Casper, Wyoming, May 29–30, 2008, 33 slides, accessed May 14, 2015, at http://www.uwyo.edu/eori/_files/co2conference08/jason%20gaines_anadarko_eori_co2%20casper%20may%2029%202008.pdf.

Garcia Quijada, Marylena, 2005, Optimization of a CO_2 flood design, Wasson field, West Texas: College Station, Texas, Texas A&M University, master's thesis, 92 p., accessed October 6, 2016, at http://oaktrust.library.tamu.edu/bitstream/handle/1969.1/4138/etd-tamu-2005B-PETE-Garcia.pdf?sequence=1&isAllowed=y.

Harpole, K.J., and Hallenbeck, L.D., 1996, East Vacuum Grayburg San Andres unit CO_2 flood ten year performance review; Evolution of a reservoir management strategy and results of WAG optimization, *in* Proceedings; 1996 SPE Annual Technical Conference and Exhibition, Denver, Colorado, October 6–9, 1996: [Richardson, Texas,] Society of Petroleum Engineers, p. 309–318, paper SPE–36710–MS.

Hervey, J.R., and Iakovakis, A.C., 1991, Performance review of a miscible CO_2 tertiary project; Rangely Weber Sand unit, Colorado: SPE Reservoir Engineering, v. 6, no. 2 (May 1991), p. 163–168, paper SPE–19653–PA.

Hill, W.J., Tinney, T.J., Young, L.C., and Stark, K.L., 1994, CO_2 operating plan, South Welch unit, Dawson County, Texas, *in* Overcoming today's challenges through shared technology, teamwork, and innovation—Proceedings; Permian Basin Oil and Gas Recovery Conference, March 16–18, 1994, Midland, Texas: [Richardson, Texas,] Society of Petroleum Engineers, p. 493−504, paper SPE–27676–MS.

Hoiland, R.C., Joyner, H.D., and Stalder, J.L., 1986, Case history of a successful Rocky Mountain pilot CO_2 flood, *in* Proceedings; SPE/DOE Fifth Symposium on Enhanced Oil Recovery, April 20–23, 1986, Tulsa, Oklahoma: [Tulsa, Oklahoma,] Society of Petroleum Engineers, p. 199−208, paper SPE–14939–MS.

Holtz, M.H., 2009, Gulf Coast CO_2 enhanced oil recovery case studies: University of Texas, class notes, 46 slides, accessed May 14, 2015, at http://www.beg.utexas.edu/pttc/archive/reservegrowth1205/holtz-casestudies.pdf.

Howard, Bruce, 2013, Wellman field case history: Presentation at the 19th Annual CO_2 Flooding Conference, Midland, Texas, December 11–13, 2013, 24 slides, accessed October 6, 2016, at http://www.co2conference.net/wp-content/uploads/2013/12/9-Wellman_Case-History-2013_CO2_Conference.pdf.

Hsie, J.C., and Moore, J.S., 1988, The Quarantine Bay 4RC CO_2 WAG pilot project; A postflood evaluation: SPE Reservoir Engineering, v. 3, no. 3, p. 809–814, paper SPE–15498–PA.

Hunt, R.D., and Hearn, C.L., 1982, Reservoir management of the Hartzog Draw field: Journal of Petroleum Technology, v. 34, no. 7, p. 1575–1582, paper SPE–10195–PA.

Imai, Nobuo, and Reeves, Scott, 2004, Feasibility study on CO_2 EOR of White Tiger field in Vietnam (CO_2 capture from Phu-My power plant): Presentation at the Third Annual DOE Conference on Carbon Capture and Sequestration, Alexandria, Virginia, May 3–6, 2004, 16 slides, accessed October 6, 2016, at http://www.netl.doe.gov/publications/proceedings/04/carbon-seq/081.pdf.

Jarrell, P.M., Fox, C.E., Stein, M.H., Webb, S.L., Johns, R.T., and Day, L.A., 2002, Practical aspects of CO_2 flooding: Society of Petroleum Engineers Monograph Series, v. 22, 220 p.

Jingcun, Zhang; Shangxian, Xie; Peihui, Han; Jiabao, Chen; Zhenghua, Zhang; and Encang, Guo, 1997, Field test of immiscible CO_2 drive in Daqing oil field: SPE Advanced Technology Series, v. 5, no. 1, p. 49−55, paper SPE 30847–PA.

Keeling, R.J., 1984, CO_2 miscible flooding evaluation of the South Welch unit, Welch San Andres field, *in* Proceedings; SPE/DOE Fourth Symposium on Enhanced Oil Recovery, April 16–18, 1984, Tulsa, Oklahoma: [Dallas, Texas,] Society of Petroleum Engineers, p. 335–346, paper SPE–12664–MS.

Kinder Morgan, 2013, North Cross Devonian unit: Kinder Morgan Web page, accessed May 14, 2015, at http://www.kindermorgan.com/business/co2/success_north_cross.cfm.

Kirkpatrick, R.K., Flanders, W.A., and DePauw, R.M., 1985, Performance of the Twofreds CO_2 injection project: Paper presented at the 60th SPE Annual Technical Conference and Exhibition of SPE, paper SPE–14439–MS, 12 p.

Kleinstelber, S.W., 1990, The Wertz Tensleep CO_2 flood; Design and initial performance: Journal of Petroleum Technology, v. 42, no. 5, p. 630–636, paper SPE–18067–PA.

Knight, William, Schechter, David, Long, Roy, and Ferguson, Daniel, 2004, Advanced reservoir characterization and evaluation of carbon dioxide gravity drainage in the naturally fractured Spraberry reservoir—Research discovers how to waterflood the Spraberry: U.S. Department of Energy, National Energy Technology Laboratory, Project Facts [Factsheet], 2 p., accessed October 6, 2016, at http://www.netl.doe.gov/KMD/cds/disk22/D-Reservoirs%20-%20Characterization%20with%20CO2%20Component/BC14942%20project%20facts.pdf.

Koottungal, Leena, ed., 2014, 2014 worldwide EOR survey: Oil and Gas Journal, v. 112, no. 4 (April 7, 2014), p. 79–84, accessed October 6, 2016, at http://www.ogj.com/articles/print/volume-112/issue-4/special-report-eor-heavy-oil-survey/2014-worldwide-eor-survey.html.

Kumar, Rajeshwar, and Eibeck, J.N., 1984, CO_2 flooding a waterflooded shallow Pennsylvanian sand in Oklahoma; A case history, *in* Proceedings; SPE/DOE Fourth Symposium on Enhanced Oil Recovery, April 16–18, 1984, Tulsa, Oklahoma: [Dallas, Texas,] Society of Petroleum Engineers, p. 367−376, paper SPE–12668–MS.

Kuuskraa, V.A., 2008, Maximizing oil recovery efficiency and sequestration of CO_2 with "next generation" CO_2-EOR technology: Presentation at the 2d Petrobras International Seminar on CO_2 Capture and Geological Storage, September 9–12, 2008, Salvador, Bahia, Brazil, 19 slides, accessed October 6, 2016, at http://www.adv-res.com/pdf/V_Kuuskraa%20Petrobras%20CO2%20SEP%2008.pdf.

Kuuskraa, V.A., 2012, CO_2 utilization with enhanced oil recovery; The new paradigm for CO_2 capture and storage: Presentation at the 10th Annual Carbon Management Workshop, Midland, Texas, December 4, 2012, 31 slides, accessed October 6, 2016, at http://www.co2conference.net/wp-content/uploads/2012/12/0815-Kuuskraa-ARI-EOR-Size-of-the-Prize-ROZ-12-4-12.pdf.

Kuuskraa, V.A., and Koperna, G.J., 2006, Evaluating the potential for "game changer" improvements in oil recovery efficiency from CO_2 enhanced oil recovery: Report to the U.S. Department of Energy, 120 p., accessed May 14, 2015, at http://www.adv-res.com/pdf/Game_Changer_Document.pdf.

Lake, L.W., and Walsh, M.P., 2008, Enhanced oil recovery (EOR) field data literature search: Technical report prepared for Danish North Sea Partner, Danish Energy Agency, and Mærsk Olie og Gas AS, 112 p., accessed May 14, 2015, at http://www.ens.dk/sites/ens.dk/files/undergrund-forsyning/olie-gas/felter-produktion-danmark/foroeget-indvinding-eor/EOR_Report_Final.pdf.

Lake, L.W., Yang, Andrew, and Pan, Zhong, 2014, Listening to the data; An analysis of the Oil and Gas Journal database: Paper presented at the 19th SPE Improved Oil Recovery Symposium, Tulsa, Oklahoma, April 12–16, 2014, paper SPE–169056–MS, 11 p.

Lee, K.H., and El-Saleh, M.M., 1990, A full-field numerical modeling study for the Ford Geraldine unit CO_2 flood: Paper presented at SPE/DOE Seventh Symposium on Enhanced Oil Recovery, April 22–25, 1990, Tulsa, Oklahoma, p. 517–528, paper SPE–20227–MS.

Lin, E.C., and Poole, E.S., 1991, Numerical evaluation of single-slug, WAG, and hybrid CO_2 injection processes, Dollarhide Devonian unit, Andrews County, Texas: SPE Reservoir Engineering, v. 6, no. 4, p. 415–420, paper SPE–20098–PA.

Lino, U.R.A., 2005, Case history of breaking a paradigm; Improvement of an immiscible gas-injection project in Buracica field by water injection at the gas-oil contact: Paper presented at the SPE Latin American and Caribbean Petroleum Engineering Conference, Rio de Janeiro, Brazil, June 20–23, 2005, paper SPE–94978–MS, 8 p.

MacAllister, D.J., 1989, Evaluation of a CO_2 flood performance; North Coles Levee CO_2 pilot, Kern County, California: Journal of Petroleum Technology, v. 41, no. 2, p. 185–194, paper SPE–15499–PA.

Magruder, J.B., Stiles, L.H., and Yelverton, T.D., 1990, Review of the Means San Andres unit CO_2 tertiary project: Journal of Petroleum Technology, v. 42, no. 5, p. 638–644, paper SPE–17349–PA.

Martin, F.D., Stevens, J.E., and Harpole, K.J., 1995, CO_2-foam field test at the East Vacuum Grayburg/San Andres unit: SPE Reservoir Engineering, v. 10, no. 4, p. 266–272, paper SPE–27786–PA.

Martin, F.D., and Taber, J.J., 1992, Carbon dioxide flooding: Journal of Petroleum Technology, v. 44, no. 4, p. 396–400, paper SPE–23564–PA.

Masoner, L.O., and Wackowski, R.K., 1995, Rangely Weber Sand unit CO_2 project update: SPE Reservoir Engineering, v. 10, no. 3, p. 203–207, paper SPE–27755–PA.

Mathiassen, O.M., 2003, CO_2 as injection gas for enhanced oil recovery and estimation of the potential on the Norwegian continental shelf: Trondheim, Norwegian University of Science and Technology, Department of Petroleum Engineering and Applied Geophysics, thesis, part 1 of 2, 96 p., accessed October 6, 2016, at http://www.co2.no/download.asp?DAFID=28&DAAID=6.

Merchant, D.H., 2010, Life beyond 80; A look at conventional WAG recovery beyond 80% HCPV injected in CO_2 tertiary floods: Paper presented at the SPE International Conference on CO_2 Capture, Storage, and Utilization, New Orleans, Louisiana, November 10–12, 2010, paper SPE–139516–MS, 14 p.

Merritt, M.B., and Groce, J.F., 1992, A case history of the Hanford San Andres miscible CO_2 project: Journal of Petroleum Technology, v. 44, no. 8, p. 924–929, paper SPE–20229–PA.

Meyer, J.P. [, 2010], Summary of carbon dioxide enhanced oil recovery (CO_2EOR) injection well technology: American Petroleum Institute, 54 p., accessed October 6, 2016, at http://www.api.org/~/media/files/ehs/climate-change/summary-carbon-dioxide-enhanced-oil-recovery-well-tech.pdf.

Mizenko, G.J., 1992, North Cross (Devonian) unit CO_2 flood; Status report: Paper presented at the SPE/DOE Eighth Symposium on Enhanced Oil Recovery, April 22–24, 1992, Tulsa, Oklahoma, p. 537–546, paper SPE–24210–MS.

Moffitt, P.D., and Zornes, D.R., 1992, Postmortem analysis; Lick Creek Meakin Sand unit immiscible CO_2 waterflood project: Paper presented at the 67th SPE Annual Technical Conference and Exhibition, Washington, D.C., October 4–7, 1992, p. 813–826, paper SPE–24933–MS.

Mohammed-Singh, L.J., and Singhal, A.K., 2005, Lessons from Trinidad's CO_2 immiscible pilot projects: SPE Reservoir Evaluation and Engineering, v. 8, no. 5, p. 397–403, paper SPE–89364–PA.

Moore, J.S., 1986, Design, installation, and early operation of the Timbalier Bay S–2B(RA)SU gravity-stable, miscible CO_2-injection project: SPE Production Engineering, v. 1, no. 5, p. 369–378, paper SPE–14287–PA.

Moore, J.S., and Clark, G.C., 1988, History match of the Maljamar CO_2 pilot performance, *in* Proceedings; SPE/DOE Sixth Symposium on Enhanced Oil Recovery, April 17–20, 1988, Tulsa, Oklahoma: [Tulsa, Oklahoma,] Society of Petroleum Engineers, p. 35–47, paper SPE–17323–MS.

Mukherjee, J., Norris, S.O., Nguyen, Q.P., Scherlin, J.M., Vanderwal, P.G., and Abbas, S., 2014, CO_2 foam pilot in Salt Creek field, Natrona County, WY; Phase I, Laboratory work, reservoir simulation, and initial design: Paper presented at the 19th SPE Improved Oil Recovery Symposium (IOR 2014), Tulsa, Oklahoma, USA, 12–16 April 2014, paper SPE–169166–MS, 21 p.

Nagai, R.B., and Redmond, G.W., 1983, Numerical simulation of a gravity stable, miscible CO_2 injection project in a West Texas carbonate reef: Paper presented at the Middle East Oil Technical Conference of SPE, Manama, Bahrain, 14–17 March 1983, p. 29–41, paper SPE–11129–MS.

National Petroleum Council (NPC), 1984, Enhanced oil recovery: Washington, D.C., National Petroleum Council, variously paged [285 p.], accessed October 6, 2016, at http://www.npc.org/reports/rd1984-Enhanced_Oil_Recovery.pdf.

Oil & Gas Journal, 2004, Cogdell unit CO_2 flood yields positive results: Oil & Gas Journal digital article from April 12, 2004, accessed October 6, 2016, at http://www.ogj.com/articles/print/volume-102/issue-14/special-report/cogdell-unit-cosub2-sub-flood-yields-positive-results.html.

Olea, R.A., 2010, Basic statistical concepts and methods for earth scientists (revised February 2010): U.S. Geological Survey Open-File Report 2008–1017, 191 p., accessed October 6, 2016, at http://pubs.usgs.gov/of/2008/1017/.

Olea, R.A., 2015, CO_2 retention values in enhanced oil recovery: Journal of Petroleum Science and Engineering, v. 129 (May 2015), p. 23–28.

Page, James, 2009, Salt Creek field; CO_2 flood performance: Presentation at the 3d Annual Wyoming CO_2 Conference, Casper, Wyoming, June 23–24, 2009, 21 slides, accessed October 6, 2016, at http://www.uwyo.edu/eori/_files/co2conference09/james%20page%20eori%202009.pdf.

Peterson, C.A., Pearson, E.J., Chodur, V.T., and Periera[sic], Carlos, 2012, Beaver Creek Madison CO_2 enhanced [oil] recovery project case history; Riverton, Wyoming: Paper presented at the 18th SPE Improved Oil Recovery Symposium, Tulsa, Oklahoma, April 14–18, 2012, paper SPE–152862–MS, 18 p.

Pittaway, K.R., Albright, J.C., Hoover, J.W., and Moore, J.S., 1987, The Maljamar CO_2 pilot; Review and results: Journal of Petroleum Technology, v. 39, no. 10, p. 1256–1260, paper SPE–14940–PA.

Pittaway, K.R., and Rosato, R.J., 1991, The Ford Geraldine unit CO_2 flood—Update 1990: SPE Reservoir Engineering, v. 6, no. 4, p. 410–414, paper SPE–20118–PA.

Plumb, L.B., and Ferrell, H.H., 1989, An evaluation of the CO_2 pilot Maljamar field, Lea County, New Mexico: U.S. Department of Energy report DOE/BC/10830–12, 24 p., accessed October 6, 2016, at http://www.netl.doe.gov/kmd/cds/disk44/D-CO2%20Injection/BC10830_12.pdf.

Pyo, K., Damián-Díaz, N., Powell, M., and Van Nieuwkerk, J., 2003, CO_2 flooding in Joffre Viking pool: Paper presented at the Petroleum Society of Canada's Canadian International Petroleum Conference, Calgary, Alberta, June 10–12, 2003, paper PETSOC–2003–109, 30 p.

Pyrcz, M.J., and Deutsch, C.V., 2014, Geostatistical reservoir modeling (2d ed.): New York, Oxford University Press, 433 p.

Resolute Energy Corporation, 2012, An update on the Greater Aneth field: Presentation at the 18th Annual CO_2 Flooding Conference, Midland, Texas, December 7, 2012, 31 slides, accessed October 6, 2016, at http://www.co2conference.net/wp-content/uploads/2012/12/02-HoppeMidland_CO2_conference_Greater_Aneth_Field_12-7-12.pdf.

Resolute Energy Corporation, 2013, An update on the Greater Aneth field: Presentation at the 7th Annual Wyoming CO_2 Conference, Casper, Wyoming, July 10–11, 2013, 32 slides, accessed October 6, 2016, at http://www.uwyo.edu/eori/conferences/co2/2013%20presentations/hoppe.pdf.

Ring, J.N., and Smith, D.J., 1995, An overview of the North Ward Estes CO_2 flood: Paper presented at the SPE Annual Technical Conference & Exhibition, Dallas, Texas, October 22–25, 1995, p. 115–122, paper SPE–30729–MS.

Rocha, P.S.; Dino, Rodolfo; Sanches, Christovam; and Le Thiez, Pierre, 2007, Assessing the CO_2 storage as a by-product of EOR activities in the Buracica oil field—Recôncavo Basin, NE Brazil: Paper presented at the 6th Annual Conference on Carbon Capture & Sequestration, Pittsburgh, Pennsylvania, May 7–10, 2007, 33 slides, accessed October 6, 2016, at http://www.netl.doe.gov/publications/proceedings/07/carbon-seq/data/papers/tue_046.pdf.

Rojas, J.H., 2002, Design and history matching of a waterflood/miscible CO_2 flood model of a mature field; The Wellman unit, West Texas: College Station, Texas, Texas A&M University, master's thesis, 188 p.

Sahin, Secaeddin; Kalfa, Ulker; and Celebioglu, Demet, 2008, Bati Raman field immiscible CO_2 application—Status quo and future plans: SPE Reservoir Evaluation and Engineering, v. 11, no. 4, p. 778–791, paper SPE–106575–PA.

Sahin, Secaeddin; Kalfa, Ulker; Celebioglu, Demet; Duygu, Ersan; and Lahna, Hakki, 2012, A quarter century of progress in the application of CO_2 immiscible EOR project in Bati Raman heavy oil field in Turkey: Paper presented at the SPE Heavy Oil Conference Canada, Calgary, Alberta, June 12–14, 2012, paper SPE–157865–MS, 14 p.

Sahin, Secaeddin; Kalfa, Ulker; Uysal, Serkan; Kilic, Harun; and Lahna, Hakki, 2014, Design, implementation and early operating results of steam injection pilot in already CO_2 flooded deep-heavy oil fractured carbonate reservoir of Bati Raman field, Turkey: Paper presented at the 19th SPE Improved Oil Recovery Symposium, Tulsa, Oklahoma, April 12–16, 2014, paper SPE–169035–MS, 14 p.

Saller, A.H.; Walden, Skip; Robertson, Steve; Nims, Robert; Schwab, Joe; Hagiwara, Hiroshi; and Mizohata, Shigeharu, 2006, Three-dimensional seismic imaging and reservoir modeling of an upper Paleozoic "reefal" buildup, Reinecke field, West Texas, United States: [AAPG] Search and Discovery Article 20044, 19 p., accessed October 6, 2016, at http://www.searchanddiscovery.com/documents/2006/06144saller/images/saller.

Schechter, D.S., Grigg, Reid, Guo, Boyun, and Schneider, Barry, 1998, Wellman unit CO_2 flood; Reservoir pressure reduction and flooding the water/oil transition zone: Paper presented at the SPE Annual Technical Conference and Exhibition, New Orleans, Louisiana, September 27–30, 1998, p. 39–50, paper SPE–48948–MS.

Schlumberger Excellence in Education Development, 2014, The Weyburn oil field; Enhanced oil recovery: Schlumberger Excellence in Education Development Web page, accessed October 6, 2016, at http://web.archive.org/web/20151231132914/http://www.planetseed.com/related-article/weyburn-oil-field-enhanced-oil-recovery.

Senocak, Didem, 2008, Evaluation of sweep efficiency of a mature CO_2 flood in Little Creek field, Mississippi: Baton Rouge, Louisiana State University, master's thesis, 178 p., accessed October 6, 2016, at http://etd.lsu.edu/docs/available/etd-10302008-040624/unrestricted/Senocak_Thesis.pdf.

Senocak, Didem, Pennell, S.P., Gibson, C.E., and Hughes, R.G., 2008, Effective use of heterogeneity measures in the evaluation of a mature CO_2 flood: Paper presented at SPE/DOE Symposium on Improved Oil Recovery, Tulsa, Oklahoma, April 20–23, 2008, paper SPE–113977–MS, 9 p.

Smith, D.J., Kelly, T.R., Schmidt, D.L., and Bowden, C.E., 2012, Katz (Strawn) unit miscible CO_2 project; Design, implementation, and early performance: Paper presented at the 18th SPE Symposium on Improved Oil Recovery, Tulsa, Oklahoma, April 14–18, 2012, paper SPE–154023–MS, 19 p.

SPE International, 2013, CO_2 miscible flooding case studies: PetroWiki page, accessed October 6, 2016, at http://petrowiki.spe.org/CO2_miscible_flooding_case_studies.

Spivak, Allan, Garrison, W.H., and Nguyen, J.P., 1990, Review of an immiscible CO_2 project, tar zone, fault block V, Wilmington field, California: SPE Reservoir Engineering, v. 5, no. 2, p. 155–162, paper SPE–17407–PA.

Stein, M.H., Frey, D.D., Walker, R.D., and Parlani, G.J., 1992, Slaughter Estate unit CO_2 flood; Comparison between pilot and field-scale performance: Journal of Petroleum Technology, v. 44, no. 9, p. 1026–1032, paper SPE–19375–PA.

Stell, Mike, 2005, Reserve booking guidelines for CO_2 floods; A practical approach from a reserve auditor: Presentation at the 11th Annual CO_2 Flooding Conference, Midland, Texas, December 7–8, 2005, 51 slides, accessed October 6, 2016, at https://www.ryderscott.com/wp-content/uploads/CO2-05-Slide-Stell.pdf.

Tanner, C.S., Baxley, P.T., Crump, J.G., III, and Miller, W.C., 1992, Production performance of the Wasson Denver unit CO_2 flood: Paper presented at the 8th SPE/DOE Symposium on Enhanced Oil Recovery, Tulsa, Oklahoma, April 22–24, 1992, p. 11–22, paper SPE–24156–MS.

Thakur, G.C., Lin, C.J., and Patel, Y.R., 1984, CO_2 minitest, Little Knife field, ND; A case history: Paper presented at the 4th SPE Symposium on Enhanced Oil Recovery, Tulsa, Oklahoma, April 15–18, 1984, p. 331–346, paper SPE–12704–MS.

Tiab, Djebbar, and Donaldson, E.C., 2012, Petrophysics; Theory and practice of measuring reservoir rock and fluid transport properties (3d ed.): Waltham, Mass., Gulf Professional Publishing, 950 p.

Tzimas, E., Geogakaki, A., Garcia Cortes, C., and Peteves, S.D., 2005, Enhanced oil recovery using carbon dioxide in the European energy system: European Commission Report EUR 21895 EN, 119 p., accessed October 6, 2016, at http://science.uwaterloo.ca/~mauriced/earth691-duss/CO2_General%20CO2%20Sequestration%20materilas/CO2_EOR_Misciblein%20Europe21895EN.pdf.

Uj, Istvan, and Fekete, Tibor, 2011, CO_2 gas + WAG + water injection in the same oil reservoir—Case study: Paper presented at the SPE Enhanced Oil Recovery Conference, Kuala Lumpur, Malaysia, July 19–21, 2011, paper SPE–143833–MS, 10 p.

van't Veld, Klaas, and Phillips, O.R., 2010, The economics of enhanced oil recovery: Estimating incremental oil supply and CO_2 demand in the Powder River Basin: Energy Journal, v. 31, no. 4, p. 31−55.

Verma, M.K., Boucherit, Michael, and Bouvier, Lucienne, 1994, Evaluation of residual oil saturation after waterflood in a carbonate reservoir: SPE Reservoir Engineering, v. 9, no. 4, p. 247–253, paper SPE–21371–PA.

Wang, F.P., Lucia, F.J., and Kerans, Charles, 1998, Integrated reservoir characterization study of a carbonate ramp reservoir; Seminole San Andres unit, Gaines County, Texas: SPE Reservoir Evaluation and Engineering, v. 1, no. 2, p. 105–113, paper SPE–36515–PA.

Wehner, S.C., 2009, A CO_2 EOR update from "no man's land"; Challenges & successes, Postle field, Texas Co[unty], Oklahoma: Presentation at the 15th Annual CO_2 Flooding Conference, Midland, Texas, December 10–11, 2009, 29 slides, accessed October 6, 2016, at http://www.co2conference.net/wp-content/uploads/2012/12/2009CO2FloodingConference_Whiting_Wehner.pdf.

Wilkinson, J.R., Genetti, D.B., Henning, G.T., Broomhall, R.W., and Lawrence, J.J., 2004, Lessons learned from mature carbonates for application to Middle East fields: Paper presented at the 11th Abu Dhabi International Petroleum Exhibition and Conference, Abu Dhabi, UAE, October 10–13, 2004, paper SPE–88770–MS, 12 p.

Willhite, G.P., 1986, Waterflooding: Society of Petroleum Engineers Textbook Series, v. 3, 326 p.

Wilson, M., and Monea, M., eds., 2004, IEA GHG Weyburn CO_2 monitoring & storage project; Summary report 2000–2004: Regina, Saskatchewan, Canada, Petroleum Technology Research Centre, 273 p., accessed October 6, 2016, at http://ptrc.ca/+pub/document/Summary_Report_2000_2004.pdf.

Winzinger, Rudi, Brink, J.L., Patel, K.S., Davenport, C.B., Patel, Y.R., and Thakur, G.C., 1991, Design of a major CO_2 flood, North Ward Estes field, Ward County, Texas: SPE Reservoir Engineering, v. 6, no. 1, p. 11–16, paper SPE–19654–PA.

Wo, Shaochang, 2007, CO_2 demand estimates for major oil fields in Wyoming basins: Presentation at the Wyoming Enhanced Oil Recovery Institute (EORI) Joint Producers Meeting, Wyoming, June 26, 2007, 26 slides, accessed October 6, 2016, at http://www.uwyo.edu/eori/_files/co2conference07/shaochang_co2_demand_estimates_v2.pdf.

Wood, Nik, 2010, Lockhart Crossing; Economically efficient reservoir operations: Presentation at the 16th Annual CO_2 Flooding Conference, Midland, Texas, December 10, 2010, 43 slides, accessed October 6, 2016, at http://www.co2conference.net/wp-content/uploads/2012/12/3-2_Wood_Denbury_LockhartCrossing.pdf.

Xiao, Chongwei, Harris, M.L., Wang, F.P., and Grigg, R.B., 2011, Field testing and numerical simulation of combined CO_2 enhanced oil recovery and storage in the SACROC field: Paper presented at the Canadian Unconventional Resources Conference, Calgary, Alberta, Canada, November 15–17, 2011, paper SPE–147544–MS, 17 p.

Yuan, M., Mosley, J., and Hyer, N., 2001, Mineral scale control in a CO_2 flooded oilfield: Paper presented at the SPE International Symposium on Oilfield Chemistry, Houston, Texas, February 13–16, 2001, paper SPE–65029–MS, 7 p.

Zhou, Dengen, Yan, Meisong, and Calvin, W.M., 2012, Optimization of a mature CO_2 flood—From continuous injection to WAG: Paper presented at the 18th SPE Improved Oil Recovery Symposium, Tulsa, Oklahoma, April 14–18, 2012, paper SPE–154181–MS, 9 p.

Table D1. Carbon dioxide (CO_2) recovery factors and other related information for petroleum-producing units in the United States, Canada, and countries outside North America

Definitions of terms in table D1 are given below by column from left to right.

Column 1: Petroleum-producing units in column 1 include fields, reservoirs, and pilot areas.

Column 2: Loc.=location by ISO (International Organization for Standardization) 3166 code; data for U.S. States come first and their codes have omitted the prefix "US" (AR, Arkansas; CA, California; CO, Colorado; LA, Louisiana; MS, Mississippi; ND, North Dakota; NM, New Mexico; OK, Oklahoma; TX, Texas; UT, Utah; WY, Wyoming); data for Canada follow, and their codes have omitted the prefix "CA" (AB, Alberta; SK, Saskatchewan); and data for countries outside North America complete the table (BR, Brazil; CN, China; HU, Hungary; IT, Italy; NO, Norway; TR, Turkey; TT, Trinidad and Tobago; UK, United Kingdom; VN, Vietnam).

Column 3: Grav.=American Petroleum Institute oil gravity, in degrees (°API).

Column 4: Conditions: M=miscible or I=immiscible or M/I=miscible and immiscible.

Column 5: Injection method: c→WAG=continuous followed by water alternating with gas; Contin.=continuous; TWAG=tapered water alternating with gas; WAG=water alternating with gas.

Column 6: Lithology (Lith.) terms: chalk, cht=chert, dl=dolomite, f.=fractured, grn=granite, ls=limestone, ss=sandstone.

Column 7: V_{DP}=Dykstra-Parsons coefficient of vertical permeability variation.

Column 8: *OOIP*=original oil in place, in millions of stock tank barrels (MMstb).

Column 9: Pr. + Sec.=primary plus secondary recovery, in percent (%); a single number denotes an aggregated value.

Column 10: *ResSo*=residual oil saturation before starting the CO_2 flooding, in percent.

Column 11: CO_2 start=initial year of CO_2 flooding.

Columns 12, 13, and 14: Last report=last mention in the literature of CO_2 flooding results.

Column 12: *RFco2*=recovery factor for CO_2 flooding (in percent of OOIP) at the date specified in column 13.

Column 13: Year=date reported in the literature.

Column 14: $HCPV_i$=hydrocarbon injected, in percent of pore volume. An asterisk (*) denotes a value estimated for this report using equation D3.

Columns 15 and 16: Ultimate recov.=predicted results at the end of the CO_2 injection.

Column 15: *Ult.RF* =final recovery factor for the CO_2-EOR, in percent of OOIP.

Column 16: $HCPV_i$=CO_2 volume necessary to inject to obtain the ultimate recovery, in percent of pore volume.

Table D1. Carbon dioxide (CO_2) recovery factors and other related information for petroleum-producing units in the United States, Canada, and countries outside North America.

[—, no data. Other terms are defined on p. D15]

General information										
Unit	Loc.	Grav. (°API)	M/I	Method	Lith.	V_{DP}	*OOIP* (MMstb)	Pr. + Sec. (%)	*ResSo* (%)	CO_2 start
United States										
Lick Creek pilot	AR	17	I	WAG	ss	—	15.8	31.9 + 11.1	—	1976
North Coles Levee pilot CLA 487.	CA	36	M	TWAG	ss	—	—	—	34	1981
North Coles Levee pilot CLA 488.	CA	36	M	TWAG	ss	—	—	—	34	1981
North Coles Levee pilot 5 spot	CA	36	M	TWAG	ss	—	—	—	34	1981
Wilmington field	CA	14	I	WAG	ss	—	69.5	—	—	1982
Rangely Weber field	CO	34	M	TWAG	ss	—	1,810	21 + 21	25	1986
Delhi field	LA	—	M	WAG	ss	—	357	57	—	—
Lockhart Crossing field	LA	42	M	—	ss	—	56	12 + 20	—	2007
Paradis pilot	LA	39	M	Contin.	ss	—	—	—	20	1984
Quarantine Bay pilot	LA	32	M	WAG	ss	—	—	—	38	1981
Timbalier Bay pilot RS-1BSU	LA	39	M	Contin.	ss	—	20.6	44 + none	29	1984
Weeks Island B reservoir	LA	32	M	Contin.	ss	—	3.3	24 + 54	22	1978
Little Creek field	MS	39	M	—	ss	0.5–0.89	102	25 + 22	21	1985
West Mallalieu	MS	38	M	—	ss	—	—	—	15	1986
Little Knife field, minitest	ND	41	M	WAG	dl	—	195	—	40	1980
East Vacuum	NM	38	M	WAG	ss/dl	—	296	25 + 15	30	1985
Maljamar 6th Zone pilot	NM	36	M	Contin.	dl	—	107	21 + 23	30	1981
Maljamar 9th Zone pilot	NM	36	M	Contin.	dl	—	26	21 + 23	40	1981
Garber field pilot	OK	47	M	Contin.	ss	—	—	—	25.3	1981
Northeast Purdy unit	OK	34.9	M	WAG	ss	—	225	16 + 22	—	1983
Postle Morrow unit	OK	42	M	TWAG	ss	—	300	34.7	—	1995
Sho-Vel-Tum	OK	25	M	—	ss	—	210	—	59	1982
Cogdell Canyon Reef unit	TX	40	M	WAG	ls	—	117	—	—	2001
Dollarhide	TX	40	M	WAG	cht	—	145.6	13.4 + 29.6	25	1985
East Ford	TX	40	M	—	ss	0.52	18.4	16 + none	49	1995
Ford Geraldine unit	TX	40	M	Contin.	ss	—	99	18 + 4.5	31	1981
Hanford San Andres field	TX	32	M	WAG	dl	—	17	17.9 + 14.2	—	1986
Hansford Marmaton field	TX	38	I	WAG	ss	0.92	12.5	13 + none	43	1980
Katz Strawn unit	TX	38	M	c→WAG	ss	0.82 0.67 0.64	206	14 + 19	—	2010

Table D1. Carbon dioxide (CO_2) recovery factors and other related information for petroleum-producing units in the United States, Canada, and countries outside North America.—Continued

[—, no data. Other terms are defined on p. D15]

Last report			Ultimate recov.		References
RFco2 (%)	Year	*HCPV*$_i$ (%)	*Ult.RF* (%)	*HCPV*$_i$ (%)	
United States—Continued					
11.1	1990	242	—	—	Moffitt and Zornes (1992); Jarrell and others (2002).
25.8	1984	38	—	—	MacAllister (1989): Jarrell and others (2002).
21.8	1984	61	—	—	MacAllister (1989); Jarrell and others (2002).
15.6	1984	38	—	—	MacAllister (1989): Jarrell and others (2002).
0.7	1986	22*	—	—	Spivak and others (1990); Merchant (2010).
4.8	2011	46	—	—	Hervey and Iakovakis (1991); Masoner and Wackowski (1995); Advanced Resources International (2006); Clark (2012).
—	—	—	17	—	Evolution Petroleum Corporation (2013); Chen and others (2014).
2.7	2010	38	—	—	Wood (2010).
14.5	1985	—	—	—	Holtz (2009).
16.9	1987	18.9	—	—	Hsie and Moore (1988); Holtz (2009).
—	—	30	23	—	Moore (1986); Kuuskraa and Koperna (2006); Holtz (2009).
8.7	1987	24	—	—	Jarrell and others (2002); Kuuskraa and Koperna (2006); Holtz (2009).
18.4	2007	—	—	—	Jarrell and others (2002); Senocak (2008); Senocak and others (2008).
—	—	—	18.5	—	Martin and Taber (1992); Jarrell and others (2002).
—	1981	—	8	—	Desch and others (1984); Thakur and others (1984).
2	1996	16	10	—	Brownlee and Sugg (1987); Martin and others (1995); Harpole and Hallenbeck (1996); Jarrell and others (2002).
16.8	1986	30.6	—	—	Pittaway and others (1987); Moore and Clark (1988); Plumb and Ferrell (1989).
10.1	1986	30.1	—	—	Pittaway and others (1987); Moore and Clark (1988); Plumb and Ferrell (1989).
11	1984	35	14	—	Kumar and Eibeck (1984).
2.8	1985	18	7.5	—	Fox and others (1988); Electric Power Research Institute (1999); Jarrell and others (2002).
6.7	2009	59	10.1	101	Jarrell and others (2002); Wehner (2009).
—	—	—	4.8	—	Electric Power Research Institute (1999); Jarrell and others (2002).
11	—	—	17	—	Oil & Gas Journal (12 April 2004); Meyer (2010).
11	1996	11.2	14	—	Lin and Poole (1991); Bellavance (1996).
1	2002	—	—	—	Jarrell and others (2002); Dutton and others (2003).
3.5	1989	24	13	—	Lee and El-Saleh (1990); Pittaway and Rosato (1991); Dutton and others (2003).
14	1989	—	—	—	Merrit and Groce (1992); Jarrell and others (2002).
9	1988	—	—	—	Flanders and others (1990); Jarrell and others (2002).
0.3	2011	18	15.8	120	Smith and others (2012).

Table D1. Carbon dioxide (CO_2) recovery factors and other related information for petroleum-producing units in the United States, Canada, and countries outside North America.—Continued

[—, no data. Other terms are defined on p. D15]

General information										
Unit	Loc.	Grav. (°API)	M/I	Method	Lith.	V_{DP}	*OOIP* (MMstb)	Pr. + Sec. (%)	*ResSo* (%)	CO_2 start
United States—Continued										
Means San Andres unit	TX	29	M	TWAG	dl	—	230	35	34	1983
North Cross unit	TX	44	M	Contin.	cht	—	53	13 + none	49	1972
North Ward Estes	TX	37	M	WAG	ss	0.85	1,100	13 + 28.5	25	1989
Port Neches pilot	TX	35	M	WAG	ss	0.7	10.4	40 + 14	30	1993
Reinecke field	TX	42	M	c→WAG	ls	—	180	50	32	1998
SACROC modern pilot	TX	41.8	M	—	ls	—	144	—	26.1	2008
Salt Creek field	TX	39	M	WAG	ls	—	700	48	—	1993
Seminole field, San Andres unit	TX	35	M	WAG	dl	—	1,100	13 + 22.3	35	1983
Sharon Ridge Canyon unit	TX	43	M	WAG	ls	—	398	50	—	1999
Slaughter Estate unit	TX	33	M	Contin.	dl	—	646	50.5	26	1984
South Welch unit	TX	34.4	M	WAG	dl	—	67	—	50	1993
Spraberry pilot	TX	—	—	—	f.ss	—	10,000	10 + 15	—	2001
Twofreds	TX	36.4	M	WAG	ss	0.5	51	12.9 + 4	—	1974
Wasson field, Denver unit	TX	33	M	WAG	dl	—	2,000	17.2 + 30.1	40	1983
Wellman unit	TX	43.5	M	Contin.	ls	—	127	33 + 11	35	1983
Aneth unit	UT	41	—	WAG	ls	—	534	—	—	1998
McElmo Creek unit	UT	40	—	WAG	ls	—	487	—	—	1985
Beaver Creek	WY	39.5	M	c→WAG	ls/dl	—	109	43.6	—	2008
Hartzog Draw field	WY	36	—	—	ss	—	370	34	—	2016
Lost Soldier Tensleep	WY	34	M	WAG	ss	—	240	19.9 + 24.4	—	1989
Monell unit	WY	43	—	—	ss	—	115	20 + 14	—	2003
Salt Creek	WY	39	M	WAG	ss	—	1,700	40	—	2004
Wertz Tensleep	WY	35	M	—	ss	0.8	172	45.1	—	1986
West Sussex pilot	WY	39	M	Contin.	ss	0.9	33.2	18.1 + 24.1	28	1982
Canada										
Caroline field	AB	42	M	WAG	ss	—	34.6	8.7 + none	—	1984
Joffre Viking pool	AB	40.5	M	WAG	ss	—	30	42	35	1984
Midale field pilot	SK	29	M	—	f.ls	—	500	—	50	1986
Weyburn field	SK	30	M	c→WAG	dl/ls	—	1,400	24	—	2000

Table D1. Carbon dioxide (CO_2) recovery factors and other related information for petroleum-producing units in the United States, Canada, and countries outside North America.—Continued

[—, no data. Other terms are defined on p. D15]

Last report			Ultimate recov.		References
RFco2 (%)	Year	$HCPV_i$ (%)	*Ult.RF* (%)	$HCPV_i$ (%)	
United States—Continued					
15	2012	55	—	—	Magruder and others (1990); Kuuskraa (2008); SPE International (2013).
23	1994	84	—	—	Mizenko (1992); Jarrell and others (2002); Kinder Morgan (2013).
4.3	1995	21	—	—	Winzinger and others (1991); Ring and Smith (1995).
—	—	—	9–15	150	Davis (1994); Holtz (2009).
4	2012	—	—	—	Jarrell and others (2002); Saller and others (2006); Zhou and others (2012).
—	—	—	9	42	Xiao and others (2011).
6	2004	35	9.5	100	Bishop and others (2004); Wilkinson and others (2004); Kuuskraa (2008).
13.7	1998	58	16.5	90	Wang and others (1998); Stell (2005); Meyer (2010).
—	—	—	13	70	Brinkman and others (1998); Yuan and others (2001).
11.5	2005	88	—	—	Stein and others (1992); Folger and Guillot (1996); Stell (2005).
—	—	—	13.2	50	Keeling (1984); Hill and others (1994); Jarrell and others (2002).
—	—	—	6.5	—	Knight and others (2004); Kuuskraa and Koperna (2006).
5	1985	27*	12	—	Kirkpatrick and others (1985); Flanders and DePauw (1993); Dutton and others (2003).
11.3	2003	63	19.5	—	Tanner and others (1992); Garcia Quijada (2005); Stell (2005); Kuuskraa (2012).
5.7	1998	—	16.7	—	Nagai and Redmond (1983); Schechter and others (1998); Rojas (2002); Kuuskraa and Koperna (2006); Howard (2013).
3	2012	20	—	—	Jarrell and others (2002); Chidsey and others (2006); Resolute Energy Corporation (2012).
8	—	45	11.9	—	Jarrell and others (2002); Stell (2005); Resolute Energy Corporation (2013).
2.4	2011	55	12	320	Peterson and others (2012).
—	—	—	7	—	Hunt and Hearn (1982); Wo (2007); van't Veld and Phillips (2010); Denbury Resources (2012).
11.5	2004	84	—	—	Wo (2007); Lake and Walsh (2008); Cook (2012).
2.6	2008	14	—	—	Gaines (2008).
0.3	2008	6	10	—	Gaines (2008); Page (2009); Bailey (2010); Meyer (2010); Mukherjee and others (2014).
9.5	2004	65	—	—	Kleinstelber (1990); Lake and Walsh (2008); Eves and Nevarez (2009).
9.5	1985	40	—	—	Hoiland and others (1986); Lake and Walsh (2008).
Canada—Continued					
5.3	1987	—	—	—	Birarda and others (1990).
11.8	2003	63	16.3	—	Pyo and others (2003).
14	1988	—	17	—	Beliveau and others (1993); Jarrell and others (2002).
2	2004	15	9	—	Wilson and Monea (2004); Schlumberger Excellence in Education Development (2014).

Table D1. Carbon dioxide (CO_2) recovery factors and other related information for petroleum-producing units in the United States, Canada, and countries outside North America.—Continued

[—, no data. Other terms are defined on p. D15]

General information										
Unit	Loc.	Grav. (°API)	M/I	Method	Lith.	V_{DP}	*OOIP* (MMstb)	Pr. + Sec. (%)	*ResSo* (%)	CO_2 start
Countries Outside North America										
Buracica field	BR	35	I	Contin.	ss	—	60.4	36.8	—	1991
Daqing pilot	CN	—	I	WAG	ss	—	—	—	—	1991
PF-A-I reservoir	HU	30.2	M/I	c→WAG	ss	—	—	27.6 + 4.6	—	1973
Armatella	IT	10.4	I	WAG	dl/ls	—	82	—	—	2015
Giaurone	IT	—	—	—	—	—	—	—	—	2015
Ekofisk field	NO	37	M	WAG	chalk	—	6,600	—	—	—
Bati Raman	TR	12	I	c→WAG	f.ls	—	1,850	2 + none	—	1986
Forrest Reserve pilot EOR 4	TT	25	I	Contin.	ss	—	36.4	41.7	—	1986
Forrest Reserve pilot EOR 26	TT	17	I	Contin.	ss	—	1.9	4.9 + none	—	1974
Forrest Reserve pilot EOR 33	TT	19	I	Contin.	ss	—	16.2	17.4	—	1976
Oropouche, pilot EOR 44	TT	29	I	Contin.	ss	—	8.7	17.9 + none	53	1990
Forties field	UK	37	—	WAG	ss	—	4,200	59	27	—
White Tiger field	VN	—	M	—	f.grn	—	3,300	—	—	—

Table D1. Carbon dioxide (CO_2) recovery factors and other related information for petroleum-producing units in the United States, Canada, and countries outside North America.—Continued

[—, no data. Other terms are defined on p. D15]

Last report			Ultimate recov.		References
RFco2 (%)	Year	*HCPV*$_i$ (%)	*Ult.RF* (%)	*HCPV*$_i$ (%)	
Countries Outside North America—Continued					
—	—	—	4.4	—	Lino (2005); Rocha and others (2007); Estublier and others (2011).
4.7	1993	—	—	—	Jingcun and others (1997).
6.5	2010	50	—	—	Uj and Fekete (2011).
—	—	—	5.4	—	Andrei and others (2010).
—	—	—	4	—	Andrei and others (2010).
—	—	—	5.6	—	Mathiassen (2003).
6	2011	20	10	—	Sahin and others (2008, 2012, 2014).
2.2	2003	40	4.7	—	Mohammed-Singh and Singhal (2005).
1.5	—	50	7.6	270	Mohammed-Singh and Singhal (2005).
5.8	2003	150	9.0	—	Mohammed-Singh and Singhal (2005).
3.1	2003	160	3.9	—	Jarrell and others (2002); Mohammed-Singh and Singhal (2005).
—	—	—	4.7	—	Mathiassen (2003).
—	—	—	20	—	Imai and Reeves (2004); Kuuskraa and Koperna (2006).

Summary of the Analyses for Recovery Factors

By Mahendra K. Verma

Chapter E of
Three Approaches for Estimating Recovery Factors in Carbon Dioxide Enhanced Oil Recovery
Mahendra K. Verma, Editor

Scientific Investigations Report 2017–5062–E

U.S. Department of the Interior
U.S. Geological Survey

U.S. Department of the Interior
RYAN K. ZINKE, Secretary

U.S. Geological Survey
William H. Werkheiser, Acting Director

U.S. Geological Survey, Reston, Virginia: 2017

Suggested citation:
Verma, M.K., 2017, Summary of the analyses for recovery factors, chap. E *of* Verma, M.K., ed., Three approaches for estimating recovery factors in carbon dioxide enhanced oil recovery: U.S. Geological Survey Scientific Investigations Report 2017–5062, p. E1–E2, https://doi.org/10.3133/sir20175062E.

ISSN 2328-0328 (online)

Contents

Chapter E. Summary of the Analyses for Recovery Factors

By Mahendra K. Verma[1]

Overview

In order to determine the hydrocarbon potential of oil reservoirs within the U.S. sedimentary basins for which the carbon dioxide enhanced oil recovery (CO_2-EOR) process has been considered suitable, the CO_2 Prophet model was chosen by the U.S. Geological Survey (USGS) to be the primary source for estimating recovery-factor values for individual reservoirs. The choice was made because of the model's reliability and the ease with which it can be used to assess a large number of reservoirs. The other two approaches—the empirical decline curve analysis (DCA) method and a review of published literature on CO_2-EOR projects—were deployed to verify the results of the CO_2 Prophet model. This chapter discusses the results from CO_2 Prophet (chapter B, by Emil D. Attanasi, this report) and compares them with results from decline curve analysis (chapter C, by Hossein Jahediesfanjani) and those reported in the literature for selected reservoirs with adequate data for analyses (chapter D, by Ricardo A. Olea).

To estimate the technically recoverable hydrocarbon potential for oil reservoirs where CO_2-EOR has been applied, two of the three approaches—CO_2 Prophet modeling and DCA—do not include analysis of economic factors, while the third approach—review of published literature—implicitly includes economics. For selected reservoirs, DCA has provided estimates of the technically recoverable hydrocarbon volumes, which, in combination with calculated amounts of original oil in place (OOIP), helped establish incremental CO_2-EOR recovery factors for individual reservoirs.

The review of published technical papers and reports has provided substantial information on recovery factors for 70 CO_2-EOR projects that are either commercially profitable or classified as pilot tests. When comparing the results, it is important to bear in mind the differences and limitations of these three approaches.

Discussion of Recovery Factors with CO_2-EOR from Three Sources

The CO_2 Prophet model was used to evaluate the potential reservoir performance of the CO_2-EOR process using geologic, reservoir, and production data from a comprehensive resource database (CRD) described by Carolus and others (in press). To demonstrate the effectiveness of the model, seven plays containing 143 clastic reservoirs within the Powder River Basin of Wyoming and Montana were chosen to determine recovery-factor (*RF*) values of individual reservoirs as well as to study the sensitivity of some of the reservoir parameters that may have significant effects on *RF* values. The median *RF* values for the seven plays within the Powder River Basin range from 9.50 to 13.43 percent of the OOIP, which seems reasonable when compared to published values adjusted for the amount of CO_2 injected during EOR, expressed as a percentage of the hydrocarbon pore volume (HCPV). The range of calculated *RF* values reflects the variations in reservoir heterogeneity as measured by the pseudo-Dykstra-Parsons coefficient, the oil viscosity, and other variables that may affect the *RF.* For each reservoir, the residual oil saturation (*Sorw*) at the initiation of CO_2-EOR that was preceded by waterflooding was assumed to be 0.25 (which can also be expressed as 25 percent), because all evaluated reservoir lithologies were clastic. Each reservoir was assumed to have a volume of CO_2 equal to 100 percent of the HCPV injected over the duration of the EOR program. However, additional runs were made to assess the impact of increasing the injection volume to 150 percent of the HCPV, and the results showed an increase of 2.5 to 3.5 percentage points in the *RF* values. Also, the incremental increases in the *RF* values due to increased injection are smaller where the value of *Sorw* is smaller.

The DCA evaluation included a total of 15 reservoirs, and the results show that the incremental *RF* values after CO_2-EOR range between 6.6 and 13.8 percent (average 10.9 percent) for the 3 clastic reservoirs and between 7.6 and 25.7 percent (average 13.8 percent) for the 12 carbonate reservoirs, which were mostly dolomites. The results do indicate higher recoveries in carbonate reservoirs compared to clastic reservoirs, but limited data in terms of a smaller number of reservoirs, especially clastic, prevent us from drawing any firm conclusions. Although there were only 15 reservoirs for DCA, their results are found to be within a reasonable range when compared with those from CO_2 Prophet modeling.

A review of technical papers and reports included 70 EOR projects located around the world, of both field-wide application and pilot tests, with the majority of them in the United States. The available information indicates that at CO_2

[1]U.S. Geological Survey.

injection volumes equivalent to 90 percent of the HCPV, the *RF* value for EOR was about 16 percent of the OOIP in carbonate reservoirs and 11.5 percent in clastic reservoirs. This *RF* value for clastic reservoirs (11.5 percent) is falling in the middle of the range of *RF* values from modeling (9.50–13.43 percent) where each reservoir was assumed to have a CO_2 injection volume equivalent to 100 percent of the HCPV.

Discussion of Some Important Variables That Have Significant Effects on *RF* Values

The review of technical papers revealed some interesting observations: (1) all other factors being the same, the larger the value of *Sorw* (oil saturation after waterflooding and prior to application of CO_2-EOR), the higher the *RF* value and (2) one of the attributes of critical importance in reservoir modeling is the *Sorw* in those portions of the reservoir thoroughly flushed by the waterflooding. Unfortunately, reported values of *Sorw* are few despite its importance in CO_2-EOR modeling. The mean values follow closely the default values of 25 percent for clastic reservoirs and 38 percent for carbonate reservoirs used by the National Petroleum Council (NPC, 1984), which later revised the value for carbonate reservoirs to 30.5 percent (Donald J. Remson, National Energy Technology Laboratory, written commun., 2015). The mean values are within the interval of 20 to 35 percent postulated by Tzimas and others (2005). However, neither the numbers from the NPC (1984) nor those from Tzimas and others (2005) are supported by data or references. In the present modeling, the *Sorw* value for clastic reservoirs was set at 25 percent (NPC, 1984), and the value for carbonate reservoirs was set at 30.5 percent (Donald J. Remson, National Energy Technology Laboratory, written commun., 2015). The reservoir information in the CRD could be used by the USGS in an assessment of hydrocarbon potential in the oil reservoirs within the United States that qualify for the application of CO_2-EOR.

Another variable of great importance in *RF* values from the CO_2-EOR modeling is the Dykstra-Parsons coefficient of vertical permeability variation (V_{DP}), as discussed by Tiab and Donaldson (2012). Unfortunately, the information available in the literature is minimal. Because of the lack of data, the algorithm developed by Hirasaki and others (1984, 1989) was used to compute the pseudo-Dykstra-Parsons coefficient. Their algorithm for computing the pseudo-Dykstra-Parsons coefficients resulted in a range in values between 0.5 and 0.98. Due to limitations of the CO_2 Prophet software, the maximum effective value of the pseudo-Dykstra-Parsons coefficient was 0.86 (J.K. Dobitz, Windy Cove Energy, written commun., 2015), and, therefore, the calculated values resulting from the algorithms of Hirasaki and others (1989) that exceeded 0.86 were set to 0.86.

References Cited

Carolus, Marshall, Biglarbigi, Khosrow, Warwick, P.D., Attanasi, E.D., Freeman, P.A., and Lohr, C.D., in press, Overview of a comprehensive resource database for the assessment of recoverable hydrocarbons produced by carbon dioxide enhanced oil recovery: U.S. Geological Survey Techniques and Methods, book 7, chap. C16.

Hirasaki, G.J., Morra, Frank, and Willhite, G.P., 1984, Estimation of reservoir heterogeneity from waterflood performance: Society of Petroleum Engineers, SPE–13415–MS, 10 p.

Hirasaki, G., Stewart, W.C., Elkins, L.E., and Willhite, G.P., 1989, Reply to discussion of the 1984 National Petroleum Council studies on EOR: Journal of Petroleum Technology, v. 41, no. 11, p. 1218–1222.

National Petroleum Council (NPC), 1984, Enhanced oil recovery: Washington, D.C., National Petroleum Council, variously paged [285 p.]. [Also available at http://www.npc.org/reports/rby.html.]

Tiab, Djebbar, and Donaldson, E.C., 2012, Petrophysics; Theory and practice of measuring reservoir rock and fluid transport properties (3d ed.): Waltham, Mass., Gulf Professional Publishing, 950 p.

Tzimas, E., Georgakaki, A., Garcia Cortes, C., and Peteves, S.D., 2005, Enhanced oil recovery using carbon dioxide in the European energy system: European Commission Report EUR 21895 EN, 119 p., accessed January 7, 2017, at http://science.uwaterloo.ca/~mauriced/earth691-duss/CO2_General%20CO2%20Sequestration%20materilas/CO2_EOR_Misciblein%20Europe21895EN.pdf.

ISSN 2328-0328 (online)
https://doi.org/10.3133/sir20175062